RESPONSE OF THE PULP, ROOT SHEATH, AND PERIODONTAL LIGAMENT TO ADRIAMYCIN TREATMENT IN RAT INCISOR

A THESIS SUBMITTED TO THE FACULTY OF GRADUATE STUDIES, UNIVERSITY OF MANITOBA, IN PARTIAL FULFILMENT OF THE REQUIREMENTS FOR THE DEGREE OF MASTER OF SCIENCE

BY

WALTER MICHAEL NIDER

SEPTEMBER, 1994

ISBN 0-612-13405-9

Name Walter M. Nider

Dissertation Abstracts International is arranged by broad, general subject categories. Please select the one subject which most nearly describes the content of your dissertation. Enter the corresponding four-digit code in the spaces provided.

Response of the pulp, root sheath, and periodontal ligament to adriamycin treatment in rat incisor.

SUBJECT TERM

0287

SUBJECT CODE

U·M·I

Subject Categories

THE HUMANITIES AND SOCIAL SCIENCES

COMMUNICATIONS AND THE ARTS
Architecture 0729
Art History 0377
Cinema 0900
Dance 0378
Fine Arts 0357
Information Science 0723
Journalism 0391
Library Science 0399
Mass Communications 0708
Music 0413
Speech Communication 0459
Theater 0465

EDUCATION
General 0515
Administration 0514
Adult and Continuing 0516
Agricultural 0517
Art 0273
Bilingual and Multicultural 0282
Business 0688
Community College 0275
Curriculum and Instruction 0727
Early Childhood 0518
Elementary 0524
Finance 0277
Guidance and Counseling 0519
Health 0680
Higher 0745
History of 0520
Home Economics 0278
Industrial 0521
Language and Literature 0279
Mathematics 0280
Music 0522
Philosophy of 0998
Physical 0523
Psychology 0525
Reading 0535
Religious 0527
Sciences 0714
Secondary 0533
Social Sciences 0534
Sociology of 0340
Special 0529
Teacher Training 0530
Technology 0710
Tests and Measurements 0288
Vocational 0747

LANGUAGE, LITERATURE AND LINGUISTICS
Language
- General 0679
- Ancient 0289
- Linguistics 0290
- Modern 0291

Literature
- General 0401
- Classical 0294
- Comparative 0295
- Medieval 0297
- Modern 0298
- African 0316
- American 0591
- Asian 0305
- Canadian (English) 0352
- Canadian (French) 0355
- English 0593
- Germanic 0311
- Latin American 0312
- Middle Eastern 0315
- Romance 0313
- Slavic and East European 0314

PHILOSOPHY, RELIGION AND THEOLOGY
Philosophy 0422
Religion
- General 0318
- Biblical Studies 0321
- Clergy 0319
- History of 0320
- Philosophy of 0322

Theology 0469

SOCIAL SCIENCES
American Studies 0323
Anthropology
- Archaeology 0324
- Cultural 0326
- Physical 0327

Business Administration
- General 0310
- Accounting 0272
- Banking 0770
- Management 0454
- Marketing 0338

Canadian Studies 0385
Economics
- General 0501
- Agricultural 0503
- Commerce-Business 0505
- Finance 0508
- History 0509
- Labor 0510
- Theory 0511

Folklore 0358
Geography 0366
Gerontology 0351
History
- General 0578
- Ancient 0579
- Medieval 0581
- Modern 0582
- Black 0328
- African 0331
- Asia, Australia and Oceania 0332
- Canadian 0334
- European 0335
- Latin American 0336
- Middle Eastern 0333
- United States 0337

History of Science 0585
Law 0398
Political Science
- General 0615
- International Law and Relations 0616
- Public Administration 0617

Recreation 0814
Social Work 0452
Sociology
- General 0626
- Criminology and Penology 0627
- Demography 0938
- Ethnic and Racial Studies 0631
- Individual and Family Studies 0628
- Industrial and Labor Relations 0629
- Public and Social Welfare 0630
- Social Structure and Development 0700
- Theory and Methods 0344

Transportation 0709
Urban and Regional Planning 0999
Women's Studies 0453

THE SCIENCES AND ENGINEERING

BIOLOGICAL SCIENCES
Agriculture
- General 0473
- Agronomy 0285
- Animal Culture and Nutrition 0475
- Animal Pathology 0476
- Food Science and Technology 0359
- Forestry and Wildlife 0478
- Plant Culture 0479
- Plant Pathology 0480
- Plant Physiology 0817
- Range Management 0777
- Wood Technology 0746

Biology
- General 0306
- Anatomy 0287
- Biostatistics 0308
- Botany 0309
- Cell 0379
- Ecology 0329
- Entomology 0353
- Genetics 0369
- Limnology 0793
- Microbiology 0410
- Molecular 0307
- Neuroscience 0317
- Oceanography 0416
- Physiology 0433
- Radiation 0821
- Veterinary Science 0778
- Zoology 0472

Biophysics
- General 0786
- Medical 0760

EARTH SCIENCES
Biogeochemistry 0425
Geochemistry 0996
Geodesy 0370
Geology 0372
Geophysics 0373
Hydrology 0388
Mineralogy 0411
Paleobotany 0345
Paleoecology 0426
Paleontology 0418
Paleozoology 0985
Palynology 0427
Physical Geography 0368
Physical Oceanography 0415

HEALTH AND ENVIRONMENTAL SCIENCES
Environmental Sciences 0768
Health Sciences
- General 0566
- Audiology 0300
- Chemotherapy 0992
- Dentistry 0567
- Education 0350
- Hospital Management 0769
- Human Development 0758
- Immunology 0982
- Medicine and Surgery 0564
- Mental Health 0347
- Nursing 0569
- Nutrition 0570
- Obstetrics and Gynecology 0380
- Occupational Health and Therapy 0354
- Ophthalmology 0381
- Pathology 0571
- Pharmacology 0419
- Pharmacy 0572
- Physical Therapy 0382
- Public Health 0573
- Radiology 0574
- Recreation 0575
- Speech Pathology 0460
- Toxicology 0383

Home Economics 0386

PHYSICAL SCIENCES
Pure Sciences
Chemistry
- General 0485
- Agricultural 0749
- Analytical 0486
- Biochemistry 0487
- Inorganic 0488
- Nuclear 0738
- Organic 0490
- Pharmaceutical 0491
- Physical 0494
- Polymer 0495
- Radiation 0754

Mathematics 0405
Physics
- General 0605
- Acoustics 0986
- Astronomy and Astrophysics 0606
- Atmospheric Science 0608
- Atomic 0748
- Electronics and Electricity 0607
- Elementary Particles and High Energy 0798
- Fluid and Plasma 0759
- Molecular 0609
- Nuclear 0610
- Optics 0752
- Radiation 0756
- Solid State 0611

Statistics 0463

Applied Sciences
Applied Mechanics 0346
Computer Science 0984
Engineering
- General 0537
- Aerospace 0538
- Agricultural 0539
- Automotive 0540
- Biomedical 0541
- Chemical 0542
- Civil 0543
- Electronics and Electrical 0544
- Heat and Thermodynamics 0348
- Hydraulic 0545
- Industrial 0546
- Marine 0547
- Materials Science 0794
- Mechanical 0548
- Metallurgy 0743
- Mining 0551
- Nuclear 0552
- Packaging 0549
- Petroleum 0765
- Sanitary and Municipal 0554
- System Science 0790

Geotechnology 0428
Operations Research 0796
Plastics Technology 0795
Textile Technology 0994

PSYCHOLOGY
General 0621
Behavioral 0384
Clinical 0622
Developmental 0620
Experimental 0623
Industrial 0624
Personality 0625
Physiological 0989
Psychobiology 0349
Psychometrics 0632
Social 0451

Nom _____

Dissertation Abstracts International est organisé en catégories de sujets. Veuillez s.v.p. choisir le sujet qui décrit le mieux votre thèse et inscrivez le code numérique approprié dans l'espace réservé ci-dessous.

_____ ☐☐☐ U·M·I

SUJET — CODE DE SUJET

Catégories par sujets

HUMANITÉS ET SCIENCES SOCIALES

COMMUNICATIONS ET LES ARTS
Architecture 0729
Beaux-arts 0357
Bibliothéconomie 0399
Cinéma 0900
Communication verbale 0459
Communications 0708
Danse 0378
Histoire de l'art 0377
Journalisme 0391
Musique 0413
Sciences de l'information 0723
Théâtre 0465

ÉDUCATION
Généralités 515
Administration 0514
Art 0273
Collèges communautaires 0275
Commerce 0688
Économie domestique 0278
Éducation permanente 0516
Éducation préscolaire 0518
Éducation sanitaire 0680
Enseignement agricole 0517
Enseignement bilingue et multiculturel 0282
Enseignement industriel 0521
Enseignement primaire. 0524
Enseignement professionnel 0747
Enseignement religieux 0527
Enseignement secondaire 0533
Enseignement spécial 0529
Enseignement supérieur 0745
Évaluation 0288
Finances 0277
Formation des enseignants 0530
Histoire de l'éducation 0520
Langues et littérature 0279
Lecture 0535
Mathématiques 0280
Musique 0522
Orientation et consultation 0519
Philosophie de l'éducation 0998
Physique 0523
Programmes d'études et enseignement 0727
Psychologie 0525
Sciences 0714
Sciences sociales 0534
Sociologie de l'éducation 0340
Technologie 0710

LANGUE, LITTÉRATURE ET LINGUISTIQUE
Langues
- Généralités 0679
- Anciennes 0289
- Linguistique 0290
- Modernes 0291

Littérature
- Généralités 0401
- Anciennes 0294
- Comparée 0295
- Médiévale 0297
- Moderne 0298
- Africaine 0316
- Américaine 0591
- Anglaise 0593
- Asiatique 0305
- Canadienne (Anglaise) 0352
- Canadienne (Française) 0355
- Germanique 0311
- Latino-américaine 0312
- Moyen-orientale 0315
- Romane 0313
- Slave et est-européenne 0314

PHILOSOPHIE, RELIGION ET THÉOLOGIE
Philosophie 0422
Religion
- Généralités 0318
- Clergé 0319
- Études bibliques 0321
- Histoire des religions 0320
- Philosophie de la religion 0322

Théologie 0469

SCIENCES SOCIALES
Anthropologie
- Archéologie 0324
- Culturelle 0326
- Physique 0327

Droit 0398
Économie
- Généralités 0501
- Commerce-Affaires 0505
- Économie agricole 0503
- Économie du travail 0510
- Finances 0508
- Histoire 0509
- Théorie 0511

Études américaines 0323
Études canadiennes 0385
Études féministes 0453
Folklore 0358
Géographie 0366
Gérontologie 0351
Gestion des affaires
- Généralités 0310
- Administration 0454
- Banques 0770
- Comptabilité 0272
- Marketing 0338

Histoire
- Histoire générale 0578
- Ancienne 0579
- Médiévale 0581
- Moderne 0582
- Histoire des noirs 0328
- Africaine 0331
- Canadienne 0334
- États-Unis 0337
- Européenne 0335
- Moyen-orientale 0333
- Latino-américaine 0336
- Asie, Australie et Océanie 0332

Histoire des sciences 0585
Loisirs 0814
Planification urbaine et régionale 0999
Science politique
- Généralités 0615
- Administration publique 0617
- Droit et relations internationales 0616

Sociologie
- Généralités 0626
- Aide et bien-être social 0630
- Criminologie et établissements pénitentiaires 0627
- Démographie 0938
- Études de l' individu et de la famille 0628
- Études des relations interethniques et des relations raciales 0631
- Structure et développement social 0700
- Théorie et méthodes. 0344
- Travail et relations industrielles 0629

Transports 0709
Travail social 0452

SCIENCES ET INGÉNIERIE

SCIENCES BIOLOGIQUES
Agriculture
- Généralités 0473
- Agronomie. 0285
- Alimentation et technologie alimentaire 0359
- Culture 0479
- Élevage et alimentation 0475
- Exploitation des pâturages 0777
- Pathologie animale 0476
- Pathologie végétale 0480
- Physiologie végétale 0817
- Sylviculture et faune 0478
- Technologie du bois 0746

Biologie
- Généralités 0306
- Anatomie 0287
- Biologie (Statistiques) 0308
- Biologie moléculaire 0307
- Botanique 0309
- Cellule 0379
- Écologie 0329
- Entomologie 0353
- Génétique 0369
- Limnologie 0793
- Microbiologie 0410
- Neurologie 0317
- Océanographie 0416
- Physiologie 0433
- Radiation 0821
- Science vétérinaire 0778
- Zoologie 0472

Biophysique
- Généralités 0786
- Medicale 0760

SCIENCES DE LA TERRE
Biogéochimie 0425
Géochimie 0996
Géodésie 0370
Géographie physique 0368
Géologie 0372
Géophysique 0373
Hydrologie 0388
Minéralogie 0411
Océanographie physique 0415
Paléobotanique 0345
Paléoécologie 0426
Paléontologie 0418
Paléozoologie 0985
Palynologie 0427

SCIENCES DE LA SANTÉ ET DE L'ENVIRONNEMENT
Économie domestique 0386
Sciences de l'environnement 0768
Sciences de la santé
- Généralités 0566
- Administration des hôpitaux 0769
- Alimentation et nutrition 0570
- Audiologie 0300
- Chimiothérapie 0992
- Dentisterie 0567
- Développement humain 0758
- Enseignement 0350
- Immunologie 0982
- Loisirs 0575
- Médecine du travail et thérapie 0354
- Médecine et chirurgie 0564
- Obstétrique et gynécologie 0380
- Ophtalmologie 0381
- Orthophonie 0460
- Pathologie 0571
- Pharmacie 0572
- Pharmacologie 0419
- Physiothérapie 0382
- Radiologie 0574
- Santé mentale 0347
- Santé publique 0573
- Soins infirmiers 0569
- Toxicologie 0383

SCIENCES PHYSIQUES
Sciences Pures
Chimie
- Généralités 0485
- Biochimie 487
- Chimie agricole 0749
- Chimie analytique 0486
- Chimie minérale 0488
- Chimie nucléaire 0738
- Chimie organique 0490
- Chimie pharmaceutique 0491
- Physique 0494
- PolymÈres 0495
- Radiation 0754

Mathématiques 0405
Physique
- Généralités 0605
- Acoustique 0986
- Astronomie et astrophysique 0606
- Électronique et électricité 0607
- Fluides et plasma 0759
- Météorologie 0608
- Optique 0752
- Particules (Physique nucléaire) 0798
- Physique atomique 0748
- Physique de l'état solide 0611
- Physique moléculaire 0609
- Physique nucléaire 0610
- Radiation 0756

Statistiques 0463

Sciences Appliqués Et Technologie
Informatique 0984
Ingénierie
- Généralités 0537
- Agricole 0539
- Automobile 0540
- Biomédicale 0541
- Chaleur et thermodynamique 0348
- Conditionnement (Emballage) 0549
- Génie aérospatial 0538
- Génie chimique 0542
- Génie civil 0543
- Génie électronique et électrique 0544
- Génie industriel 0546
- Génie mécanique 0548
- Génie nucléaire 0552
- Ingénierie des systèmes 0790
- Mécanique navale 0547
- Métallurgie 0743
- Science des matériaux 0794
- Technique du pétrole 0765
- Technique minière 0551
- Techniques sanitaires et municipales 0554
- Technologie hydraulique 0545

Mécanique appliquée 0346
Géotechnologie 0428
Matières plastiques (Technologie) 0795
Recherche opérationnelle 0796
Textiles et tissus (Technologie) 0794

PSYCHOLOGIE
Généralités 0621
Personnalité 0625
Psychobiologie 0349
Psychologie clinique 0622
Psychologie du comportement 0384
Psychologie du développement 0620
Psychologie expérimentale 0623
Psychologie industrielle 0624
Psychologie physiologique 0989
Psychologie sociale 0451
Psychométrie 0632

RESPONSE OF THE PULP, ROOT SHEATH, AND PERIODONTAL LIGAMENT TO ADRIAMYCIN TREATMENT IN RAT INCISOR

BY

WALTER MICHAEL NIDER

A Thesis submitted to the Faculty of Graduate Studies of the University of Manitoba in partial fulfillment of the requirements for the degree of

MASTER OF SCIENCE

ABSTRACT

Light and electron microscopy techniques, as well as radioautography were used to study the responses of the pulp, root sheath, and periodontal ligament to adriamycin in the rat incisor. Young male Sprague-Dawley rats (13 days old) were injected subcutaneously with a single dose of adriamycin (5.0 mg/kg) and sacrificed by perfusion at 1, 2, and 3 weeks following adriamycin administration. Serial sections of the incisors were digitized and three dimensional reconstructions of the experimental incisors were created using an IBM computer. The radioautography portion of the study comprised 100 gram Sprague-Dawley rats which were intravenously injected with a single dose of adriamycin (5.0 mg/kg) and sacrificed by perfusion at 2 or 3 weeks following adriamycin administration. Animals were given an intravenous injection of ^{3}H-thymidine (2 μCi/g), 6 hours prior to sacrifice.

Following the administration of adriamycin, apoptotic death of dental papilla and root sheath cells was observed in the rat incisor. In areas where root sheath apoptosis had occurred, an associated failure in dentinogenesis was observed. Although dentin was not present in these areas, an associated fibrous "lesion", similar in composition to normal PDL, was formed. Based on the radioautography results, it appears that this "lesion" originated from proliferation of dental follicle cells.

For my Mom

ACKNOWLEDGEMENTS

I would like to thank all the members of the Departments of Preventive Dental Science and Anatomy, for without whose assistance, the preparation of this thesis would have been impossible.

First and foremost I express my appreciation and thanks to my research supervisor, Dr. Algernon Karim. His guidance, support and supreme patience allowed a dentist to get a taste of what research is all about and made my graduate education an enjoyable and worthwhile experience.

A special thank you to Dr. C.L.B. Lavelle for his supervision, insight, and constant encouragement throughout this project.

I also express my thanks to Dr. J.E. Scott for his sound guidance and advice in the preparation of the thesis as well as his help with statistics and graphs.

Thanks are due to Mr. Paul Perumal for his tireless technical assistance in the laboratory and Mr. Roy Simpson for help with photography and art work. My appreciation to Dr. J. Anderson for the use of her reconstruction program.

Lastly I gratefully acknowledge my indebtedness to all my friends and family for their unfailing encouragement and understanding throughout the last three years - it has not gone unnoticed.

TABLE OF CONTENTS

INTRODUCTION

In order to present the literature on the impact of adriamycin on tooth development as a coherent summary, this section is divided into the following topics:

I) Development of the Tooth

II) Development of the Periodontal Ligament

III) Periodontal Ligament Structure

- i) Collagen
- ii) Cells
- iii) Cell Kinetics

IV) Adriamycin

I. Development of the Tooth

In recent times, odontogenesis has been subjected to intense investigation (Slavkin, 1989, 1990, 1991; Thesleff *et al.*, 1990, 1991; Slavkin *et al.*, 1992; MacNeil and Somerman, 1993) but although the biological mechanism responsible for tissue induction have been defined, the largely speculative data require further investigation and appraisal. The neural crest cells predominantly control all aspects of odontogenesis and play a major inductive role in the formation of connective tissues (Le Douarin, 1984). Migrating as ectomesenchyme, the neural crest cells move into the maxillary and mandibular arch processes to interact with the lining epithelium. These

epithelio-mesenchymal interactions are essential for odontogenesis. For instance, tooth formation is prevented if odontogenic epithelial and dental mesenchymal tissues are enzymatically separated (Kollar and Baird, 1969). Yet, if recombined, odontogenesis may still proceed normally. In addition, if epithelium, obtained from a site distant from the developing oral cavity, is combined with dental mesenchyme, the epithelium will form functional ameloblasts (Kollar and Baird, 1970).

Following neural crest migration, proliferation of the oral epithelium results in the formation of the dental lamina. This tissue extends into the underlying mesenchyme to form the initial enamel organ (Sharawy and Bhussry, 1986). The enamel organ subsequently increases in size and takes on the shape of a cap. The ectomesenchyme apposing the depression in the cap proliferates and becomes more dense to initiate the formation of the dental papilla. Although the mesenchyme of the dental papilla is generally assumed to originate from neural crest cells (Ten Cate, 1975), the only conclusive evidence for this belief was demonstrated in amphibians by Chibon (1967). The dental papilla is the formative organ of the pulp and dentin, whereas a condensation of ectomesenchyme, surrounding both the enamel organ and the dental papilla, forms the dental follicle (dental sac). The cells of the dental follicle eventually form the tissues of tooth attachment, ie. alveolar bone, cementum, and periodontal ligament.

Growth of the cap results in a bell shaped enamel organ comprising four distinct layers: inner enamel epithelium, stratum intermedium, stellate reticulum, and outer enamel epithelium. The cells of the inner enamel epithelium develop into preameloblasts. These induce the mesenchymal cells of the dentinal papilla to differentiate into odontoblasts which lay down predentin and begin the complex process of dentinogenesis (Bronckers *et al.*, 1989; Linde and Goldberg, 1993). Kollar and Baird (1969) have shown that the mesenchyme controls tooth shape and promotes epithelial differentiation. The deposition of dentin subsequently induces the onset of amelogenesis.

Root formation begins after coronal dentine and enamel deposition has reached the cervical loop, the site of the future dento-enamel junction. Hertwig's epithelial root sheath, comprising the outer and inner enamel epithelium, appears then to guide root formation by inducing the transformation of dental papilla cells into odontoblasts. Once root dentine has been laid down, the epithelial root sheath loses its structural continuity and the remnants give rise to the Epithelial Rests of Malassez. Mesenchymal cells of the dental follicle next to the dentine, differentiate into cementoblasts and initiate cementogenesis (Ten Cate *et al.*, 1970). Changes in the follicle are seen as principal fibre formation starts. Work by Wise *et al.* (1992) suggests that TGF-β_1 induces the fibroblasts of the dental follicle to secrete the extracellular matrix necessary for periodontal

ligament development. However, at the root apex, the dental follicle is composed of three distinct layers as seen in the bell stage of tooth development (Tonge, 1963). The outer layer, comprised of a vascular mesenchyme, lies next to the developing alveolus. A similar fibrovascular layer, 3 - 4 cells thick, forms the inner layer. A loose, relatively avascular connective tissue lies between these layers. Berkovitz *et al.* (1984) have alluded to the fact that unlike the inner layer which is derived from neural crest, the middle and outer layers are mesodermal in origin. Ten Cate (1969) has stated that the inner layer is the precursor of the periodontium's major components. This view is supported by transplantation and radioautography studies. When this inner, vascular layer was implanted into mouse parietal bone, new bone, tooth roots, and periodontal ligament formed (Freeman *et al.*, 1975). Ten Cate *et al.* (1970), using H^3-thymidine, showed that the inner layer gave rise to cementoblasts and fibroblasts of the periodontal ligament.

Odontogenesis, therefore, involves complex interactions between the epithelial and mesenchymal components of the tooth germ, although the detailed mechanisms involved with their control remain largely obscure at this time.

II. Development of the Periodontal Ligament

Periodontal ligament formation in teeth without primary predecessors differs from that in teeth with secondary succedaneous teeth (Grant *et al.*, 1972). The following section will describe the sequential histogenesis of the principal collagen fibre groups of the ligament in teeth with and without predecessors, as well as in teeth that are continually erupting.

Formation and organization of the secondary succedaneous tooth periodontal ligament

The work by Grant and Bernick (1972) on squirrel monkey premolars is of seminal importance, and will therefore be used in this section. The premolars are encased in a bony crypt prior to eruption. When approximately one third of the root has formed, fibres near the cementoenamel junction, the future dentogingival fibres, appear as a mass of loosely structured collagenous elements coursing coronally, following the outline of the crown. At this point, no fibres are seen emerging from the crestal bone. In the middle three quarters of the periodontal ligament, loosely arranged fibres are aligned parallel to the long axis of the root. "Osteoblasts [line] the surface of the bone and only an occasional fibre [can] be seen emerging from bone" (Grant and Bernick, 1972). At the apex,

fine fibres course occlusal-ward, parallel to the root's long axis, toward the middle third of the periodontal ligament. In addition, fibre bundles emerging from the periapical tissues course coronally, and become more densely packed as they approach the bony margin. The bundles then become oriented in a superior-oblique direction, from bone toward the centrally located periodontal ligament core. Although many authors have confirmed these morphologic descriptions in a variety of other models (Grant *et al.*, 1972; Owens, 1974), the processes involved in their control remain largely obscure.

Emergence into the oral cavity

The direction of the principal fibres appear to depend on the degree of adjacent tooth eruption. When next to a tooth in functional occlusion, well formed dentogingival fibres appear to emerge and course occlusally to terminate in the lamina propria of the interproximal gingiva. Transeptal fibre groups extend from the cementum of the developing tooth, in a superior-oblique direction, over the forming alveolar crest. There is also an intermediate zone separating these fibres from those of the adjacent, developed tooth. On the side next to an unerupted tooth, the transeptal fibres develop beneath the dentogingival fibres to extend apico-obliquely towards the cementoenamel junction. Toward the middle third of the root, the ligament is continuous, extending from bone to cementum.

At the bone, these fibres are separated from short, brush-like cemental fibres by a wide central zone of loosely arranged connective tissue elements (Grant and Bernick, 1972). However, Berkovitz and Moxham (1990) were able to demonstrate fibres passing between bone and cementum at this stage. The central zone was not seen by Trott (1962) or Zwarych and Quigley (1965), who described the fibres as being continuous from cementum to bone. Grant *et al.* (1972) and Grant and Bernick (1972) believed an intermediate plexus is present only during tooth eruption, but not in a functioning tooth. According to their theory, cells of this zone secrete precursors of collagen and mucopolysaccharide complexes which may participate in lengthening and thickening of principal fibres. The failure of other researchers to see this zone is thought by Grant *et al.* (1972) to be due to rapid principal fibre formation in primary teeth. However, evidence derived from electron microscopy and radioautography (Melcher, 1986) have shown that in the non-continuously erupting tooth, the so called intermediate plexus is an artifact resulting from the fact that collagen fibres do not remain in one bundle but branch into other bundles.

First occlusal contact

At this stage, the dentogingival and transeptal fibre groups are well developed, more so than the more apical alveolar crest and horizontal fibres. The transeptal fibres appear as dense, intact, and closely approximated when stained with silver nitrate. In the upper one third of the ligament, heavy widely spaced fibres emerge from the bone as Sharpey's fibres, and seem to unravel as they join the finer groups from the cementum. Progressing apically, the fibres emanating from the cementum remains separated from the bony fibres by a central zone (Grant and Bernick, 1972).

Full articulation

With continuing occlusal function, the alveolodental fibres thicken, intermesh and pass uninterrupted from bone to cementum.

Formation and organization of the PDL in teeth without primary predecessors

The sequence of principal fibre formation is the same for teeth with and without predecessors, with the following exceptions (Grant *et al.*, 1972). During the pre-eruptive stage in the molar (a tooth without a predecessor), well defined

dentogingival and alveolodental fibres are seen. The reason for this may be related to timing. In the molar, alveolar bone deposition is completed mainly before the crown enters the mouth, however, the tooth with a predecessor is completely enclosed by a bony crypt. Principal fibre formation must therefore await the deposition of alveolar bone (Bernick and Grant, 1982).

The development of the PDL in the continuously erupting rodent incisor

Relatively little information is available with regard to the development of the periodontal ligament associated with the rat incisor (Smith, 1976). Within the first two days post-natally, odontoblasts develop following root sheath differentiation. No fibrous ligament is present, with only loosely organized fibroblasts, capillaries, and large venous channels on the labial surface. Cementoblasts become prominent along the dentine by day six and the ligament becomes wider and more prominent. Fibroblasts flatten, and they and collagen fibres become more angled in relation to the dentine surface. At day sixteen, collagen fibres run almost perpendicular to the dentine surface. The ligament next to the alveolar bone is the last to develop. By day 32, "the periodontal ligament is fully developed with characteristic interstitial pockets of loose connective tissue enclosed between larger fibre bundles

near the socket wall." (Smith, 1976) Sharpey's fibres are evident inserting into the alveolar bone.

III. Periodontal Ligament Structure

Occupying the space between the tooth root and alveolar bone, the periodontal ligament's (PDL) functions include: support, sensation, nutrition, homeostasis, and repair (Melcher, 1980). The width of the PDL varies according to functional load and age (Kronfeld, 1931; Coolidge, 1937). In general, the width decreases with age, and with hypofunction. As with other soft connective tissues, the PDL consists of cells, a fibrous matrix, and interstitial tissue, with ground substance, blood vessels and nerves.

i) Fibrous Matrix (Collagen)

The majority of the collagen present in the PDL is type I, with up to 20% being type III (Butler *et al.*, 1975a, 1975b; Limeback and Sodek, 1979; Sodek and Limeback, 1979). Immunofluorescence studies (Wang *et al.*, 1980; Takita *et al.*, 1987) and immunohistochemical studies (Becker *et al.*, 1991; Huang *et al.*, 1991) have shown type III collagen to be dispersed throughout the periodontal ligament and is greater

in erupting, than erupted teeth (Takita *et al.*, 1987). This finding is consistent with the fact that type III collagen is present in higher quantities in fetal and granulation tissues, than in adult connective tissues (Epstein, 1974; Shuttleworth and Forrest, 1975; Barnes *et al.*, 1976). Henkel and Glanville (1982) have demonstrated that type I and III collagen may be present in the same fiber: this finding is confirmed by immunohistochemical localization, where periodontal fibres and Sharpey's fibres consisted of cofibrils of type I and type III collagen (Huang *et al.*, 1991). The function of type III collagen in the PDL has not been determined, but it may act as a collagen fibre scaffold (Bailey *et al.*, 1975; Gay *et al.*, 1978; Konomi *et al.*, 1989), initiate organogenesis (Mao *et al.*, 1990), regulate collagen fibre size (Konomi *et al.*, 1981; Miller and Gay, 1987), prevent mineralization of Sharpey's fibres (Wang *et al.*, 1980; Huang *et al.*, 1991), or impart flexibility to allow occlusal forces to be absorbed or dissipated (Huang *et al.*, 1991).

Karimbux *et al.* (1992) have studied the structural alteration of the periodontal ligament with reference to changes in the expression of certain collagenous proteins. Using *in situ* hybridization, they investigated the expression of α1(XII) collagen, a Fibril-Associated Collagen with Interrupted Triple helices (FACIT) thought to contribute to fibril arrangement, α1(XII) was limited to the mature stage of PDL development and may be involved in collagen fibril

arrangement.

The initial theory that the collagen fibres of the PDL were randomly oriented and formed an indifferent fibre plexus (Shackleford, 1971a, 1971b; Svejda and Skach, 1973) was shown to be an artifact related to specimen preparation ie. disc grinding (Sloan *et al.*, 1976). It is now recognized that the collagen is arranged in fibre bundles with specific orientations depending on location. The PDL of the rabbit incisor may be separated into three zones (Sloan, 1978). The alveolar zone, comprising 40% of the ligament, is composed of thick fibre bundles 10-20 μm in diameter which are continuous with Sharpey's fibres in the alveolar bone. The cemental zone, formed by bundles 3-10 μm in diameter, comprises 10% of the ligament. The remaining bundles, interposed between the cemental and alveolar zones, are finer, being 1-4 μm in diameter. There is extensive branching and anastomosing of fibres with overlapping of the bundles in adjacent layers (Sloan 1979, 1982).

Using biochemical and radioautographical methods, a number of authors (Van den Bos and Tonino, 1984; Imberman *et al.*, 1986; Sodek and Ferrier, 1988) have shown the turnover of periodontal ligament collagen to be among the most rapid in the body. This high turnover rate may be needed for tissue adaptation during tooth movement, however this area is not clearly understood. Collagen turnover rates are increased in teeth whose antagonist has been extracted (Rippin, 1978;

Kanoza *et al.*, 1980), although, no increase was noted i) when eruption rates are doubled in the rat incisor (Van den Bos and Tonino, 1984), ii) between erupted and erupting rat molars (Berkovitz *et al.*, 1984), and iii) when an incisor is removed from occlusion (Beersten and Everts, 1977; Van den Bos and Tonino, 1984).

An area of study which even today remains unresolved is the precise location of a shear zone which allows the tooth to erupt. Sicher (1942) described an intermediate zone or plexus, although this may be merely an optical effect caused by the orientation of the middle layer of collagen (Sloan, 1978). Radioautography studies (Beertsen and Everts, 1977; Rippin, 1978; Perera and Tonge, 1981a) have shown an even uptake of radiolabel across the width of the PDL, while certain authors (Melcher and Correia, 1971; Kanoza *et al.*, 1980) have suggested that turnover may be faster in the zone along the alveolar bone.

In the continuously erupting rodent incisor, Beertsen and Everts (1977), Beertsen *et al.* (1982, 1984) have speculated that the zone of shear is associated with the middle zone of the PDL, while Berkovitz *et al.* (1980) believe it to be located nearer to the tooth.

It is recognized that the average half-life of the collagen in the PDL is less in the apical regions of molars as opposed to the crestal portion (Rippin, 1978; Perera and Tonge, 1981a).

Oxytalan Fibres

These pre-elastin fibres tend to lie parallel to the root surface (Fullmer *et al.*, 1974) and course between cementum and the periodontal vessels (Sims, 1975, 1976) without attaching to the alveolar bone. In the human PDL, oxytalan fibres account for 3% of the volume (Jonas and Riede, 1980), while occupying only 0.3% in the rat PDL (Shore *et al.*, 1984). Ultrastructurally, the fibres range from 0.2 μm to 1.5 μm depending on site and species (Shore *et al.*, 1984; Sims, 1984). To date, the exact function of the oxytalan fibres is unknown. An increase in the amount of oxytalan fibres in the PDL of teeth with increased functional loading has lead a number of investigators to believe that the oxytalan fibres increase the rigidity of the ligament (Fullmer *et al.*, 1974; Edmunds *et al.*, 1979; Jonas and Riede, 1980). Beertsen *et al.* (1974) have postulated that the oxytalan fibres may act as a guide for fibroblast migration during tooth eruption. Because of their close relationship with periodontal blood vessels, Sims (1973, 1977, 1983) has speculated that the fibres may act as part of a vascular mechanoreceptive system.

ii) Cells

According to Berkovitz and Shore (1982) there are four major cell types present in the PDL; connective tissue, epithelial, defense, and vascular. Rests of Malassez, formed following the breakup of the root sheath, form the epithelial cell component. Present in both healthy and inflamed tissues, defense cells include macrophages, lymphocytes, mast cells, and leucocytes (Schroeder, 1986). Fibroblasts, osteoblasts, osteoclasts, and cementoblasts comprise the connective tissue component. Fibroblasts constitute the most numerous cell population in the PDL, occupying 50 % of the volume of the collagenous portion in the rat and mouse incisor ligament (Beertsen and Everts, 1977; Shore and Berkovitz, 1979; Shore *et al.*, 1984). This discussion of the cells in the PDL will focus on the fibroblast. The shape of the fibroblast is often determined by the surrounding fibre network. Where fibres are tightly packed and have a definite orientation between tooth and bone, the fibroblasts appear elongated, lying parallel to the fibre bundles. In loose, interstitial tissue, the fibroblasts have an ovoid, spindle, or elongated shape. Roberts and Chamberlain (1978), using scanning electron microscopy, have concluded that the cells are pleomorphic and have described four general cell shapes in the rat PDL. These include irregular, oblong-shaped cells (16-22 μm long); stellate-shaped (8-13 μm long); nodular spheroid-shaped cells

(7-12 μm long) located in perivascular areas, and elongated, stellate shaped cells (up to 60 μm long), with pseudopodia-like cytoplasmic extensions. It must be remembered that while these classifications were made, perceived cell shape is determined by the plane of section (Beertsen and Everts, 1977; Shore and Berkovitz, 1979). Shore and Berkovitz (1979) have shown that the rat incisor contains a group of fibroblasts with a preferential orientation. When sectioned either longitudinally or transversely, the fibroblasts of the inner, cementum-related PDL had a similar appearance, with a mean diameter of 30 μm. It was concluded that these fibroblasts were flattened discs.

At the ultrastructural level, the fibroblast contains a nucleus which is euchromatin-rich and includes at least one nucleolus. This nucleus occupies approximately 25% of the cellular volume (Beertsen and Everts, 1977; Yamasaki *et al.*, 1987). The fibroblast also contains an abundance of organelles used in the synthesis and secretion of protein; rough endoplasmic reticulum, mitochondria, vesicles, and Golgi apparatus. Rough endoplasmic reticuli have been shown to encompass 5-10% of the cell volume (Beertsen and Everts, 1977; Bervovitz *et al.*, 1984; Yamasaki *et al.*, 1987). Collagen synthesis by periodontal fibroblast closely follows that seen by other tissues (Cho and Garant, 1981). Within 5 minutes following injection, radiolabelled proline can be identified in the rough endoplasmic reticulum and by 20 minutes this is

concentrated in the Golgi apparatus. Secretory granules containing labelled procollagen are visible by 30 minutes, and radiolabelled extracellular collagen is present 4 hours following proline administration. Bienkowski *et al.* (1978) have postulated that collagen synthesis by a fibroblast may be greater than its requirement, resulting in intracellular breakdown. Bienkowski (1983) has indicated that 10% to 40% of newly synthesised procollagen is degraded before being processed into collagen fibrils. This intracellular breakdown is supported by other investigations (Ten Cate and Syrbu, 1974; Garant, 1976) which have demonstrated that collagen containing intracellular vesicles contain acid and alkaline phosphatase. Svoboda *et al.* (1979a, 1979b) and Melcher and Chan (1981) have shown that in addition to degrading newly synthesised collagen intracellularly, fibroblasts will degrade exogenous collagen from the intercellular environment. Biosynthesis, phagocytosis, and degradation of collagen occur concurrently.

Microfilaments and microtubules are important functioning organelles within the PDL fibroblast. Microfilaments have been documented as serving a number of functions in many different types of cells (Allison, 1973; Willingham *et al.*, 1981). Located beneath the cell memebrane, with a diameter of 6 nm, these microfilaments participate in endocytosis, exocytosis and cell locomotion and motility. Also present are microtubules, non-branching cylinders with a diameter of 22

nm, which participate in intracellular transport and maintenance of cell shape.

The cytoplasm of fibroblasts often come into contact with one another. The most frequent type is the simplified desmosome where a narrow intercellular space of 15 nm separate adjacent cells with increased cytoplasmic and cell membrane density. Unlike typical desmosomes, these simplified desmosomes do not contain bundles of inserting tonofilaments (Shore *et al.*, 1981). Gap junctions and close contact junctions may also be present.

The relationship between the contractile properties of fibroblasts and tooth eruption has been studied. Melcher and Beertsen (1977) have postulated that the microtubules and microfilaments may provide structural support for a motile system. According to these authors, cytoplasmic, pseudopodic contractility could pull collagen fibres together which would result in occlusal tooth movement. Bellows *et al.* (1982a) supported this theory where tooth and bone fragments were pulled together when on collagen gels in vitro. However, this phoenomenon was not seen when colcemid and cytochalasin D. were added to the gels, indicating that microtubules and microfilaments were involved in the process.

In gel contraction studies, the fibroblasts appear spindle-shaped and similar to myofibroblasts (Bellows *et al.*, 1982a, 1982b). However, fibroblasts in vivo generally have an irregular disc-shape. Studies comparing teeth which were

erupting with those that were non-erupting (Berkovitz *et al.*, 1984) or those that were immobilized (Shore *et al.*, 1985) showed few morphological differences.

Cahill and Marks (1982), using erupting dog premolars, demonstrated that the collagenous PDL did not attach into the alveolar bone, even though the tooth erupted, thus showing that the PDL may not be directly responsible for eruption. Only when the tooth pierced the gingiva, did the fibres show bony attachment. Also, in support of this theory, Carl and Wood (1980) have shown that eruption did occur in rootless teeth. Whether fibroblasts, through contractility, play a direct role in tooth eruption is still under debate, Marks and Cahill (1987) have shown that the coronal portion of the follicle, the precursor of the PDL, is required for bone resorption, while the basal portion initiates bone deposition. Without both parts, eruption is impeded. Prior to eruption, there is an increase in monocyte numbers in the coronal follicle. Marks *et al.* (1988) believe that these aid eruption by either becoming osteoclast precursors or releasing local mediators such as prostaglandins or growth factors.

Garant and Cho (1979) and Cho and Garant (1985) are of the impression that the position of certain cytoplasmic organelles is related to migration. These authors believe that the leading edge of polarized fibroblasts is where collagen is secreted (Cho and Garant, 1984) and migration closely follows secretion. In addition, Beertsen *et al.* (1979) have shown that

fibroblasts in the continuously erupting rat incisor were polarized, while those in the erupted molar ligament were not.

iii) Cell Kinetics

Radioautography shows the periodontal ligament to be a dynamic tissue (Toto and Kwan, 1970; Roberts and Jee, 1974; McCulloch and Melcher, 1983c), with age (Jensen and Toto, 1968; Toto and Borg, 1968; Tonna *et al.*, 1972; Toto *et al.*, 1975; McCulloch and Melcher, 1983c) and location being the principal determinants (Toto and Borg, 1968; Toto and Kwan 1970; Gould *et al.*, 1982).

Rather than comprising a single tissue, McCulloch and Bordin (1991) have described various fibroblast sub-populations, mediated by i) clonal expansion of a highly proliferative population, ii) clonal deletion by selective cell death and/or inhibition of proliferation by chemical mediators, and iii) directed migration of subsets into a site by chemoattractants. The origin of these specific subpopulations remains unclear, although the majority appear to originate from precursor cells associated with blood vessels (Ten Cate, 1972; McCulloch and Melcher, 1983b; McCulloch, 1985). These cells not only have a high basal rate of proliferation, but also proliferate during a repopulation response, and show kinetic characteristics similar to stem

cells (McCulloch and Bordin, 1991). As the number of cells in the PDL does not increase with age, a homeostatic mechanism must equilibrate cell growth with cell death or migration (Schellens *et al.*, 1982; McCulloch and Melcher, 1983a, 1983c).

While the PDL has been considered a slowly renewing tissue (Perera and Tonge, 1981b), this renewal can be altered [eg. by orthodontic forces (Roberts and Chase, 1981), trauma (Gould *et al.*, 1977, 1980) and electrical stimulation (Davidovitch *et al.*, 1980)]. But since cells labelled following trauma were primarily paravascular in nature (Gould *et al.*, 1977, 1980), while widely distributed cells proliferate following orthodontic stimulation (Roberts and Chase, 1981), cell precursors may be heterogenous. Moreover, since continuous labelling shows 50% of the PDL cells have not entered mitosis after 60 days (Gould *et al.*, 1982; McCulloch and Melcher, 1983a), either the cell cycle is greater than 60 days or some cells lose their ability to divide. Yet recombination experiments (Yoshikawa and Kollar, 1981) support a single stem cell whereas more recent research indicates "there is no compelling data to demonstrate the existence of phenotypically stable and heterogeneous populations of fibroblasts in periodontal ligament" (McCulloch and Bordin, 1991). Changes in EGF-receptor expression (Partanen and Thesleff, 1987) and cell-surface proteoglycans in different mesenchyme cells during tooth development (Thesleff *et al.*,

1988) may indicate sorting of cells along specific phenotypic pathways, but may also indicate site-specific modulation. Conceivably, the cellular environment imposes heterogeneic function on certain cells. For instance, changes in the ground substance is seen with tooth maturation (Pearson *et al.*, 1975). Cell surface receptors are crucial in fibroblast function (Yamada, 1983), eg. for extracellular matrix components, cytokines and complement proteins, although their roles remain obscure.

Possibly, only cells from incompletely developed teeth can synthesize all types of periodontal tissues (Barrett and Reade, 1981), while phenotypically stable cell lines occur in mature teeth. Yet Roberts and Morey (1985) have demonstrated discrete cellular populations in the PDL with varying ability to form osteoblasts and fibroblasts. At present, we know that progenitor cells are located throughout the periodontal ligament. What is not known is whether a totipotent precursor exists.

IV Adriamycin

As adriamycin plays a major role in this study, a more detailed examination of this drug with specific reference to its mode of action and effect on tooth development is

warranted.

Doxorubicin (adriamycin) is an anthracycline chemotherapeutic, commonly used in the treatment of neoplasms of the lung (Myers, 1990), bladder (Seidman and Scher, 1991; Miller and Torti, 1992), liver (d'Arville and Johnson, 1990; Ku *et al.*, 1993), ovary (Tsuruchi *et al.*, 1993), breast (Ahern *et al.*, 1994), and stomach (Kusumoto *et al.*, 1991; Sugarbaker, 1991; Wils, 1991; Weese and Nussbaum, 1992); both Hodgkin's and non-Hodgkin's lymphoma (Bader *et al.*, 1993, Diehl, 1993), sarcomas (Patel and Benjamin, 1992; Hays, 1993; Mameghan *et al.*, 1993), and the acute leukemias (Jehn and Heinemann, 1991; Yokose *et al.*, 1993).

The anthracyclines are members of a group of antibiotics termed rhodomycins, which are metabolites of various *Streptomyces sp.*, characterized by a glycosidic structure, where a tetracyclic chromophore is linked to one or more sugar residues (Meyers, 1982). With adriamycin, the sugar is daunosamine with the A ring possessing a methoxy group and the B ring containing hydroquinone functionalities.

The antracyclines' mode of action, although studied by many investigators, is not certain. Historically, the ability of doxorubicin to bind to DNA was the first mechanism of action to be noted (Myers, 1982). The chromophore of the doxorubicin molecule positions itself between base pairs perpendicular to the DNA double helix. The amino sugar of the

anthracycline molecule interacts ionically with the DNA's sugar phosphate backbone (Patel and Canuel, 1978), while the A and D rings extend beyond the double helix. The resultant intercalation results in partial DNA helix unwinding with nucleic acid synthesis being impaired. Other investigators (Schwartz, 1975; Ross *et al.*, 1979) have demonstrated single- and double-stranded DNA breaks. Tewey *et al.* (1984) have demonstrated that the protein associated breaks are the result of the anthracyclines' effect on topoisomerase-II. This enzyme promotes DNA strand cleavage and resealing. The anthracyclines, through intercalation, alter the DNA conformation such that topoisomerase-II action is stopped at the cleavage stage.

Depending on the concentration of the administered drug, different parts of the cell cycle are affected. Ritch *et al.* (1981) demonstrated that at high concentrations, adriamycin will cause an S-phase block. However, when cells in G_1 are exposed to lower concentrations, they will proceed through S phase normally, then stop and die in G_2. This phenomenon may be explained by the fact that doxorubicin inhibits preribosomal RNA synthesis (Daskal *et al.*, 1978).

Sato *et al.* (1977), have demonstrated the formation of free superoxide radicals following the action by the microsomal enzyme P450 reductase (in the presence of NADPH) upon doxorubicin and daunorubicin. Oxidative damage to cell membranes and cleavage of DNA results from these superoxide

radicals (Fridovich, 1978). Bachur *et al*. (1977) and Thayer (1977) have shown that following doxorubicin administration, superoxide formation results in the peroxidation of cardiac mitochondrial lipids. Bachur *et al*. (1977) have also suggested that doxorubicin may have a similar effect on cardiac sarcosomes. Work by Goormaghtigh *et al*. (1980a, 1980b) may explain why mitochondrial targetting occurs. They have shown that of the cell membrane phospholipids, doxorubicin has the highest affinity for cardiolipin; mitocondrial membranes demonstrate the highest concentration of cardiolipin. The biologic effects of the anthracyclines are complex and should not be viewed as necessarily independent nor mutually exclusive.

Adriamycin effects on the rat incisor have been studied. It has been shown that one day following an I.V. injection of adriamycin, a zone of cell degeneration 2.2 mm long, starting 300 μm from the apex and extending incisally, is produced in the rat incisor (Karim, 1985a; Karim and Pylypas, 1985). The affected cells were shown to be early preodontoblasts and the precursors of preodontoblasts, while more differentiated cells capable of initial dentine secretion were resistant to the drug's effect (Dahl and Koppang, 1985; Karim, 1985a). Between three and seven days after adriamycin administration, aggregations of mesenchymal cells, incisal to the zone of cells degeneration, were noted (Karim, 1985b). These abnormally differentiated pulp mesenchymal cells

contained high levels of rough endoplasmic reticulum and secretory granules, and were responsible for subsequent osteodentin formation (Karim, 1985b; Karim and Pylypas, 1986). Daeninck and Karim (1987) demonstrated that these odontoblast-like cells showed a high alkaline phosphatase activity, indicating that they may be involved in osteodentin mineralization as well as protein secretion (Karim and Pylypas, 1986). Karim and Eddy (1984) demonstrated that the osteodentin formation can progress to a point where the entire pulpal chamber becomes obliterated. While osteodentin formation is stimulated in the rat incisor following adriamycin administration, reduced dentin formation by odontoblasts (Dahl, 1984; Dahl and Koppang, 1985) and defects in the lingual dentin (Karim, 1990), with a subsequent sheath of fibroblasts bridging the gap have been noted.

The present study was undertaken to examine the mesenchymal-epithelial cellular interactions that occur during tooth development by studying the response of these elements to adriamycin.

MATERIALS AND METHODS

Morphology and Reconstruction Studies

Animals

All animals used in this study were obtained from the Central Animal Care Facility, where they were housed and cared for during the experimental period. Twelve young (13 days old) male Sprague-Dawley rats (35 ± 4 g) were used. These animals were divided into two groups. Group 1 (control) comprised three animals used to study normal tooth and periodontal ligament developmental morphology, in addition to changes induced by the trauma of injection. Group 2 (experimental) comprised nine animals and was used to study the periodontal response following Adriamycin administration.

Injection of Animals

Group 1: The animals were injected with 0.1 ml of physiological saline.

Group 2: These animals were subcutaneously injected with a single dose of Adriamycin (Adria Laboratories of Canada, Ltd.) at a dose of 5.0 mg/kg; a concentration previously shown to produce a lingual dentin defect in the incisor with the subsequent formation of a fibroblast bridge (Karim, 1990).

Perfusion of Animals

The animals were sacrificed in the following sequence:

i) At 1 week post-Adriamycin injection (20 day old animals): One control (Group 1) and three experimental animals (Group 2);

ii) At 2 weeks post-Adriamycin injection (27 day old animals): One control (Group 1) and three experimental animals (Group 2);

iii) At 3 weeks post-Adriamycin injection (34 day old animals): One control (Group 1) and three experimental animals (Group 2).

All rats were anaesthetized by ether inhalation and perfused through the left ventricle; initially with physiologic saline (45 - 60 seconds) to clear the vascular system of blood, followed by a glutaraldehyde solution (Appendix A) for 15 minutes (Warshawsky and Moore, 1967).

Decalcification

Following the methods of Warshawsky and Moore (1967), the incisors were dissected with the jaws (Figure 1), after perfusion, and stored in a cold glutaraldehyde solution for an additional 2-3 hours. After removal from the fixative, the jaws were stored in a 0.15 M phosphate buffer solution (*p*H 7.2) at 4.0 °C for 24 hours. The jaws were then tied in gauze bags and suspended in 4.13% disodium EDTA (*p*H 7.4) [Appendix

A] for 6 weeks. During the period of decalcification, the solution was maintained at 4.0 °C, continuously agitated, and changed weekly.

Processing of Tissue

After demineralization, the incisors were cut into 1 mm cross sectional segments. Mandibular incisor segments were arranged on a fine plastic thread to maintain the order and orientation of the individual segments. All segments were washed several times over a 24 hour period in 0.15 M phosphate buffer solution (*p*H 7.2) at 4.0 °C.

Post-Fixation

The washed samples were post-fixed in a 1% osmium tetroxide solution (Appendix A) at 20 °C for 3 hours. Following post-fixation, the tissue was washed in several changes of 0.15 M phosphate buffer solution.

Dehydration

The post-fixed material was dehydrated in graded concentrations of acetone as follows:

Concentration of Acetone	Dehydration Time
30%	10 minutes (1 change)
50%	10 minutes (1 change)
70%	10 minutes (1 change)
80%	10 minutes (1 change)
85%	10 minutes (1 change)
90%	10 minutes (1 change)
95%	10 minutes (1 change)
100%	10 minutes (3 changes)

Infiltration

After the final change in 100% acetone, the tissue samples were placed in a 3:1 acetone-Epon mixture (Appendix A) to begin the infiltration process. This process was continued in the following manner:

Acetone:Epon	Time
3:1	12 hours
1:1	12 hours
1:3	12 hours
Pure Epon	24 hours

This process was carried out at room temperature, with the samples being agitated in the mixtures prior to letting them stand.

Embedding

The tissues were embedded in pure Epon. Beam capsules were partially filled (0.1 ml) with Epon, and the tissue (one segment per capsule) orientated with its cross sectioned surface towards the bottom of the capsule. The capsules were completely filled with Epon and placed in a 60 °C oven for a 48 hour polymerization.

Sectioning

The blocks were gross trimmed using a razor blade under a dissecting microscope. One μm thick sections were obtained using a diamond knife on a Reichert OM U3 ultramicrotome. An

evaluation was made as to which incisors (one incisor chosen from an experimental animal group sacrificed at i) 1 week, ii) 2 weeks, and iii) 3 weeks -post Adriamycin administration) would be the most appropriate for serial sectioning. Once the three specific incisors were chosen, 1 μm thick serial sections were obtained. Every 20 μm, 2 sections were placed on a previously cleaned glass slide. Random, non-serial, 1 μm thick sections of control animals were also obtained.

Ultrathin sections (pale gold or silver interference colour) were cut with a diamond knife on a Reichert OM U3 ultramicrotome. These sections were placed on naked 300 mesh copper grids for subsequent electron microscopic observation.

Staining

Glass slides, containing sections for subsequent light microscopic reconstruction, were flooded with 1% toluidine blue (Appendix A) for 45-50 seconds at 85 °C. These were washed under a stream of double distilled water and dried on a hot plate.

Grids for electron microscopy were contrast stained using uranyl acetate (Appendix A) and lead citrate (Appendix A)

Uranyl Acetate

The stain was pipetted from midway in the bottle and filtered directly onto a wax staining plate. The section side

of the copper grids were placed upon the surface of the drops for 2 hours. After staining, the grids were doused with 70% ethyl alcohol and rinsed in 3 changes of double distilled water, using straight up and down movements. The grids were dried on filter paper.

Lead Citrate

Filtered solution was dropped onto a clean staining plate. Previously UA-stained ultrathin sections on grids were placed section-side down on the drops for 5 minutes. They were washed, rinsed and dried as described above.

Computer Generated Incisor Reconstruction

The following procedure was carried out for an incisor from each of the following experimental groupings (ie. an animal sacrificed at i) 1 week, ii) 2 weeks, and iii) 3 weeks -post Adriamycin administration).

Using an Olympus BH-2 microscope, with an attached camera lucida, the serial sections were traced directly onto 125 μm thick acetate sheets. One section was traced every 60 μm, at a magnification of 40 x. The acetate sheets were stacked and orientated to one another using vascular and neural canals (canals within and outside of the incisor proper were used to reduce the chance of orientation error).

The traced sections were electronically digitized using a three dimensional reconstruction computer program, PC 3D (Jandel Scientific, USA), on an IBM computer.

Electron Microscopy

Microscopic observations were carried out on a Philips 201 electron microscope operated at 75 kv.

Radioautography Study

Animals

Eight male Sprague-Dawley rats (100 ± 8 g) were used in this part of the study. They were divided into two groups. Group A comprise control animals, used to determine normal periodontal ligament fibroblast incorporation of ^{3}H-thymidine. In group B (experimental), six animals injected with ^{3}H-thymidine were used to study the kinetics of the fibroblasts associated with the Adriamycin-induced dentin incisor defect.

Injection of Animals

The control animals (Group A) were injected with 0.25 ml of physiologic saline. Group B animals were given a single subcutaneous injection of Adriamycin (5 mg/kg).

Group A animals were injected intravenously with ^{3}H-thymidine [2 μCi/g (Appendix A)], 2 weeks post-saline injection, and were sacrificed via intra-cardiac perfusion 6 hours after ^{3}H-thymidine injection.

Group B animals were treated in the following manner:

Number of rats	Time of sacrifice after Adriamycin Injection (5 mg/kg)	Time of sacrifice after ^{3}H-thymidine Injection (2 μCi/g)
3	2 weeks	6 hours
3	3 weeks	6 hours

The incisors and associated jaws were dissected out, demineralized and processed in a manner similar to that described previously, with the following exceptions.

Radioautographic Procedures

Light microscopy

One μm sections were collected on cleaned slides and prestained with iron hematoxylin (see staining procedure). The slides were processed according to the technique of Kopriwa and Leblond (1962), [with the exception that Amersham LM-1 liquid emulsion was used], exposed in the dark for 37 days at 4 °C, developed in a diluted solution of D-19 (10:1, DD H_2O:D-19) at 20 °C for 3 minutes, and fixed in 30% sodium thiosulfate for 10 minutes.

Staining Procedure

Iron hematoxylin (Appendix A)

The slides were heated on a hot plate at 85 °C. The

slides were flooded with 5% iron alum for 15 minutes. Bubbles were removed from the surface of the sections by running a fine plastic filament over the surface. The iron alum was poured off, the slides were rinsed in distilled water. The backs of the slides were wiped dry, replaced on the hot plate, and the sections flooded with iron hematoxylin for 10 minutes. The slides were not allowed to dry. The iron hematoxylin was discarded and the slides were rinsed in several changes of distilled water. The backs of the slides were dried. The slides were once again heated on the hot plate with tap water for approximately 3 minutes to differentiate the stain, then dried on edge at room temperature.

Counting of Labelled Cells

The slides were examined microscopically at 400x magnification. A grid measuring 40 μm x 200 μm was used to delineate an area in which the number of labelled cells was determined. A cell was considered labelled if the nucleus contained 6 or more silver grains.

Analysis of Radioautography

Cell counts were analyzed using Duncan's multiple range test. A difference was considered significant at a confidence level of $p < 0.01$.

RESULTS

The aim of this section is to show the responses of the periodontium, at various time periods, to the administration of adriamycin. In order to present a coherent account, a series of subsections are presented:

1) Light Microscopy
2) Description of Serial Reconstruction
3) Electron Microscopy
4) Radioautography

1. LIGHT MICROSCOPY

In this section, the histologic structure of control incisors is described first in order to form a basis for comparison with the experimental animals. The sections were viewed mainly at x 200 magnification, although estimates of cell size and areas were based on x 1000 magnification. The description of a particular, representative section may contain elements which are not readily visible in the associated photomicrograph as space limitations have resulted in low power photomicrographs.

1.1 Control (Figures 1.1.a - 1.1.g)

This is a description of the sequential cross sectional morphology (apical to incisal) of the continuously erupting mandibular incisors of a control animal, based on representative sections.

Figure 1.1.a is a cross section through the "U"-shaped part of the odontogenic organ, as described by Smith and Warshawsky (1975a). At this point in development, the incisor consists of a central labial portion and two lingual extensions. The lingual extensions are not approximated, resulting in a lingual apical foramen.

Low columnar ameloblasts form the inner wall of the central portion of the "U". Lying pulpally to the ameloblasts, low columnar odontoblasts with polarized nuclei function to secrete predentin. Moving laterally toward the lingual projections, the cuboidal or ovoid odontoblasts do not produce visible dentin matrix. The pulp consists of loose, stellate mesenchymal cells with minimal organization. Labial to the ameloblasts, flattened or ovoid cells form the provisional stratum intermedium and stellate reticulum, although these two groups of cells are difficult to distinguish at this magnification. The outer enamel epithelium (OEE) lies labial to these cells and comprises a single cell layer of loosely packed squamous cells.

As the outer enamel epithelium moves lingually to form the outer surface of the medial and lateral limbs of the

odontogenic organ, the cells become more cuboidal and more tightly packed. At the cervical loop, the OEE makes an abrupt, labial bend, becoming continuous with the inner enamel epithelium (IEE). This IEE layer is composed of a layer of tightly packed columnar cells, which run labially and meet the cuboidal shaped ameloblasts at the future site of the cemento-enamel junction. The periodontal ligament is composed of a loose arrangement of stellate mesenchymal cells with no visible fibrous matrix. Numerous, large vascular channels are evident.

Figure 1.1.b demonstrates the point at which the inner and outer enamel epithelium, previously forming the limbs of the odontogenic "U" organ, have been replaced by Hertwig's Epithelial Root Sheath (RS). While the odontogenic "U" contains tall columnar cells and several different cell layers, the root sheath consists of short cells that are only a few layers thick. The stellate reticulum presents as a single layer of squamous cells between the inner and outer epithelial layers, and extends labially from the cervical loop for approximately 150 μm. The inner layer of the root sheath comprises a single layer of cuboidal or low columnar cells, 6 to 8 μm in height, which can be followed labially to the dentin. A cell free zone, 1 to 2 μm, occurs between the inner layer of the root sheath and the adjacent pulp. Near the cervical loop, the outer layer is cuboidal in shape, which

becomes progressively flatter and less tightly packed on progressing labially. Near the future CEJ, the outer layer of the root sheath is disrupted and a fine fibrous matrix is noted in the PDL space. On the pulpal side, tall columnar odontoblasts producing dentin are present along the labial one quarter of the root sheath. Cells deeper in the pulp, adjacent to the tall columnar odontoblasts are organized as a flattened subodontoblastic layer, 2 to 3 cells thick. Progressing lingually along the root sheath, pulpal cells differente first into cuboidal, and then low columnar pre-odontoblasts. The ameloblasts are tall columnar cells with polarized nuclei. A thin layer of unmineralized enamel matrix is seen adjacent to the dentin layer. At the edge of the cervical loops, there is a condensation of spindle shaped cells, extending approximately 150 μm into the apical foramen.

Figure 1.1.c, is incisal to the two previous sections. This section shows the root sheaths of the medial and lateral arms nearing approximation. The cellular condensations of elongated spindle shaped cells adjacent to the cervical loops of the root sheaths have met in the apical foramen area as a scaffold, closing off the apical foramen. While the outer layer of the root sheath consists of cuboidal cells near the cervical loop, this feature is lost labially as dentinogenesis continues. The outer layer of the root sheath loses continuity and round to ovoid shaped cells are seen near the tooth

surface. At this point in development, dentinogenesis has progressed half way up the mesial surface of the incisor. A fine fibrous matrix is seen near the CEJ, while the cells of the PDL remain as undifferentiated mesenchymal cells.

Figure 1.1.d demonstrates closure of the apical foramen through root sheath approximation. Differentiation of odontoblasts, from ovoid to columnar cells, progresses lingually, parallel to dentin formation. The PDL is becoming more cellular, comprising round to spindle shaped cells. The cells in the labial half of the pulp are more ovoid in shape, with hyperchromatic nucleoli.

Figure 1.1.e represents an area of development where the lingual portion of the incisor is enclosed by a layer of dentin. On the lingual surface, the thickness of the dentin is approximately 40 μm, with 20 μm of predentin. In the subodontoblastic layer, the cells are ovoid in shape, while the pulp cells, located more centrally, have a stellate appearance. The odontoblasts lining the predentin are all tall columnar with polarized nuclei, and there are multiple vascular channels between these cells. On the labial surface of the incisor, both the enamel and dentin layers are each 90-100 μm in thickness.

The periodontal ligament shows a definite fibrous organization. The fibres run in an oblique direction with the

insertion into cementum being more lingual than those into alveolar bone. In the lingual one third of the incisor, the PDL fibres run perpendicular to the dentinal surface. Throughout the ligament, fibroblasts with elongated nuclei are oriented between the fibrous matrix. Along the dentin surface, cementoblasts with round and hyperchromatic nucleoli are visible.

Figure 1.1.f is similar to Figure 1.1.e, except that dentinogenesis and amelogenesis is more advanced, leading to a reduced pulp space. On the lingual aspect, the dentin layer is approximately 120 μm thick, while on the labial it is 200 μm. The enamel layer is approximately 140 μm thick, and is stained less intensely than the previous sections due to matrix mineralization. The PDL remains highly fibrous with an orientation similar to that seen in the preceding Figure (1.1.e). Fibroblasts with elongated nuclei are oriented between the fibres. The pulp demonstrates a reduced cellular density with the cells being stellate in shape.

Figure 1.1.g is a section through the incisal end of the rat incisor. The pulpal space is greatly diminished as the dentin thicknes has increased to 400-425 μm. The only remnant of the acid-soluble enamel is a space 150 μm thick. The odontoblast layer next to the dentin comprises cells fusiform in shape with nuclei at various levels. The ovoid pulp cells

are few in number. The PDL fibres course perpendicular to the dentin surface, except for a narrow band at the CEJ where they run from the cementum to the alveolar bone in a lingual-labial direction. Fibroblasts with elongated nuclei are present between the fibre bundles.

1.2 Experimental

The following is a description of the sequential (apical to incisal) cross sectional morphology associated with the continuously erupting mandibular incisor of experimental animals at: i) one, ii) two, and iii) three weeks post-adriamycin injection. While the entire cross sectional morphology of the incisor is described in the text, only the lingual half of the incisor is depicted photographically to allow a more detailed examination of the areas of interest at a higher magnification.

1.2.1 One Week Post-adriamycin Administration

Figure 1.2.1.a represents a section through the "U" portion of the odontogenic organ (Oo). At this stage, the tooth consists of a central labial portion and with two lingual extensions. The medial and lateral projections of the "U" comprise the IEE, stellate reticulum, and OEE. The IEE is

composed of multiple layers of tightly packed columnar cells. Toward the cervical loop, these cells become more cuboidal and thin to one layer. 120 μm labial to the cervical loop, the IEE is deformed away from the pulp, whereas an area of cell death is represented by a cell free zone. The cell free zone is larger on the medial projection, being 60 x 80 μm, while 30 x 30 μm on the lateral side. With the exception of the cell free zone, normal morphology is noted. At the cervical loop, the OEE comprises a single layer of cuboidal cells that progressively become more squamous toward the labial portion of the incisor. The PDL is a loose arrangement of stellate shaped mesenchymal cells with no visible fibrous matrix. At the cervical loops, there is a condensation of ovoid shaped cells streaming toward the apical foramen. Between these condensations there appears to be a loosely arranged network of stellate cells, 10 to 15 cells thick.

Figure 1.2.1.b illustrates a point in development where the vertical arms of the "U" are replaced by the root sheath. Unlike the previous section, the sides of the incisor are not distorted laterally. The inner layer of the root sheath is formed by a layer of cuboidal cells, one to two cells in thickness, which are flattened where they contact the area of pulpal cell death. This area is approximately 80 x 20 μm on the medial side and 60 x 20 μm on the lateral side, with the larger dimension being in a labio-lingual direction. At the

cervical loop area of the root sheath, the condensation is more dense with elongated cells on the future PDL side, and more ovoid cells pulpally. At this stage, the PDL comprises a loose arrangement of stellate mesenchymal cells. A loosely arranged cellular network of stellate cells lying lingually between the cervical loop condensations is still present.

Figure 1.2.1.c shows that normal incisor development is altered in the lingual half of the incisor approximately 360 μm from the medial CEJ. Proceeding lingually, there is a disrupted arrangement of flattened and small ovoid shaped cells, 3 - 4 layers thick. The ovoid cells lie pulpal to the flattened cells. Lingually, this disrupted area is continuous with a portion of lingual root sheath. The root sheath contains an inner layer of tightly packed cuboidal cells and an outer layer of squamous cells. At the labial extent of the root sheath segment, the cells of the inner and outer layers flatten and become less distinct. Pulpal to the lingual root sheath, there is a condensation of round to ovoid preodontoblasts with prominent nuclei. On the lateral surface of the incisor, the root sheath ends in a fine taper with a disrupted area of cells mentioned previously.

Figure 1.2.1.d shows the lingual root sheath has been replaced by odontoblasts involved with dentinogenesis. The thickness of dentin on the lingual surface is approximately 2-

3 μm. On both the medial and lateral walls, the thickness of the dentin is increasing. Lingual to the free dentin margin on the medial wall of the incisor, there is a disrupted area comprising flattened cells, 3-4 cells thick pulpally, and round cells with small round nuclei, 2 layers thick, toward the PDL side. There does not appear to be a fibrous matrix associated with this disruption. On the lateral surface, the disruption has a similar composition, although the flattened cells appear to be associated with a fine fibrous matrix.

Figure 1.2.1.e illustrates a section through the incisor where dentin production has encircled the pulp. There are small breaks in the dentin layer, 3-5 μm thick, on the medial, lateral, and lingual surfaces. Unlike the sides of the incisor, dentinogenesis has not followed a uniform and regular pattern. The pulpal surface of the dentin is irregular and convoluted, an indication that this is most likely osteodentin. In the lingual portion of the pulp, there is an aggregation of ovoid cells 5 to 7 layers thick in the subodontoblastic region. The cellular density of the pulp is greater in the lingual portion than in the labial half. The PDL space contains a high number of round to ovoid shaped cells near the cementum, although the cellular density decreases with only a few stellate mesenchymal cells being present toward the alveolar bone.

1.2.2 Two Weeks Post-adriamycin Administration

Figure 1.2.2.a is a cross section through the "U"-shaped part of the odontogenic organ. The lingual extensions have not approximated, resulting in an apical foramen on the lingual surface. The pulp comprises a loose arrangement of stellate mesenchymal cells. As the outer dental epithelium moves lingually, the cells next to the inner dental epithelium become more cuboidal and more tightly packed, while the outer layers of the ODE are more squamous in shape. At the cervical loop, the ODE makes an abrupt, labial bend, becoming continuous with the inner dental epithelium (IDE). This IDE layer comprises tightly packed columnar cells, which run labially and meet the cuboidal shaped ameloblasts at the future site of the cemento-enamel junction. Pulpal to the IDE, there is a condensation of preodontoblasts, but no area of pulpal cell death is evident. The periodontal ligament is composed of a loose stellate cell arrangement with no visible fibrous matrix. Numerous, large vascular channels are evident. This section does not show deviation from the normal morphology as seen in Figure 1.1.a.

Figure 1.2.2.b shows that normal development is altered in the lingual half of the incisor. At approximately 900 μm from the medial CEJ, the presence of tall columnar

odontoblasts stops. A fine fibrous network with interposed elongated cells, radiates from the free end of the dentin. This fibrous arrangement courses lingually for approximately 270 μm, where it is replaced by a disrupted arrangement of small ovoid cells with no specific orientation. This feature is seen for approximately 200 μm, at which point it meets a double layered root sheath to close off the apical foramen. Pulpal to the lingual root sheath, a condensation of round to ovoid preodontoblasts with prominent nuclei are noted. On the lateral surface of the incisor, tall columnar odontoblasts producing dentin are present lingual to the CEJ for approximately 500 μm . At the edge of the lateral dentin, a radiating condensation of disrupted ovoid cells is present for approximately 120 μm. At its widest mediolateral dimension, this condensation measures 10 cell layers in thickness. These ovoid cells abut the previously mentioned lingual root sheath.

Figure 1.2.2.c demonstrates a point in incisor development where a disrupted area of small ovoid cells radiates lingually, for approximately 600 μm, from the free edge of the dentin. Associated with this disruption is a fine fibrous matrix. Pulpal to the disrupted area, mesenchymal cells with a typical stellate appearance are evident. At the lingual end of the incisor tall columnar odontoblasts separate the pulp from the PDL. On the lingual surface of this lingual cap, the root sheath has begun to break up. The dentin wall

forming the lateral surface of the incisor extends 720 μm from the lateral CEJ. A cellular disruption, 240 μm in length, with a fine fibrous matrix is seen bridging the gap between the free dentin margins of the lateral wall and the lingual dentin cap. This diruption is approximately 90-100 μm wide and contains many ovoid shaped cells. At its midpoint, the cells appear to meld with the adventitia of a pulpal vessel.

Figure 1.2.2.d illustrates a stage in development of the incisor where a dentin cap has formed on the lingual surface of the incisor, measuring 60 μm at its greatest labiolingual dimension. The medial side of the incisor demonstrates a highly organised fibrous "lesion" coursing between the medial dentin wall and the lingual dentin cap. The "lesion" measures 100 μm x 600 μm and comprises a fibrous matrix with flattened cells oriented parallel to one another between the fibre bundles. The fibres insert not only to the dentin edge but also along its lateral surface for approximately 80 μm. On the lateral side of the incisor, the "lesion" is shorter in length, (240 μm), but its mediolateral dimension is 180 μm. The cellular component of the lateral lesion primarily comprises ovoid cells. At the most lingual portion of the lingual cap, the fibre bundles of the PDL are arranged perpendicular to the dentin surface, with a clear distinction between these normal PDL fibre bundles and the fibres of the "lesion".

1.2.3 Three Weeks Post-adriamycin Administration

Figure 1.2.3.a is a cross section through the "U"-shaped part of the odontogenic organ. The pulp consists of a loose arrangement of stellate mesenchymal cells. As the outer enamel epithelium moves lingually to form the outer surface of the medial and lateral limbs of the odontogenic organ, the cells next to the IEE become more cuboidal and more tightly packed, while the outer layers of the OEE are more squamous in shape. At the cervical loop, the OEE makes an abrupt, labial bend, becoming continuous with the inner enamel epithelium (IEE). This IEE layer is composed of tightly packed columnar cells which run labially. This section shows no deviation from the normal morphology as seen in Figure 1.1.a.

Figure 1.2.3.b illustrates a point in development where the vertical arms of the "U" are replaced by the root sheath. This section is very similar to Figure 1.2.1.b, although, no area of pulpal cell death is visible. At the cervical loop area of the root sheath, there is a condensation of elongated cells on the future PDL side, and more ovoid cells pulpally. At this stage, the PDL is comprised of a loose arrangement of stellate mesenchymal cells.

Figure 1.2.3.c resembles the control Figure 1.1.c. Morphologically normal, well formed root sheaths are present

at the future sites of the medial and lateral walls of the incisor. Cellular condensations radiating from the edge of the root sheaths are approximately 100 μm in length and arch toward the apical foramen.

Figure 1.2.3.d is the most apical section in the 3 weeks post-adriamycin injected animal that shows a deviation from normal developmental morphology. 960 μm from the lateral CEJ, both the inner and outer layers of the root sheath are disrupted with a condensation of small ovoid cells 80 μm x 80 μm replacing the normal architecture of the root sheath. The condensation gives the impression that the root sheath has been constricted pulpally in this area. Lingual to the condensation, a double layered root sheath comprising cuboidal cells is seen. On the medial side, disruption of the root sheath is seen at 1200 μm lingual to the CEJ. This disruption is characterized by a condensation of small ovoid cells, 80 μm x 140 μm with the larger dimension being in the labiolingual direction. There also appears to be less disruption of the outer layer of the root sheath, with a loose layer of squamous cells transversing the disrupted area. An organised inner layer cannot be visualized.

Figure 1.2.3.e demonstrates a section where a disrupted layer of cells is seen coursing between the free margins of the dentin. Near the dentin margins, the cellular component of

the disruption comprises flattened cells. Approximately 200 μm from the dentin, the cells of the disruption are more ovoid and less organized.

Figure 1.2.3.f shows continuing dentinogenesis with the medial free edge of dentin being 100 μm thick while the lateral free edge is 80 μm thick. The "lesion" can be seen coursing from the medial to lateral dentin edges. The "lesion" is well organised with a width of approximately 15-20 μm. The cells have attained a fine spindle shape. All other features of the incisor remain normal.

2. DESCRIPTION OF RECONSTRUCTION

While this section briefly summarizes the previous section, the apico-incisal extent of the cellular disruptions and fibrous "lesion" are expressed quantitatively.

One Week Post-adriamycin Administration (1.2.1)

At approximately 100 μm from the apex, a pulpal cellular necrosis is found adjacent to the IEE layer of the medial and lateral limbs of the odontogenic organ. This area of cell death is present for approximately 460 μm from the apex, at which point it is not visible. At 1080 μm from the apex, there is a cellular disruption of the medial and lateral root sheaths. This disruption is present for approximately 720 μm,

to 1800 μm from the apex. 1500 μm from the apex, the disruption is associated with a fine fibrous matrix and is present incisally for 240 μm. At 1920 μm from the apex, a normal tooth morphology is noted.

Two Weeks Post-adriamycin Administration (1.2.2)

Unlike the one week post-adriamycin administration, the two week experimental animal does not demonstrate any pulpal cell death adjacent to the IEE or root sheath. At 920 μm from the apex, there is a disruption on the medial and lateral root sheaths. This disruption is present incisally for approximately 420 μm. At 1420 μm from the apex the cellular disruption attains an associated fibrous matrix. 1980 μm from the apex, a lingual cap of dentin is present with a medial and lateral ligamentous "lesion" bridging the gap between the lingual dentin cap and the sides of the incisor. The "lesion" extends incisally, 4080 μm from the apex.

Three Weeks Post-adriamycin Administration (1.2.3)

Unlike the one week post-adriamycin administration, the three week experimental animal does not demonstrate pulpal cell death adjacent to the IEE or root sheath. At 1320 μm from the apex, there is a disruption of the lingual most portion of

the root sheath. This is in contrast to the one week and two weeks post-adriamycin injected animals, which showed mesial and distal dentin breaks with a resultant lingual the root sheath remnant. 1740 μm from the apex, this lingual disruption has an associated fibrous component. 2100 μm from the apex, the "lesion" which bridges the open lingual dentinal gap demonstrates a highly structured organisation with large quantities of fibrous material as well as elongated fibroblasts running parallel to the fibre bundles. This appearance is present to approximately 5940 μm from the apex. Between 6000 and 6540 μm from the apex, multiple lingual accessory canals are evident.

Estimation of the Rate of Tooth Eruption (Figure 2)

This examination was based on a sample of two to estimate the rate of incisor eruption by calculating the relative distance a specific point has moved over a period of time. Between the one and two week post-adriamycin injected animals, the presence of lingual dentin breaks (accessory canals) was noted at 1920 μm and 4080 μm from the apex, respectively. This results in an eruption rate of approximately 2160 μm in one week, or approximately 308 μm/day. Between the two and three week post-adriamycin injected animals, the presence of lingual dentin breaks was noted at 4080 μm and 6540 μm from the apex,

respectively. This results in an incisor eruption of 2460 μm/week, or approximately 351 μm/day.

3. ELECTRON MICROSCOPY

This section is designed to explore the ultrastructural developmental morphology of the "lesion" found in experimental animals. Administration of adriamycin alters the structure of the experimental tooth, making direct comparisons between exact experimental and control sites impossible. When comparing cellular densities or the quantities of organelles present in a cell, descriptive terms such as high, low, many, and few are employed to represent a qualitative assessment, although no specific quantitation was performed.

3.1 Control

As shown in Figure 3.1.1, various electon micrographs were taken (Figures 3.1.1.a-d) to show the more detailed structures of the odontogenic organ and adjacent tissues. Figure 3.1.1 is a section through the "U" portion of the odontogenic organ, where the IEE and OEE forming the medial limb of the "U" are becoming an epithelial root sheath.

Figure 3.1.1.a is an electron micrograph of an area along the OEE. The OEE is composed of squamous shaped cells with

elongated nuclei. There exists a double layered membrane between the OEE cells and the PDL space. Collagen bundles, running perpendicular to the plane of section, are numerous along the OEE. Towards the alveolar bone, large intercellular spaces are noted.

Figure 3.1.1.b shows the cervical loop, with cuboidal cells with round nuclei forming the OEE. A double membrane is present surrounding the OEE and IEE. Collagen fibres are present, but are not organised into discrete bundles as seen in Figure 3.1.1.a, nor do they exhibit as regular an orientation pattern. Cells of the dental follicle are lateral to the cervical loop, and contain round to cuboidal shaped nuclei with intensely staining nucleoli, but few organelles.

Figure 3.1.1.c is lingual to Figure 3.1.1.b, and demonstrates a decrease in cellular density. The stellate cells of the dental follicle demonstrate ovoid to elongated nuclei depending on the plane of section. The cytoplasm contains abundant mitochondria, although the number of rough endoplasmic reticuli is low. Collagen fibre bundles are present, although their density is lower than that seen in Figure 3.1.1.b

Figure 3.1.1.d shows the cells at the lingual extent of the apical foramen demonstrate elongated nuclei. Cytoplasmic

inclusions are minimal. Collagen fibre bundles are located adjacent to the cytoplasmic membrane.

Figure 3.1.2 represents a light microscopy section through the incisor at a point in development where the apical foramen is open, and the vertical limbs of the "U" are formed by the root sheath. As shown in Figure 3.1.2, various electon micrographs were taken (Figures 3.1.2.a-d) to show the more detailed structures of the odontogenic organ and adjacent tissues.

Figure 3.1.2.a demonstrates the outer layer of the root sheath enclosed by a double layer membrane. As was seen in the younger control (Figure 3.1.1.a), collagen fibre bundles are seen near the root sheath, oriented perpendicular to the plane of section. Laterally, elongated follicular cells with ovoid nuclei are evident, and the cytoplasm contains lysosomes and RER. While the cells are tightly packed near the root sheath, greater intercellular spaces are noted laterally.

Figure 3.1.2.b illustrates the cellular organization at the cervical loop of the epithelial root sheath. At cervical loop, the cells of the inner and outer layer are columnar with elongated nuclei. A double layered membrane surrounds the root sheath. Lateral to the cervical loop, the inner layer of follicular cells contain elongated nuclei and polarized

organelles. Towards the pulp, the cells contain nuclei which are round or ovoid. Medially, there is a zone of low cellular density that appears to form a natural separation between the dental papilla and dental follicle. The dental papilla cells associated with the pulp exhibit a stellate appearance with associated collagen fibre bundles. These cells have not yet come into approximation with the inner layer of the root sheath.

Figure 3.1.2.c shows the follicle cells in this region have attained a definite orientation, running from labial to lingual. The nuclei vary in shape from ovoid to squamous. While lysosomes are present, the number of cytoplasmic inclusions, (RER and mitochondria) are low. Collagen fibre bundles are seen coursing between the cells, perpendicular to the plane of section.

Figure 3.1.2.d shows the pulp comprising stellate cells with round to ovoid nuclei. Collagen fibre bundles associated with the pulp cells are coarse, and large intercellular spaces are present.

3.2 Experimental

The experimental subjects were sacrificed three weeks post-adriamycin administration. Figure 3.2.1 represents a

young "lesion", which has not yet totally enclosed the lingual portion of the incisor ie. the medial and lateral halves have not yet approximated. As shown in Figure 3.2.1, various electon micrographs were taken (Figures 3.2.1.a-d) to show the more detailed structures of the young "lesion" and adjacent tissues.

Figure 3.2.1.a represents an area of normal PDL labial to the "lesion" area. Near the dentin surface, flattened fibroblasts with elongated nuclei are noted. The polarized cytoplasm contains a large quantity of organelles, particularly RER and mitochondria. Collagen fibre bundles are seen running between tightly packed fibroblasts, perpendicular to the plane of section.

Figure 3.2.1.b shows the PDL side of the partially formed "root" dentin. The odontoblast processes wrap around the free edge and are seen between the PDL and dentin. Collagen fibre bundles are present next to the odontoblast and separate the odontoblast processes from adjacent fibroblasts with elongated nuclei.

Figure 3.2.1.c represents an area lingual to figure 3.2.1.b. Medially stellate shaped pulp cells with round to ovoid nuclei are present. A low cell density is noted in the pulp with a fine, non-bundled collagenous matrix present

between the pulp cells. Lateral to the pulp, intensely stained spindle shaped fibroblasts with elongated nuclei exist. The predominant cellular inclusions are RER and mitochondria.

Figure 3.2.1.d is representative of the region where the lateral and medial halves of the "lesion" have not yet met. The nuclei of the cells are ovoid in shape and less intensely stained than the fibroblasts in the "lesion". The collagen fibre bundles demonstrate a delicate, fine appearance. RER and mitochondria still form the major part of the cytoplasmic organelles.

3.2.2 represents a fully formed, mature lesion enclosing the lingual half of the incisor. As shown in Figure 3.2.1, various electon micrographs were taken (Figures 3.2.1.a-d) to show the more detailed structures of the young "lesion" and adjacent tissues. Since the general structure of the mature "lesion" was constant, a lower power (x 1360) series is used to illustrate the differences between the "lesion" and adjacent tissues.

Figure 3.2.2.a is located at the edge of the free dentin margin on the medial side of the incisor. Fibroblasts with elongated nuclei lie parallel to the dentin surface. These cells, which contain large amounts of RER, are polarized with the organelles toward the lingual end of the incisor. Moving

toward the alveolar bone, the cell density decreases, with more intercellular collagen bundles present.

Figure 3.2.2.b shows the pulp is composed of stellate shaped cells with large, round to ovoid nuclei and large intercellular spaces. The "lesion" is seen next to the pulp, and comprises tightly packed, intensely staining spindle shaped cells, 6-8 cells in thickness. The cytoplasm of these cells contain relatively few organelles. Lingual to the intensely staining layer, fibroblasts with plump, ovoid nuclei are present. These cells contain a high quantity of organelles similar to the fibroblasts in Figure 3.2.1.a.

Figure 3.2.2.c is similar to Figure 3.2.2.b, except that the intensely staining layer has thinned to 3-4 cells in thickness.

Figure 3.2.2.d shows the intensely staining layer of 1-2 cells of the "lesion" next to the pulp. Lingual to this region, there are fibroblasts with elongate nuclei and abundant organelles.

4. RADIOAUTOGRAPHY

This section describes the incorporation of tritiated thymidine (^{3}H-Tdr) at various locations of the tooth and peridontium in the control and experimental animals. All animals were sacrificed 6 hours post-^{3}H-Tdr. Experimental animals were injected with ^{3}H-Tdr at either i) 2 weeks post-adriamycin administration, or ii) 3 weeks post-adriamycin administration. While ^{3}H-Tdr was incorporated throughout the tooth, only selective areas were actually quantified and compared. In the experimental group these included i) lingual periodontal ligament, ii) midroot periodontal ligament, iii) disruption or fibrous "lesion" [depending on the stage of maturation], iv) pulpal tissue near the disruption or "lesion", v) pulpal tissue away from the disruption or "lesion". At 1320 μm from the apex, the most apical region studied autoradiographically, the tooth consisted of a root sheath and open foramen. As a result, only two areas were quantified i) pulp near the root sheath, and ii) midroot area.

The administration of adriamycin alters the structure of the experimental tooth, restricting direct comparisons between experimental and control sites. As a result the control quantitation includes an area termed "approximate lesion PDL", an area of the PDL in the same labial-lingual position of the incisor as the adriamycin-induced root defect of the experimental rat. The areas studied in the control include i)

lingual PDL, ii) "approximate lesion PDL", iii) pulp, iv) midroot PDL.

The following section will briefly describe the incorporation pattern of ^{3}H-Tdr in the control and experimental animals as well as significant findings. Counts of labelled cells were made within a 40 μm x 200 μm grid at x 400 magnification. Comparisons were done using Duncan's multiple range test and significance was based at the $p < 0.01$ level.

4.1 **Control** (Graph 1)

At 1320 μm from the apex, the pulp exhibited a significantly higher incorporation than did the midroot PDL (16.4 labelled cells/800 μm^2, 3.4 labelled cells/800 μm^2 respectively). As the distance from the apical end increased, the incorporation of ^{3}H-Tdr decreased in the pulp and midroot PDL.

At 2160 μm from the apical end, the highest incorporation was seen in the lingual PDL (15.2 labelled cells/800 μm^2) followed by the "approximate lesion PDL" with 8.3 labelled cells/800 μm^2. As with the pulp and midroot counts, the incorporation of ^{3}H-Tdr decreased in the "approximate lesion area" and lingual PDL with increasing distance from the apex.

4.2 Experimental

4.2.1 Two weeks post-adriamycin administration (Graph 2)

At 1320 μm from the apex, the pulp near the "lesion" demonstrated a significantly higher number of labelled cells than did the midroot PDL (22.8 labelled cells/800 μm^2 versus 6.5 labelled cells/800 μm^2). Between 1960 μm and 2160 μm from the apex, the pulp associated with the "lesion" had a higher incorporation of ^{3}H-Tdr than the pulp not associated with the "lesion". The pulp not associated with the "lesion" was located at a similar labio-lingual position as the pulp associated with the "lesion". While the lingual PDL and "pulp associated with the lesion" had a significantly higher incorporation than the "lesion" between 1960 and 2060 μm from the apex, all three areas had a comparable ^{3}H-Tdr incorporation at 2160 μm from the apex. At 3300 μm from the apex, the incorporation of ^{3}H-Tdr was higher in the "lesion" than in any other area (6.1 labelled cells/800 μm^2).

4.2.2 Three weeks post-adriamycin Administration (Graph 3)

At 1320 μm from the apex, the pulp near the "lesion" demonstrated a significantly higher number of labelled cells than did the midroot PDL (24.1 labelled cells/800 μm^2versus

15.1 labelled cells/800 μm^2). This midroot area had a significantly higher incorporation than did the comparable midroot PDL of a control or two week post-adriamycin administration experimental animal.

Between 2680 and 2880 μm from the apex, the midroot PDL demonstrated a significantly higher 3H-Tdr incorporation than any other area at this location (4.3 and 6.3 labelled cells/800 μm^2 respectively). The other areas had incorporation rates no higher than 2.1 labelled cells/800 μm^2.

At 3850 μm (see Figures 4.3.a, 4.3.b, and 4.3.c) from the apex, the "lesion" showed the highest 3H-Tdr incorporation of the areas quantitated at this apico-incisal position. The same situation was seen at 4200 μm.

Comparing similar areas between the control and the two experimental groups, the pulp associated with the disrupted root sheath showed a significantly higher rate of ^{3}H-Tdr incorporation in the experimental groups than in the control (Graph 4, Figures 4.1.a, 4.1.b, 4.1.c). This difference was only present to 2160 μm from the apex, after which point the incorporation in the three groups was similar.

In the apical end of the incisors, the ^{3}H-Tdr incorporation in the "lesion" of the experimental groups was significantly lower than in the control (Graph 5). However, the two and three week adriamycin treated groups showed a higher ^{3}H-Tdr incorporation than the control at areas incisal to 3300 μm from the apex (See Figure 4.2.a, 4.2.b, 4.2.c).

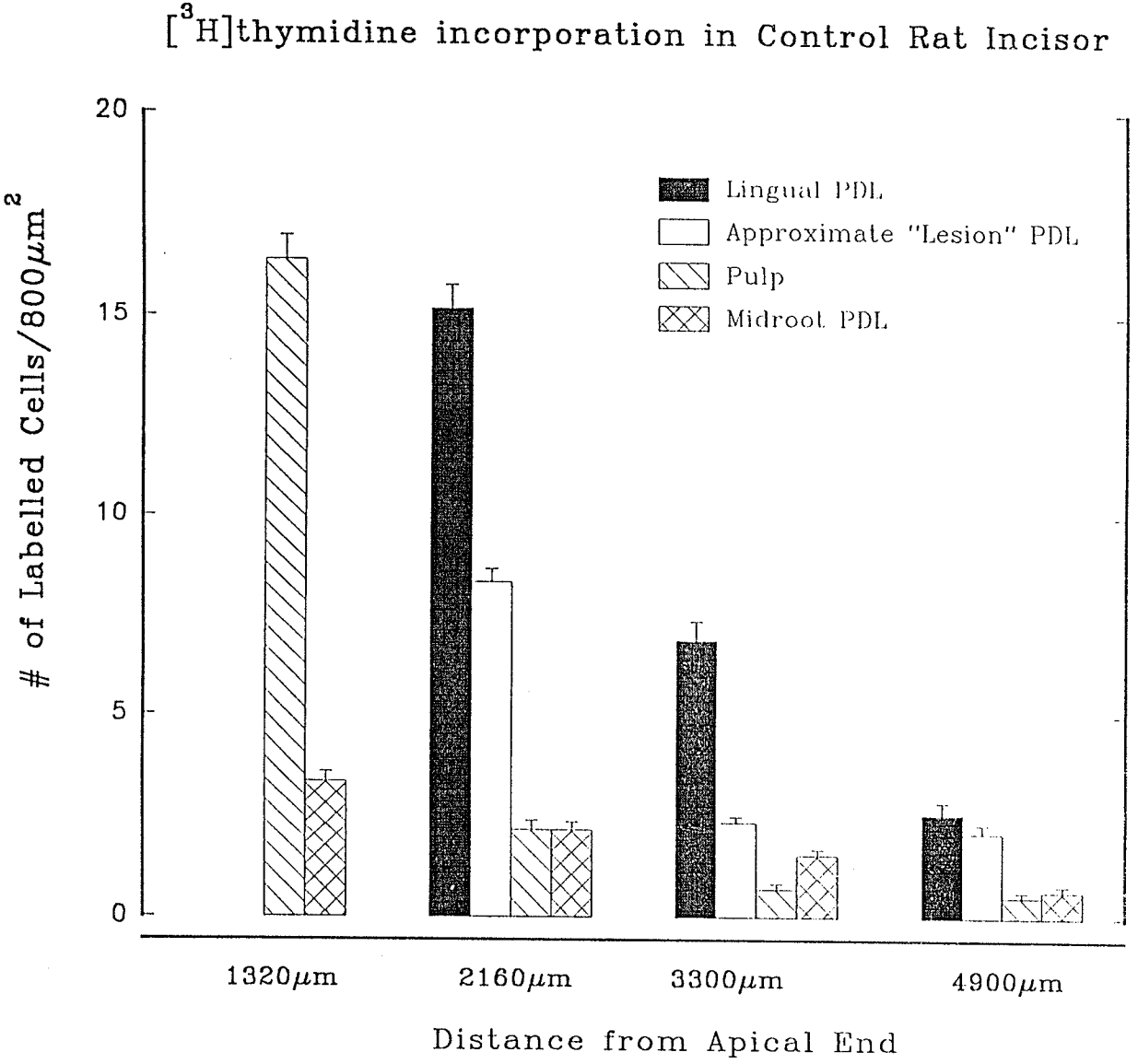
[3H]thymidine incorporation in Control Rat Incisor
# of Labelled Cells/800μm2
20
15
10
5
0
Lingual PDL
Approximate "Lesion" PDL
Pulp
Midroot PDL
1320μm
2160μm
3300μm
4900μm
Distance from Apical End

Graph 1

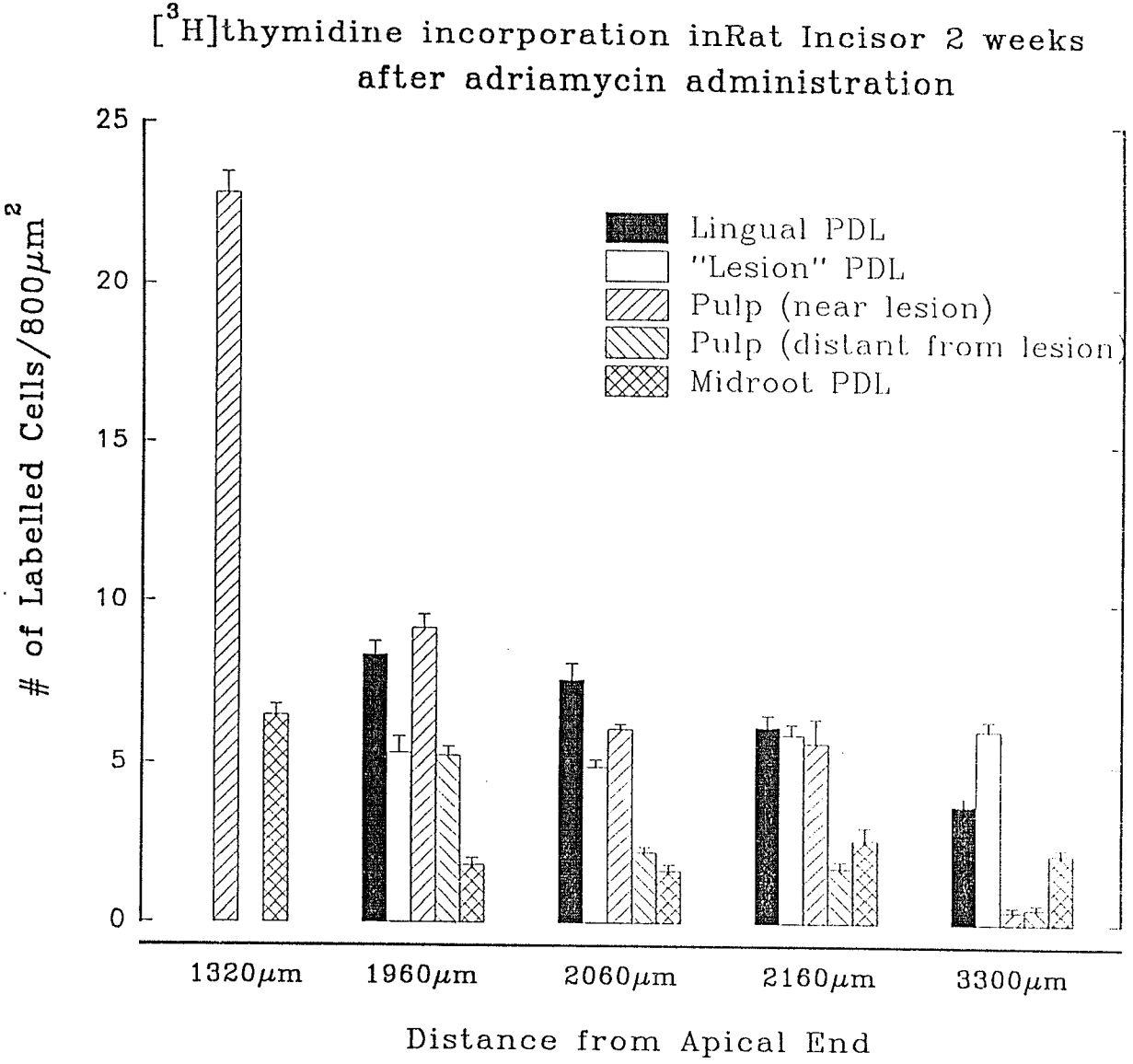
[3H]thymidine incorporation inRat Incisor 2 weeks after adriamycin administration
# of Labelled Cells/800μm2
25
20
15
10
5
0
Lingual PDL
"Lesion" PDL
Pulp (near lesion)
Pulp (distant from lesion)
Midroot PDL
1320μm
1960μm
2060μm
2160μm
3300μm
Distance from Apical End

Graph 2

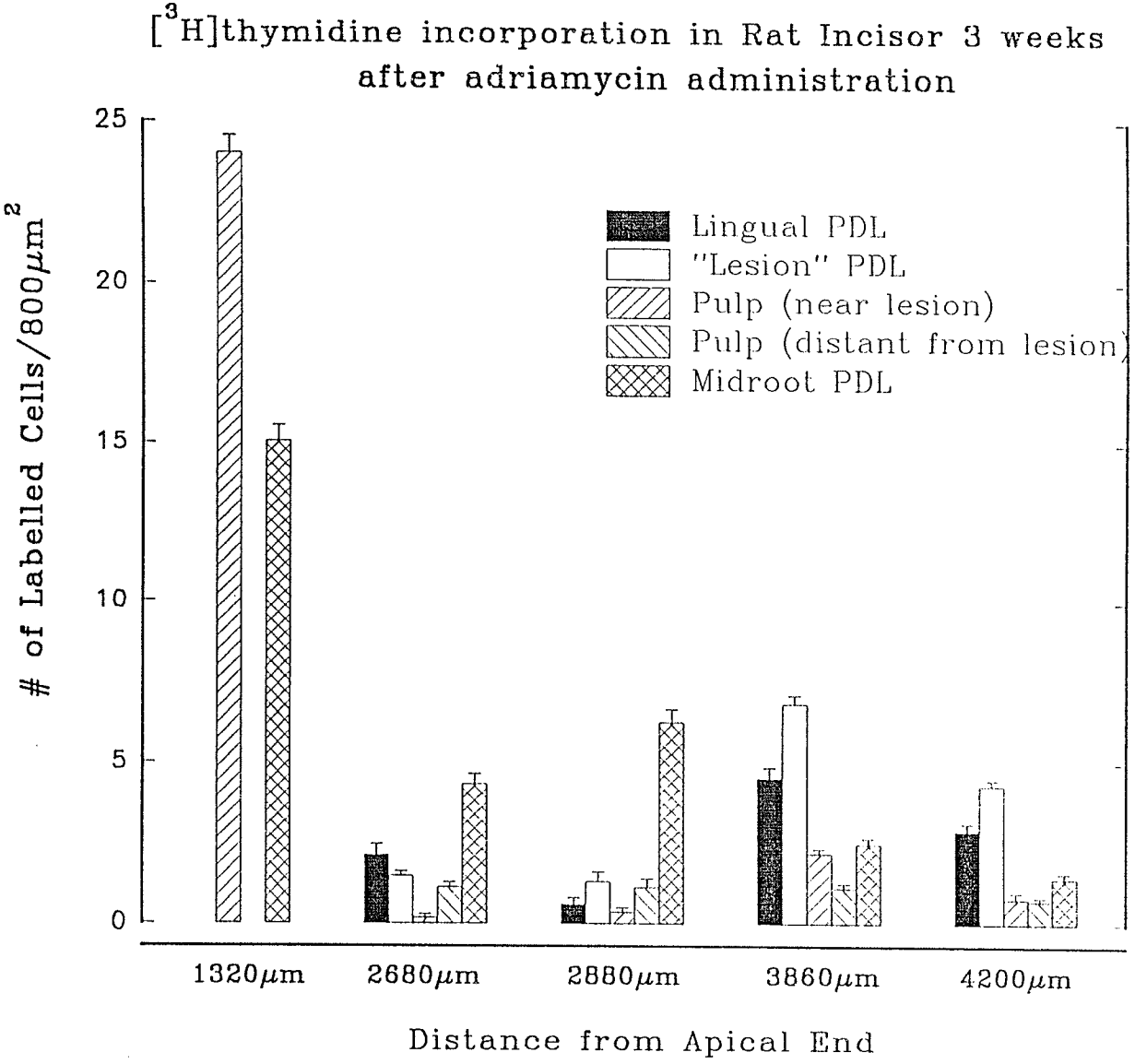
[3H]thymidine incorporation in Rat Incisor 3 weeks after adriamycin administration
# of Labelled Cells/800μm2
25
20
15
10
5
0
Lingual PDL
"Lesion" PDL
Pulp (near lesion)
Pulp (distant from lesion)
Midroot PDL
1320μm
2680μm
2880μm
3860μm
4200μm
Distance from Apical End

Graph 3

Incorporation of [^{3}H]thymidine into Pulp Cells associated with the "Lesion"

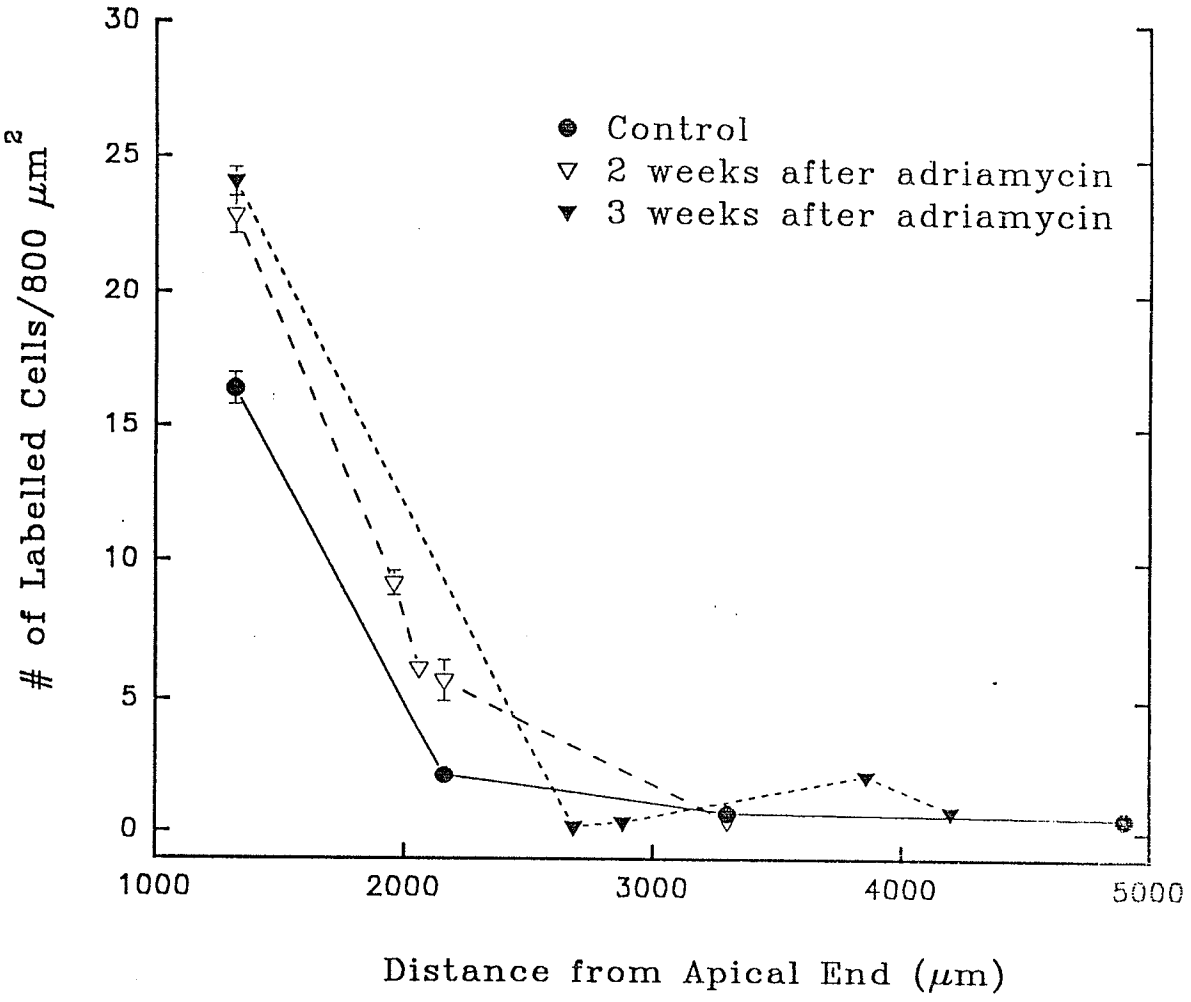

Graph 4

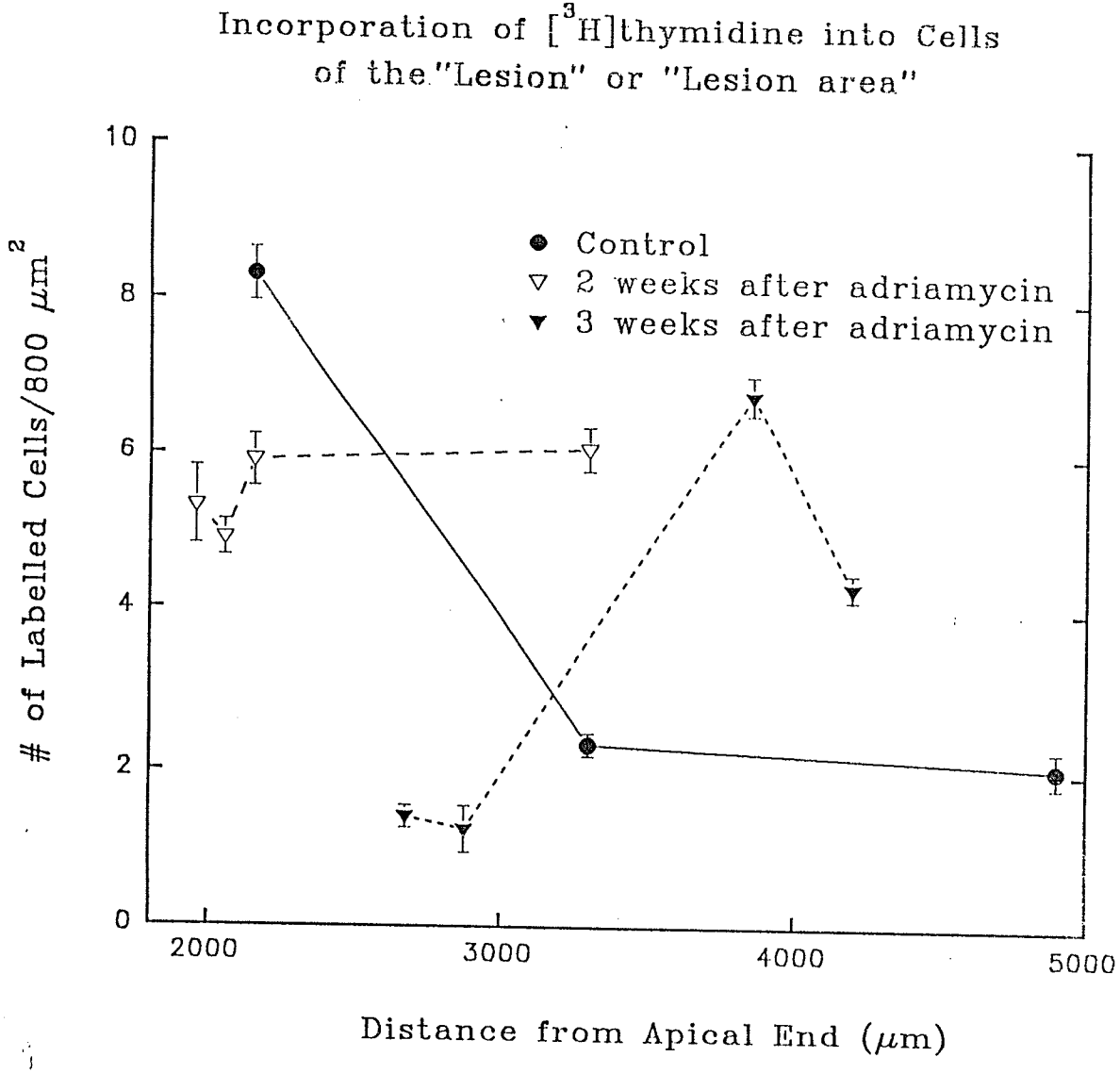
Incorporation of [3H]thymidine into Cells
of the "Lesion" or "Lesion area"
# of Labelled Cells/800 μm2
Control
2 weeks after adriamycin
3 weeks after adriamycin
0
2
4
6
8
10
2000
3000
4000
5000
Distance from Apical End (μm)

Graph 5

DISCUSSION

The primary finding of this investigation was that adriamycin induced changes in the odontogenic organ of the rat incisor. Such changes were noted one week following adriamycin administration, so the primary focus of the Discussion is devoted to the probable inherent cellular mechanisms. Unfortunately, the morphologic nature of this study prohibits testing of the suggested cellular and metabolic pathways involved. Consequently, the Discussion is necessarily limited pending more detailed investigation of the common underlying process - apoptosis. Although other adriamycin-induced features of the "lesion" are discussed, the primary change induced by this agent appears to be apoptosis: a physiologic mechanism that is only now the subject of intense investigation thoughout the world.

Adriamycin-induced apoptosis

One week following the administration of adriamycin, a series of changes in the cellular morphology of the incisor were observed in this study. For instance, in the "U" shaped portion of the odontogenic organ (Smith and Warshawsky, 1975a), next to the IDE, there was cell death in the dental papilla [Figure 1.2.1.a]. A similar zone of cell death was

also evident more incisally, next to the HERS [Figure 1.2.1.b]. Edematous zones in the apical end of the rat incisor have been previously noted following a number of insults, including irradiation (Hansen and English, 1957; Adkins, 1967; Medak *et al.*, 1952), vincristine (Stene, 1978), cyclophosphamide (Koppang, 1973a; Adatia, 1975), actinomycin D (Dahl *et al.*, 1981; Moule *et al.*, 1993) and adriamycin (Dahl, 1984; Karim, 1985a; Karim and Pylypas, 1985). In the majority of these studies, cell death associated with the edema was termed necrosis, although such terminology may be incorrect.

By definition, necrosis includes those events "that accompany and follow irreversible cell injury in living organisms" (Buga *et al.*, 1993). For instance, following severe injuries from ischemia, hypoxia, trauma, infection, and chemical toxins, coagulation necrosis results from cellular protein coagulation and denaturation (Farber, 1982). These proteins may be further degraded by hydrolytic enzymes derived from such sources as polymorphonuclear leukocytes or neutrophils, resulting in colliquative necrosis, as in liquification of protein-poor cerebral tissue. The characteristic histologic changes associated with coagulation necrosis include karyorrhexis, karyolysis, cytoplasmic hypereosinophilia and nuclear pyknosis, preservation of cell outlines, and cell swelling (Serle *et al.*, 1982; Trump *et al.*, 1973; Farber, 1982). In the late stages of necrosis, cellular

fragmentation resulting from autolysis and heterolysis due to inflammatory cells generally follow cell death. Progressive membrane damage is a key event in the pathogenesis of necrosis (Buja *et al.*, 1993). The pathophysiology of this damage involves: i) alterations in ionic transport systems, ii) increases in membrane permeability, and finally iii) physical membrane disruption. Conceivably, loss of membrane integrity (membrane disruption) may result from i) membrane phospholipid degradation (Chien *et al.*, 1984), ii) amphipathic lipid production (Buja, 1991), iii) cytoskeleton damage (Steenbergen *et al.*, 1987), and iv) generation of oxygen free radicals (Burton *et al.*, 1990).

Karim (1985a), however did not observe inflammatory activity associated with adriamycin-induced cell death in the dental papilla. The term "liquification necrosis" has been used to describe mesenchymal cell death following adriamycin administration (Dahl, 1984), although Moule *et al.* (1993) discounted this description as polymorphonuclear leukocytes were not present in the affected tissue. Moule *et al.* (1993) have indicated that the mechanism of cell death is apoptosis rather than necrosis.

Pathophysiology of apoptosis

Apoptosis, derived from the Greek word describing falling leaves or petals, is defined as multifocal single-cell death exhibiting a distinct set of morphological characteristics (Kerr *et al.*, 1972). While the terms apoptosis and "programmed cell death" are often used interchangeably, this usage is incorrect (Martin et al, 1994). Programmed cell death describes specific cell death that is a normal part of a multicellular organism's life cycle, while apoptosis is a descriptive term of a cell's response to a variety of environmental changes. These changes may be induced by various factors including cytotoxic drugs, physical stimuli, and certain pathological conditions including viral hepatitis and graft versus host disease (Eigenbrodt *et al.*, 1990; Gerschenson and Rotello, 1992).

Nuclear and cytoplasmic condensation (shrinkage) of single cells is the first morphologic sign of apoptosis. The changes in cell shape are most probably due to reorganization of the cell's cytoskeleton (Martin and Cotter, 1990; Cotter *et al.*, 1992). This is followed by nuclear membrane loss, nuclear chromatin fragmentation, and subsequent "formation of multiple fragments of condensed nuclear material and cytoplasm" (Buja *et al.*, 1993). These apoptotic bodies are engulfed by nearby cells, while inflammatory responses comprising leukocyte infiltrates are rarely present.

Perturbation of nuclear chromatin appears to be the mode of pathogenesis in apoptotic cell death (Gerschenson and Rotello, 1992). Such changes appear to be initiated by activation or synthesis of endonucleases. These cleave DNA at linker regions between nucleosomes, resulting in 180-200 base pair multiple fragments (Arends *et al.*, 1990). This cleavage is more ordered and less extensive than in other forms of cell death.

Control mechanisms for apoptosis

Apoptosis appears to be controlled by gene products. The *c-myc* gene, important in promoting cell proliferation, has been implicated in apoptosis in some cell types depending on the abundance of certain growth factors in the media (Evan *et al.*, 1992; Shi *et al.*, 1992). A gene involved with DNA repair, (p53), may induce apoptosis in cells which are unrepairable, thereby serving to prevent subsequent malignant transformations.

Other mechanisms may also be involved. For instance, Ca^{++} ions appear to play an important role in cellular signalling. Prior to observable structural changes associated with apoptotic cell death, intracellular free Ca^{++} appears to be greatly increased (Arends *et al.*, 1990). In addition, apoptosis is diminished or delayed in areas of low extracellular Ca^{++}. Such intracellular Ca^{++} influxes may

activate transglutamase or the endonuclease responsible for internucleosomal cleavage, both of which are Ca++ dependent (Fesus *et al.*, 1991). Ca^{++} may also play a role in the changes in shape and size of cells undergoing apoptosis.

At this time, a specific biomarker for apoptosis is unavailable. Visualization of specific cell changes, followed by cell death, in the absence of inflammation is currently the only marker to identify apoptosis. Such a deficiency hampered the interpretation of changes into the effects of adriamycin on the developing rat incisor at a minimum of one-week following its administration. For instance, only zones of previous apoptosis were visible, with the elimination of dead cells having already taken place. However, the zone of cell death closely resembles those illustrated by Moule *et al.* (1993), who have indicated that papillary cell death following actinomycin-D is the result of apoptosis. Karim (1985a) was also unable to observe inflammatory changes associated with adriamycin-induced cell death of the dental papilla. This author is convinced that the adriamycin changes observed in this study resulted from apoptosis rather than necrosis.

Anthracyclines have been shown to induce apoptosis-associated DNA fragmentation and apoptosis-related cell shrinkage (Skladanowski and Konopa, 1993). The underlying mechanisms remain obscure at this time, although the incubation of HeLa S_3 with adriamycin leads to the suppression of cell proliferation due to induction of G_2 block followed by

cell death by apoptosis.

The degree of cellular differentiation primarily determines a cell's sensitivity to exogenous agents. In this study, once the odontoblasts were committed to dentin matrix production, they appear to be resistant to the effects of the drug. By contrast, more immature cells (preodontoblasts), involved in cell to cell interactions and other activities requiring the synthesis of a variety of RNA's, appeared to be more sensitive to adriamycin. Triatiated glycine studies have also shown that odontoblasts are most sensitive to cyclophosphamide just prior to predentin secretion (Koppang, 1973b), before the commencement of collagen synthesis. Interestingly, an area of cell death associated with the dental papilla was not seen in experimental animals sacrificed at two or three weeks following adriamycin administration. This indicates that the cells were replaced either through migration or proliferation; a subject to be more thoroughly examined in the Radioautography Section of the Discussion. Of interest, is the fact that cells in the bulbous portion of the odontogenic organ (Smith and Warshawsky, 1975a) were insensitive to the effects of adriamycin. Such stem cell resistance may result from their lack of differentiation, position in the cell cycle, or the fact that the nuclear repair may be occurring subsequent to adriamycin-induced damage. In addition, Zn^{++} has been shown to block the process of apoptosis (Giannakis *et al.*, 1991), and the Bcl-2 protein

to repress the process (Korsmeyer, 1992). Such metabolic determinants underscore the need for further investigation of this important histological process.

The major response to adriamycin, seen in the one-, two-, and three week post-injection experimental animals was a disruption of Hertwig's Epithelial Root Sheath (HERS). This initially manifested as a loss of intercellular membrane contacts followed by loss of the normal cuboidal shape of the inner layer with the cells becoming rounded and shrunken in size (Figures 1.2.1.c, 1.2.3.b, 1.2.3.d-e). During this process, no inflammatory changes were evident, suggesting the possible role of apoptosis in the disruption of the HERS. Although, the membrane damage suggests that necrosis may be involved, since progressive membrane damage is central to the pathogenesis of necrosis (Buja *et al.*, 1993). However, membrane damage may also be an important step in apoptosis. Anthracyclines cause an increase in plasma membrane fluidity (Sugiyama *et al.*, 1986; Deliconstantinos *et al.*, 1987; Oth *et al.*, 1987; Lameh *et al.*, 1989). These fluidity changes may lead to an increased turnover of phosphatidylinositol resulting in the production of diacylglycerol. Such diacylglycerol accumulation may then act as an intracellular activator of protein kinase C (Posada *et al.*, 1989a; 1989b). This enzyme phosphorylates a number of substrates including topoisomerase II (Sayhoun *et al.*, 1986). As mentioned

previously, topoisomerase II promotes DNA strand cleavage and resealing. Adriamycin, through intercalation, can then alter the DNA conformation such that topoisomerase-II action is stopped at the cleavage stage (Tewey *et al.*, 1984) resulting in DNA damage and subsequent cell death. This model offers a possible explanation for the mode of cell death associated with adriamycin, utilizing both the membrane and nuclear effects. Further research is however needed to delineate the details of this pathway.

Osteodentin formation

While it was not the purpose of this study to investigate the formation of osteodentin following adriamycin administration, its ubiquitous presence was noted in all the experimental teeth (Figure 1.2.1.e). This osteodentin was located incisal to the disrupted HERS and had a globular appearance similar to that noted in other studies (Karim and Eddy, 1984; Karim, 1990). The osteodentin layer had an irregular pattern of deposition (Figure 1.2.3.e) with odontoblasts being trapped on the PDL side of the osteodentin. The presence of trapped cells was a feature also noted by Mikkelsen (1978), using vinblastine. The initiation of osteodentin is not, however, a feature unique to adriamycin.

Vinblastine (Moe, 1977), vincristine (Stene and Koppang, 1976; Stene, 1979), colchicine (Noguiera *et al.*, 1980), and cyclophosphamide (Koppang, 1973a) produce similar effects. It appears that adriamycin has a reversible effect on the function of secretory odontoblasts, resulting in osteodentin deposition (Karim, 1990).

Induction of root dentinogenesis by ERS has long been accepted (Sharawy and Bhussry, 1986), however, direct experimental evidence to support this theory has only recently been provided (Thomas and Kollar, 1989). Using recombinants of isolated ERS and dental papilla, these investigators induced odontoblast differentiation within cells of the dental papilla with subsequent formation of dentin. These findings were supported by the the current study, which showed that dentinogenesis did not occur in areas of previous root sheath disruption (Figures 1.2.1.d, 1.2.2.d, 1.2.3.f).

The adriamycin-induced "fibrous" lesion

While dentinogenesis was not induced in specific areas of the incisor following adriamycin administration, a fibrous "lesion" bridging the dentin free area was always noted. This "lesion" appeared one week following adriamycin administration, (Figure 1.2.1.d), and comprised a distinct layer of flattened cells, 3-4 cells thick, adjacent to the

pulp. The cells were associated with a fine collagen matrix, but its extent was limited at this stage in development. Two weeks following adriamycin administration, a definite "lesion", with an associated fibrous matrix was noted (Figures 1.2.2.c-d); a similar "lesion" was also seen three weeks following adriamycin administration (Figures 1.2.3.e-f).

Ultrastructural (electron microscopy) comparisons (Figures 3.1.1, 3.1.2, 3.2.1, 3.2.2), between developing control PDL and the adriamycin-induced "lesion" showed relatively few differences. Normal PDL development followed a pattern of cellular differention from ovoid to flattened cells with an increasing organization of collagen into discrete fibre bundles. It appears that even in areas of low cellularity, where cellular proliferation and differentiation have yet to be actively initiated (Figures 3.1.1.d and 3.1.2.d), a definite collagen framework was present which may have acted as a developmental guide. Such a theory has been proposed by a number of investigators in other parts of the body (Bailey *et al.*, 1975; Gay *et al.*, 1978; Konomi *et al.*, 1989). The cells of the "lesion" also demonstrated a pattern of cellular differentiation from ovoid to flattened cells. While the cells of the control showed few cytoplasmic organelles, the cells of the "lesion" demonstrated prominent cellular inclusions (Figures 3.2.1.c-d). However, the effects of adriamycin complicates any comparison between experimental and control animals. The electron photomicrographs of the

control were based on more immature areas than the experimental. The fibroblasts seen in the "lesion" may therefore be at a more advanced stage in development, where collagen secretion is progressing at a heightened level, necessitating a high organelle to cytoplasmic ratio.

The fully formed fibrous "lesion" demonstrated an interesting fibroblastic feature. The "lesion" fibroblasts adjacent to the pulp were intensely hyperchromatic (Figure 3.2.2.b-d). A similar cellular appearance was seen in recombination experiments (MacNeil and Thomas, 1993). Using immunohistochemical staining, these investigators showed intensely staining cells to occupy an area where epithelial root sheath cells would normally be found, but, at the ultrastructural level, the cells were more fibroblastic than epithelial in nature. While epithelial-mesenchymal transformation occurs in other developmental systems (Greenburg and Hay, 1982; Nichols DH, 1981), MacNeil and Thomas (1993) have postulated that the hyperchromatic cells may represent root sheath epithelium which has undergone phenotypic alteration. Further investigation is therefore necessary before the source or function of these cells is made.

The component fibroblasts of the mature "lesion" demonstrated polarized cellular organelles. This is a feature generally associated with migrating cells (Garant and Cho, 1979). The question could therefore be raised as to the origin

of the fibroblasts of the "lesion". Conceivably the "lesion" was formed through normal differentiation and proliferation of dental follicle. Alternatively, cellular migration may be involved. While fibroblast migration occurs following wounding (Gould *et al.*, 1977), fibroblast migration is a "normal" physiological condition. (McCulloch and Melcher, 1983b; 1983c). The radioautography portion of the current study has also shown that ^{3}H-Tdr was incorporated into the fibroblasts of the developing "lesion". From the electron microscopy and radioautography experiments of this study, the "lesion" appears to be normally developed periodontal ligament, whereas the altered orientation appears to be due to the fact that a continuous layer of dentin was not present.

Recombination experiments (Palmer and Lumsden, 1987) have demonstrated the formation of PDL and bone following recombination of the enamel organ and follicle. However, MacNeil and Thomas (1993) showed that PDL formation could only be initiated following recombination involving root dentin basement membrane, dental follicle, and epithelial root sheath. If root dentin basement membrane was absent the process of PDL genesis was halted. The general concensus holds that the dentin portion is necessary for PDL formation, a feature not found in the current study. It is possible that the root dentin basement membrane is not directly required for differentiation of dental follicle cells, but rather for HERS degeneration. If this is the case, adriamycin may play the

same role as the root dentin basement membrane, that is to signal its demise. Once the signal for disruption has been provided, the ERS could mediate inductive changes in neighboring undifferentiation cells through i) changes of its basement membrane or ii) alteration of the extracellular matrix (Merilees and Scott, 1980) through the release of proteins similar to enamalin or amelogenin (Slavkin *et al.*, 1989), or growth factors such as transforming growth factor-β_1 (Wise *et al.*, 1992). The presence of TGF-β_1 in dental tissues during their development adds further credibility to this theory of follicular differentiation (D'Souza *et al.*, 1990; Wise and Fan, 1991).

^{3}H-Thymidine incorporation

An autoradiographic technique, using ^{3}H-Tdr, was used to study the DNA synthetic activity of fibroblasts. The highest incorporation in the control incisor was evident in the apical end, (Graph 1), a finding which has been supported by other investigators (Chiba *et al.*, 1967; Zajicek, 1974; Beertsen, 1975; Michaeli *et al.*, 1979). This incorporation into the cells diminishes dramatically at about 5 mm from the apical end (Michaeli *et al.*, 1987; 1988). The tissues associated with the lingual portion of a given incisor section had a greater incorporation than tissues on the labial. This finding is expected as the lingual tissues are more immature than the

labial tissues, and would be undergoing mitosis during formation.

Two weeks following the administration of adriamycin (Graph 2), a pattern similar to that seen in the control is present; a higher incorporation of ^{3}H-Tdr is present in the apical tissues as compared to those more incisally. However, this pattern is not seen in the "lesion". The incorporation of radioisotope in the "lesion" is relatively constant between 1960 μm and 3300 μm. A possible explanation for the fact that the incorporation does not decrease with increasing distance from the apex may be found in previous cell kinetic work (Roberts and Jee, 1974; Gould *et al.*, 1977; 1980). Following perturbation of the periodontal system, these investigators found a increase in fibroblast proliferation. It is therefore possible that the absence of dentin is recognized by the body as an insult with subsequent proliferation of fibroblasts to maintain a protective or reparative barrier.

Three weeks following the administration of adriamycin, a very different pattern of ^{3}H-Tdr incorporation was noted (Graph 3). While incorporation was noteable at 1320 μm from the apex, this was dramatically reduced between 2680 - 2880 μm, with only midroot PDL showing any significant labelling. At present, no definite explanation for this phenomenon is available. It is possible that some local factor may have caused a decrease proliferation of cells in this area, and due to the low number of experimental incisors sampled (6), the

results were skewed.

However, at 3850 μm from the apex, the incorporation of ^{3}H-Tdr into the "lesion" was significantly higher ($p < 0.01$, Duncan's multiple range test) than any other area tested at that distance from the apex. This same finding is seen 3300 μm from the apex in the two week post-adriamycin administered animal and at 4200 μm in the three week post-adriamycin administered animal. It appears that the proliferative component of the "lesion" is further incisal in the 3 week experimental animal, than in the 2 week experimental animal (Graph 5). This fact can be explained by the fact that the incisor is continually erupting. As a result, the "lesion" has moved incisally, carrying its proliferative component incisally as well.

As mentioned previously, adriamycin induces apoptosis of the dental papilla. One week following the administration of adriamycin, this apoptosis is visualized as a zone of edema next to the HERS. However, this disturbance within the dental papilla is not present in the two and three week post-adriamycin administered animals. Repopulation of this area would require an increase in cell proliferation and such a scenerio is seen (Graph 4). The incorporation of ^{3}H-Tdr into the pulp associated with the "lesion" was significantly higher ($p < 0.01$) than in the pulp of the control incisor.

Reconstruction

The three dimensional reconstruction proved valuable in assessing the extent of the dentin defect and "lesion". Of particular interest was the fact that two basic dentin defects could be elucidated. The first variation was seen in the one and two week post-adriamycin administered animals (Figure 2). In these animals, mesial and distal dentin defects were noted, with an intervening lingual portion of dentin. The second variation was seen in the three week post-adriamycin administered animal. In this situation, the dentin defect encompassed the entire lingual surface of the incisor. While all animals were given the drug via a similar route, the only explanation for this variability lies in anatomic differences related to the delivery of the adriamycin to the affected tissues. The arterial system of the mandibular rat incisor has been shown to have two basic variations (Kindlova and Metena, 1959). In some animals, the mandibular artery courses through the mandibular canal and supplies the apical portion of the incisor, while in others, the mental artery runs apically to supply the apical portion of the incisor with the mandibular artery being thinner and running from the mandibular canal to the mesial part of the fibrous periodontium.

Figure 1.2.3, which represents a mandibular right incisor illustrates that the dentin defect and subsequent "lesion" are skewed toward the mesial surface. This is fitting with the

concept of cell susceptibility to adriamycin at a specific point in their differentiation. Smith and Warshawsky (1976) have stated that the lateral side of the incisor takes longer to develop than the medial side, indicating that the cells on the medial side are susceptible earlier, possibly resulting in the bilateral asymmetry.

The rate of eruption of the lower incisor has been studied by a number of investigators (Sturman, 1957; Sessle, 1966; Weinreb *et al.*, 1967), with the average being 400 μm/day. Karim (1990) using radioautography methods has indicated that adriamycin has no effect on tooth eruption. The current study has shown that between one and two weeks post-adriamycin administration, the increase in incisor length was 308 μm/day and 351 μm/day between two and three weeks post-adriamycin administration. In addition, Smith and Warshawsky (1975b) have demonstrated that the apical end of a young rat incisor will also grow posteriorly. As a result, the actual growth of the incisor will be greater than the 400 μm/day which is erupting out of the oral cavity. This data tends to imply that adriamycin may slow the rate of incisor eruption, however, it must be remembered that the sample size used was small.

The formation of accessory canals was shown to occur following the administration of adriamycin. While Kovacs (1967) claimed that coursing blood vessels caused the formation of accessory canals, the current study points to

localized defects in the root sheath, a view held by other investigators (Seltzer, 1971; Scott and Symons, 1977; Kuroiwa *et al.*, 1992).

SUMMARY AND FUTURE INVESTIGATIONS

Following the administration of adriamycin, apoptotic death of dental papilla and root sheath cells is observed in the rat incisor. Incisal to these areas, odontoblasts committed to dentin matrix secretion begin production of osteodentin. In areas where root sheath apoptosis has occurred, an associated failure in dentinogenesis is observed. Although dentin is not present in these areas, an associated fibrous "lesion", similar in composition to normal PDL, forms. Based on the radioautography results, it appears that this "lesion" originated from proliferation of dental follicle cells.

Although periodontal ligament formed in the rat incisor in areas devoid of dentin, it cannot be claimed that dentin is not necessary for normal PDL formation. In this study, adriamycin caused root sheath disruption, however, in the normal situation, the basement membrane of the dentin may be necessary for this occurrence.

While much has been learned from the present study, more work in this area is necessary. Future studies must

concentrate on the ultrastructural changes of the root sheath, following adriamycin administration and during normal development. The only possible way of determining whether dentin is necessary for PDL development is through the use of in vitro recombination experiments comparing the results of i) adriamycin treated root sheath cells and follicular tissue, with ii) follicular tissue and root sheath +/- dentin basement membrane. These experiments would also benefit from immunohistochemical labelling which would identify the possible messangers (eg. TGF-β_1) involved in the differentiation of the dental follicle.

REFERENCES

Adatia AK (1975). The effect of cyclophosphamide on odontogenesis in the rat. Arch Oral Biol 20:141-144.

Adkins KF (1967). The effect of actinomycin D on differentiation of odontoblasts in the rat. Arch Oral Biol 17:323-328.

Ahern V, Barraclough B, Bosch C, Langlands A, Boyages J (1994). Locally advanced breast cancer: defining an optimum treatment regimen. Int J Radiat Oncol Biol Phys 28:867-875.

Allison AC (1973). The role of microfilaments and microtubules in cell movement, endocytosis and exocytosis. In: Locomotion of tissue cells. Ciba Symposium 14 Amsterdam:Elsevier, 110-143.

Arends MJ, Morris RG, Wyllie AH (1990). Apoptosis: the role of the endonuclease. Am J Pathol 136:593-608.

Bachur NR, Gordon SL, Gee MV (1977). Anthracycline antibiotic augmentation of microsomal electron transport and free radical formation. Mol Pharmacol 13:901-910.

Bader SB, Weinstein H, Mauch P, Silver B, Tarbell NJ (1993). Pediatric stage IV Hodgkin disease. Long-term survival. Cancer 72:249-255.

Bailey AJ, Bazin S, Sims TJ, Le Lous M, Nicoletis C, Delaumay A (1975). Characterization of the collagen of human hypertrophic and normal scars. Biochem Biophys Acta 405:412-421.

Barnes MJ, Morton LF, Bennett RC, Bailey AJ, Sims TJ (1976). Presence of type III collagen in guinea-pig dermal scar. Biochem J 157:263-266.

Barrett AD, Reade PC (1981). The relationship between degree of development of tooth isografts and the subsequent formation of bone and periodontal ligament. J Periodontal Res 16:456-465.

Becker J, Schuppan D, Rabanus JP, Rauch R, Niechoy U, Gelderblom HR (1991). Immunoelectron microscopic localization of collagens type I, V, VI and of procollagen type III in human periodontal ligament and cementum. J Histochem Cytochem 39:103-110.

Beertsen W (1975). Migration of fibroblasts in the periodontal ligament of the mouse incisor as revealed by autoradiography. Arch Oral Biol 20:659-666.

Beertsen W, Everts V (1977). The site of remodelling of collagen in the periodontal ligament of the mouse incisor. Anat Rec 189:479-497.

Beertsen W, Everts V, Brekelmans M (1979). Unipolarity of fibroblasts in rodent periodontal ligament. Anat Rec 195:535-544.

Beertsen W, Everts V, Hoeben K, Niehof A (1984). Microtubules in periodontal ligament cells in relation to tooth eruption and collagen degradation. J Periodont Res 19:489-500.

Beertsen W, Everts V, Niehof A, Bruins H (1982). Loss of connective tissue attachment in the marginal periodontium of the mouse following blockage of eruption. Light microscopic observations. J Periodont Res 17:640-656.

Bellows CG, Melcher AH, Aubin JE (1982a). Association between tension and orientation of periodontal ligament fibroblasts and exogenous collagen fibres in collagen gels *in vitro*. J Cell Sci 50:299-314.

Bellows CG, Melcher AH, Bhargava U, Aubin JE (1982b). Fibroblasts contractin three-dimensional collagen gels exhibit ultrastructure consistent with either contraction or protein secretion. J Ultrastruc Res 78:178-192.

Berkovitz BKB (1990). The structure of the periodontal ligament: an update. Eur J Orthod 12:51-76.

Berkovitz BKB, Holland GR, Moxham BJ (1984). A colour atlas and textbook of oral anatomy. Holland: Wolfe Medical Publications.

Berkovitz BKB, Moxham BJ (1990). The development of the periodontal ligament with special reference to collagen fibre ontogeny. J Biol Buccale 18:227-236.

Berkovitz BKB, Shore RC (1982). Cells of the periodontal ligament. In: Berkovitz BKB, Moxham BJ, Newman HN, editors. The periodontal ligament in health and disease. Oxford: Pergamon Press, 25-50.

Berkovitz BKB, Shore RC, Moxham BJ (1984). Ultrastructural studies on the developing periodontal ligament. In: Ruch JV, Belcourt AB, editors. Tooth morphogenesis and differentiation. Colloquiium of the Institut De La Santé Et De La Recherche Médicale 125:545-556.

Berkovitz BKB, Shore RC, Sloan P (1980). Histology of the periodontal ligament of rat mandibular incisors following root resection, with special reference to the zone of shear. Arch Oral Biol 25:235-244.

Bienkowski RS (1983). Intracellular degradation of newly synthesised secretory proteins. Biochem J 214:1-10.

Bienkowski RS, Cowan MJ, McDonald JA, Crystal RG (1978). Degradation of newly synthesised collagen. J Biol Chem 253:4356-4363.

Bronckers AL, Lyaruu DM, Woltgens JH (1989). Immunohistochemistry of extracellular matrix proteins during various stages of dentinogenesis. Connect Tissue Res 22:65-70.

Buja LM (1991). Lipid abnormalities in myocardial cell injury. Trends Cardiovasc Med 1:40-45.

Buja LM, Eigenbrodt ML, Eigenbrodt EH (1993). Apoptosis and necrosis: basic types and mechanisms of cell death. Arch Pathol Lab Med 117:1208-1214.

Burton KP, Morris AC, Massey KD, Buja LM, Hagler HK (1990). Free radicals alter ionic calcium levels and membrane phospholipids in cultured rat ventricular myocytes. J Mol Cell Cardiol 22:3060-3067.

Butler WT, Birkedal-Hansen H, Taylor RE (1975b). Proteins of the periodontium: The chain structure of the collagens of bovine cementum and periodontal ligament. In: Slavkin HC, Greulich RC, editors. Extracellular matrix influence on gene expression. New York:Academic Press, 371-377.

Butler WT, Birkedal-Hanson H, Taylor RE, Chung E (1975a). Proteins of the periodontium. Identification of collagens with the $\alpha1(I)_2\alpha2$ and $[\alpha1(III)]_3$ structures in bovine periodontal ligament. J Biol Chem 250:8907-8912.

Cahill DR, Marks SC Jr. (1982). Chronology and histology of exfoliation and eruption of mandibular premolars in dogs. J Morphol 171:213-218.

Carl W, Wood R (1980). Effects of radiation on the developing dentition and supporting bone. J Am Dent Assoc 101:646-648.

Chiba M, Nakagawa R, Minura T (1967). DNA synthesis and cell division cycle at the base of the maxillary incisor tooth of the young rat. Arch Oral Biol 12:865-876.

Chibon P (1967). Etude expérimentale par ablations, greffes et autoradiographie de l'origine des dents chez l'amphibien unrodèle Pleurodeles Waltii Michah. Arch Oral Biol 12:745-755

Chien KR, Han A, Sen A, Buja LM, Willerson JT (1984). Accumulation of unesterified arachidonic acid in ischemic canine myocardium: relationship to a phosphatidylcholine deacylation-recylation cycle and depletion of membrane phospholipids Circ Res 54:313-322.

Cho MI, Garant PR (1981). An electron microscopic radioautographic study of collagen secretion in periodontal ligament fibroblasts of the mouse. I. Normal fibroblasts. Anat Rec 201:115-119.

Cho MI, Garant PR (1984). The effect of beta-aminoproprionitrile on the periodontal ligament. II. Radioautographic study of collagen secretion from fibroblasts. Anat Rec 209:41-52.

Cho MI, Garant PR (1985). Mirror symmetry of newly divided rat periodontal ligament fibroblasts in situ and its relationship to cell migration. J Periodont Res 20:185-200.

Coolidge ED (1937). The thickness of the human periodontal membrane. J Am Dent Assoc 24:1260-1270.

Cotter TG, Lennon SV, Glynn JG, Green DR (1992). Microfilament-disrupting agents prevent the formation of apoptotic bodies in tumor cells undergoing apoptosis. Cancer Res 52:997-1005.

d'Arville CN, Johnson PJ (1990). Growth factors, endocrine aspects and hormonal treatment in hepatocellular carcinoma-an overview. J Steroid Biochem Mol Biol 37:1007-1012.

D'Souza RN, Happonen RP, Ritter NM, Butler WT (1990). Temporal and spatial patterns of transforming growth factor-β_1 expression in developing rat molars. Arch Oral Biol 35:957-965.

Daeninck PJ, Karim AK (1987). Effect of adriamycin on alkaline phosphatase activity of pulp cells. Proceedings of the 30th Annual Meeting of CFBS:93.

Dahl JE (1984). Influence of doxorubicin on rat incisor mesenchymal cells. Scand J Dent Res 92:6-13.

Dahl JE, Koppang HS (1985). Renewal and migration of rat incisor mesnchymal cells after doxorubicin administration. Acta Odontol Scand 43:97-102.

Dahl JE, Stene T, Koppang HS, Koppang R, Stokke T (1981). B-lumicolchicine as a tool to elucidate micro-tubular function in dentinogenesis. Acta Odont Scand 39:195-200.

Daskal G, Woodward C, Crooke ST, Busch H (1978). Comparative ultrastructural studies on nucleoli of tumor cells treated with adriamycin and the newer anthracyclines, carminomycin and marcellomycin. Cancer Res 38:467-473.

Davidovitch Z, Finkelson MD, Steigman S, Shanfeld JL, Montgomery PC, Korostoff E (1980). Electrical currents, bone remodelling, and orthodontic tooth movement. II. Increase in rate of tooth movement and periodontal cyclic mucleotide levels by combined force and electric current. Am J Orthod 77:33-47.

Deliconstantinos G, Kopeikina-Tsiboukidou L, Villiotou V (1987). Evaluation of membrane fluidity effects and enzyme activities alterations in adriamycin neurotoxicity. Biochem Pharmacol 36:1153-1161.

Diehl V (1993). Dose-escalation study for the treatment of Hodgkin's disease. The German Hodgkin Study Group (GHSG). Ann Hematol 66:139-140.

Edmunds RS, Simmons TA, Cox CF, Avery JK (1979). Light and ultrastructural relationship between oxytalan fibres in the periodontal ligament of the guinea pig. J Oral Path 8:109-120.

Eigenbrodt ML, Eigenbrodt EH, Thiele DL (1990). Histologic similarity of murine colonic graft-versus-host disease (GVHD) to human colonic GVHD and inflammatory bowel disease. Am J Pathol 137:1065-1076.

Epstein EH (1974). $[1(III)]_3$ Human skin collagen. J Biol Chem 249:3225-3231.

Evan GI, Wyllie Ah, Gilbert CS, Littlewood TD, Land H, Brooks M, Waters CM, Penn LZ, Hancock DC (1992). Induction of apoptosis in fibroblasts by c-myc protein. Cell 69:119-128.

Farber JL (1982). Biology of disease: membrane injury and calcium homeostasis in the pathogenesis of coagulative necrosis. Lab Invest 47:114-123.

Fesus L, Davies PJ, Piacentini M (1991). Apoptosis: molecular mechanisms in programmed cell death. Eur J Cell Biol 56:170-177.

Freeman E, Ten Cate AR, Dickson J (1975). Development of a gomphosis by tooth germ implants in the parietal bone of the mouse. Arch Oral Biol 20:139-140.

Fridovich I (1978). The biology of oxygen radicals. Science 201:875-880.

Fullmer HM, Sheetz JH, Narkates AJ (1974). Oxytalan connective tissue fibres: A review. J Oral Pathol 3:291-316.

Garant PR (1976). Collagen resorption by fibroblasts. A theory of fibroblastic maintenance of the periodontal ligament. J Periodont 47:380-390.

Garant PR, Cho MI (1979). Cytoplasmic polarisation of periodontal ligament fibroblasts. Implications for cell migration and collagen secretion. J Periodont Res 14:95-106.

Gay S, Miller EJ (1978). Collagen in the physiology and pathology of connective tissue. Stuttgart: Gustav Fischer Verlag, 1978.

Gerschenson LE, Rotello RJ (1992). Apoptosis: a different type of cell death. FASEB J 6:2450-2455.

Giannakis C, Forbes IJ, Zalewski PD (1991). Ca^{2+}/Mg^{2+}-dependent nuclease: tissue distribution, relationship to inter-nucleosomal DNA fragmentation and inhibition by Zn^{2+}. Biochem Biophys Res Commun 181:915-920.

Goormaghtigh E, Chatelain P, Caspers J, Ruysschaert JM (1980b). Evidence of a complex between adriamycin derivatives and cardiolipin: possible role in cardiotoxicity. Biochem Pharmacol 29:3003-3010.

Goormaghtigh E, Chatelain P, Caspers J, Ruysschaert JM (1980a). Evidence of a specific complex between adriamycin and negatively charged phospholipids. Biochem Biophys Acta 597:1-14.

Gould TRL, Brunette DM, Dorey J (1982). Cell turnover in the periodontal ligament determined by continuous infusion of H^3-thymidine using osmotic minipumps. J Periodont Res 17:662-668.

Gould TRL, Melcher AH, Brunette DM (1977). Location of progenitor cell populations in periodontal ligament of mouse molar stimulated by wounding. Anat Rec 188:133-141.

Gould TRL, Melcher AH, Brunette DM (1980). Migration and division of progenitor cell populations in periodontal ligament after wounding. J Periodont Res 15:20-42.

Grant DA, Bernick S (1972). Formation of the periodontal ligament. J Periodontol 43:17-25.

Grant DA, Bernick S, Levy BM, Dreizen S (1972). A comparative study of periodontal ligament development in teeth with and without predecessors in marmosets. J Periodontol 43:162-169.

Grant DA, Bernick S, Levy BM, Dreizen S (1972). A comparative study of periodontal ligament development in teeth with and without predecessors in marmosets. J Periodont 43:162-169.

Greenburg G, Hay ED (1982). Epithelia suspended in collagen gels lose polarity and express characteristics of migrating meenchymal cells. J Cell Biol 95:333-339.

Hansen LS, English JA (1957). Histological changes in the incisor of rats serially sacrificed after receiving 1500 R of 200 kv X-ray irradiation. J Dent Res 36:417-431.

Hays DM (1993). Rhabdomyosarcoma. Clin Orthop (289):36-49.

Henkel W, Glanville, RW (1982). Covalent crosslinking between molecules of type I and type III collagen. The involvement of the N-terminal, nonhelical regions of the 1(I) and 1(iii) chains in the formation of intermolecular crosslinks. Eur J Biochem 122:205-213.

Huang YH, Ohsaki Y, Kurisu K (1991). Distribution of type I and type III collagen in the developing periodontal ligament of mice. Matrix 11:25-35.

Imberman M, Ramamurthy N, Golub L, Schnier M (1986). A reassessment of collagen half-life in rat periodontal tissues: application of the pool expansion approach. J Periodont Res 21:396-402.

Jehn U, Heinemann V (1991). New drugs in the treatment of acute and chronic leukemia with some emphasis on m-AMSA. Anticancer Res 11:705-711.

Jensen JL, Toto PD (1968). Radioactive labeling index of the periodontal ligament in aging rats. J Dent Res 47:149-153.

Jonas IE, Riede UN (1980). Reaction of oxytalan fibers in human periodontium to mechanical stress. J Histochem Cytochem 28:211-216.

Kanoza RJJ, Kelleher L, Sodek J, Melcher AH (1980). A biochemical analysis of the effect of hypofunction on collagen metabolism in the rat molar periodontal ligament. Arch Oral Biol 25:663-668.

Karim AC (1985a). The effect of adriamycin on rat incisor one day after administration. Anat Rec 211:17-23.

Karim AC (1985b). The initiation of osteodentin formation in the rat incisor after adriamycin administration. Anat Rec 213:377-384.

Karim AC (1990). The effect of adriamycin on dentinogenesis and ^{3}H-thymidine incorporation into the enamel organ of the rat incisor. Exp Pathol 40:1-18.

Karim AC, Eddy EL (1984). A light and electron microscopic study of osteodentin formation in the rat incisor after adriaycin administration. Am J Anat 169:207-219.

Karim AC, Pylypas SP (1985). The extent of the necrotic lesion in the apical end of the rat incisor pulp seen after adriamycin administration. Exp Path 27:105-110.

Karim AC, Pylypas SP (1986). Osteodentin formation in rat incisor as visualized by radioautography after ^{3}H-proline administration. Anat Rec 216:19-26.

Karimbux NY, Rosenblum ND, Nishimura I (1992). Site-specific expression of collagen I and XII mRNAs in the rat periodontal ligament at two developmental stages. J Dent Res 71:1355-1362.

Kerr JFR, Wyllie AH, Currie AR (1972). Apoptosis: a basic biological phenomenon with wide-ranging implications in tissue kinetics. Br J Cancer 26:239-257.

Kindlova M, Matena V (1959). Blood circulation in the rodent teeth of the rat. Acta Anat 37:163-192.

Kollar EJ, Baird GR (1969). The influence of the dental papilla on the development of tooth shape in embryonic mouse tooth germs. J Embryol Exp Morphol 21:131-148.

Kollar EJ, Baird GR (1970). Tissue interactions in embryonic mouse tooth germs. I. Reorganisation of the dental epithelium during tooth-germ reconstruction. J Embryol Exp Morphol 24:159-171.

Konomi H, Arima M, Tanaka H, Hayashi T, Ikeda S (1989). Increased deposition of type III and V collagen in neurofibroma tissue from patients with von Recklinghausen disease. Brain Dev 11:378-383.

Konomi H, Sano J, Nagai Y (1981). Immunohistochemical localization of type I, III, IV (basement membrane) collagens in the lymph node: co-distribution of type I and III collagens in the reticular fibres. Biomed Res 2:536-545.

Koppang HS (1973a). Histomorphologic investigations of the effect of cyclophosphamide on dentinogenesis of the rat incisor. Scan J Dent Res 81:383-396.

Koppang HS (1973b). Autoradiographic investigations on the effect of cyclophosphamide on dentinogenesis of the rat incisor. Scan J Dent Res 81:397-405.

Korsmeyer SJ (1992). Bcl-2: a repressor of lymphocyte death. Immunol Today 13:285-288.

Kovacs I (1967). Contribution to the ontogenetic morphology of roots of human teeth. J Dent Res 46:865-874.

Kronfeld R (1931). Histologic study of the influence of function on the human periodontal membrane. J Nat Dent Ass 18:1242-1247.

Ku Y, Saitoh M, Iwasaki T, Tominaga M, Maekawa Y, Shiki H Samizo M, Fukumoto T, Kuroda Y, Sako M (1993). Intraarterial infusion of high-dose adriamycin for unrespectable hepatocellular carcinoma using direct hemoperfusion under hepatic venous isolation. Eur J Surg Oncol 19:387-392.

Kuroiwa M, Kodaka T, Abe M, Higashi S (1992). Three-dimensional observations of accessory canals in mature and developing rat molar teeth. Acta Anatomica 143:130-138.

Kusumoto H, Kumashiro R, Kido K, Inutsuka S (1991). Simultaneous adenocarcinoma of the stomach and fourth portion of the duodenum: case report and review of the literature. Radiat Med 9:223-228.

Lameh J, Chuang RY, Israel M, Chuang LF (1989). Nucleoside uptake and membrane fluidity studies on N-trifluoroacetyladriamycin-14-o-hemiadipate-treated human leukemia and lymphoma cells. Cancer Res 49:2905-2908.

Le Douarin NM (1984). Cell migrations in embryos. Cell 38:353-360.

Limeback HF, Sodek J (1979) Procollagen synthesis and processing in periodontal ligament *in vivo* and *in vitro*. A comparative study using slab-gell fluorography. Eur J Biochem 100:541-550.

Linde A, Goldberg M (1993). Dentinogenesis. Crit Rev Oral Biol Med 4:679-728.

MacNeil RL, Somerman MJ (1993). Molecular factors regulating development and regeneration of cementum. J Periodontal Res 28:550-559.

MacNeil RL, Thomas HF (1993). Development of the murine periodontium. II. Rolte of the epithelial root sheath in formation of the periodontal attachment. J Periodontol 64:285-291.

Mameghan H, Fisher R, Tobias V, Kern IB, O'Gorman-Hughes D, Vowels M, Mameghan J (1993). Local failure in childhood rhabdomyosarcoma and undifferentiated sarcoma: prognostic factors and implications for curative therapy. Med Pediatr Oncol 21:88-95.

Mao YQ, Ohasaki Y, Kurisu K (1990). Immunohistochemical study on the relationship between extracellular matrix and root bifurcation in mouse molars. Arch Oral Biol 35:583-591.

Marks SC Jr., Cahill DR (1987). Regional control of alveolar bone metabolism by the dental follicle during tooth eruption. J Oral Pathol 16:164-169.

Marks SC Jr., Gorski JP, Cahill DR, Wise GR (1988). Tooth eruption - A synthesis of experimental observations. In: Davidovitch Z, editor. Biological mechanisms of tooth eruption and root resorption, 1988 Apr 28-30, Columbus(OH). Birmingham(AL):EBSCO media, 237-242.

Martin SJ, Cotter TG (1990). Disruption of microtubules induces an endogenous suicide pathway in human leukaemia HL-60 cells. Cell Tissue Kinet 23:545-559.

Martin SJ, Green DR, Cotter TG (1994). Dicing with death: dissecting the components of the apoptosis machinery. TIBS 19:26-30.

McCulloch CAG (1985). Progenitor cell populations in the periodontal ligament of mice. Anat Rec 211:258-262.

McCulloch CAG, Bordin S (1991). Role of fibroblast subpopulations in periodontal physiology and pathology. J Periodont Res 26:144-154.

McCulloch CAG, Melcher AH (1983a). Continuous labelling of the periodontal ligament of mice. J Periodont Res 18:231-241.

McCulloch CAG, Melcher AH (1983b). Cell migration in the periodontal ligament of mice. J Periodont Res 18:339-352.

McCulloch CAG, Melcher AH (1983c). Cell density and cell generation in the periodontal ligament. Am J Anat 167:43-58.

Medak H, Weinreb M, Sicher H, Weinmann JP, Schour I (1952). The effect of single doses of irradiation upon the tissues of the upper rat incisor. J Dent Res 31:559-574.

Melcher AH (1980). Periodontal ligament. In: Bhaskar SN, editor. Orban's oral histology and embryology, 9 th edition. Toronto:Mosby, 204-209.

Melcher AH (1986). Periodontal Ligament. In: Bhaskar SN, editor. Orban's Oral histology and embryology. 10th edition. Toronto: CV Mosby, 198-231.

Melcher AH, Beertsen W (1977). The physiology of tooth eruption. In: McNamara JA, editor. The biology of occlusal development. Monograph No. 7 Craniofacial growth series. Ann Arbor, Center for Human Growth and Development, University of Michigan, 1-23.

Melcher AH, Correia MA (1971). Remodelling of periodontal ligament in eruptin molars of mature rats. J Periodont Res 6:118-125.

Merilees MJ, Scott L (1980). Interaction of epithelial cells and fibroblasts in culture: effect on glycosaminoglycan levels Dev Biol 76:396-409.

Michaeli Y, Steigman S, Barad A, Weinreb M Jr (1988). Three-dimensional presentation of cell migration in the periodontal ligament of the rat incisor. Anat Rec 221:584-590.

Michaeli Y, Weinreb M Jr, Barad A, Steigman S (1987). Three-dimensional presentation of the fibroblast progenitor compartment in the periodontal ligament of the rat incisor. Am J Anat 180:243-248.

Michaeli Y, Zajicek G, Gineo I (1979). Cell production in the normal and lathyrogenic rat periodontal ligament. J Dent Res 58:511-516.

Mikkelsen HB (1978). Acute and protracted effects of vinblastine on ameloblasts and dentinogenesis in rat incisors. Scand J Dent Res 86:313-324.

Miller EJ, Gay S (1987). The collagens: an overview and update. Method Enzymol 144:3-41.

Miller RS, Torti FM (1992). Chemotherapy of advanced transitional-cell carcinoma of the bladder. Cancer Chemother Pharmacol 30 (Suppl):S99-S110.

Moe H (1977). On the effect of vinblastine on ameloblasts of rat incisors in vivo. 3 acute and protracted effects on differentiating ameloblasts. A light microscopical study. Acta Pathol Microbiol Scand 85:330-334.

Moule AJ, Young WG, Adkins KF (1993). Early cellular events in an actinomycin D-created dentin niche in the rat incisor. J Oral Pathol Med 22:159-167.

Myers CE (1982). Anthracyclines. In: Chabner B, editor. Pharmacologic principles of cancer treatment. Philadelphia: Saunders, 416-434.

Myers CE, Chabner BA (1990). Anthracyclines. In: Chabner BA, Collins JM, editors. Cancer chemotherapy: principles and practice. Philadelphia: Lippincott, 356-381.

Nichols DH (1981). Neural crest fromation in the head of the mouse embryo as observed using a new histological technique. J Embryol Exp Morph 64:105-120.

Noguiera JO, Stene T, Koppang HS (1980). Long-term effects of colchicine on dentinogenesis in rat incisors. Scand J Dent Res 88:15-21.

Oth D, Begin M, Bischoff P, Leroux JY, Mercier G, Bruneau C (1987). Induction, by adriamucin and mitomycin C, of modifications in lipid composition, size distribution, membrane fluidity and permeability of cultured RDM4 lymphoma cells. Biochem Biophys Acta 900:198-208.

Owens PDA (1974). A light microscopic study of the development of the roots of premolar teeth in dogs. Arch Oral Biol 19:525-538.

Palmer RM, Lumsden AGS (1987). Development of periodontal ligament and alveolar bone in homografted recombinations of enamel organs and papillary, pulpal and follicular mesenchyme in the mouse. Arch Oral Biol 32:281-289.

Partanen AM, Thesleff I (1987). Localization and quantification of ^{125}I-epidermal growth factor binding in mouse embryonic tooth and other embryonic tissues at different developmental stages. Dev Biol 120:186-197.

Patel DJ, Canuel LL (1978). Anthracycline antitumor antibiotic nucleic acid interactions. Structural aspects of the daunomycin poly(dA-dT) complex in solution. Eur J Biochem. 90:247-254.

Patel S, Benjamin RS (1992). Standard and high dose chemotherapy for advanced soft tissue sarcomas. Ann Oncol 3 (Suppl 2):S81-S83.

Pearson CH, Wohllebe M, Carmichael DJ, Chovelon A (1975). Bovine periodontal ligament. An investigation of the collagen, glycosaminoglycan and insoluble glycoprotein components at different stages of tissue development. Connect Tiss Res 3:195-206.

Perera KAS, Tonge CH (1981a). Metabolic turnover of collagen in the mouse molar periodontal ligament during tooth eruption. J Anat 133:359-370.

Perera KAS, Tonge CH (1981b). Fibroblast cell population kinetics in the mouse molar periodontal ligament and tooth eruption. J Anat 133:281-300.

Posada J, Vichi P, Tritton TR (1989b). Protein kinase C in adriamycin action and resistance in mouse sarcoma 180 cells. Cancer Res 49:6634-6639.

Posada JA, McKeegan EM, Worthington KF, Morin MJ, Jaken S, Tritton TR (1989a). Human multidrug resistan KB cells overexpress protein kinase C: involvement in drug resistance. Cancer Commun 1:285-292.

Rippin JW (1978). Collagen turnover in the periodontal ligament under normal and altered functional forces. II. Adult rat molars. J Periodont Res 13:149-154.

Ritch PS, Occhipinti SJ, Cunningham RE, Shackney SE (1981). Schedule-dependent synergism of combinations of hydroxyurea with Adriamycin and 1-beta-D-arabinofuranosylcytosine with adriamycin. Cancer Res. 41:3881-3884.

Roberts WE, Chamberlain JG (1978). Scanning electron microscopy of the cellular elements of rat periodontal ligament. Arch Oral Biol 23:587-589.

Roberts WE, Chase DC (1981). Kinetics of cell proliferation and migration associated with orthodontically-induced osteogenesis. J Dent Res 60:174-181.

Roberts WE, Jee WSS (1974). Cell kinetics of orthodontically stimulated and non-stimulated periodontal ligament in the rat. Arch Oral Biol 19:17-21.

Roberts WE, Morey ER (1985). Proliferation and differentiation sequence of osteoblast histogenesis under physiological conditions in rat periodontal ligament. Am J Anat 174:105-118.

Ross WE, Zwelling LA, Kohn KW (1979). Relationship between cytoxicity and DNA strand breakage produced by adriamycin and other intercalating agents. Int J Radiat Oncol Biol Phys 5:1221-1224.

Sato S, Iwaizumi M, Handa K, Tamura Y (1977). Electron spin resonance study on the mode of generation of free radicals of daunomycin, adriamycin and carboquone in NAD(P)H-microsome system. Gann 68:603-608.

Sayhoun N, Wolf M, Besterman J, Hsieh T, Sander M, Levine H, Chang K, Cuatrecasas P (1986). Protein kinase C phosphorylates topoisomerase II: topoisomerase activation and its possible role in phorbol ester induced differentiation of HL-60 cells. Proc Natn Acad Sci USA 83:1603-1607.

Schellens JPM, Everts V, Beertsen W (1982). Quantitative analysis of connective tissue resorption in the supra-alveolar region of the mouse incisor ligament. J Periodont Res 17:407-422.

Schroeder HE (1986). Handbook of microscopic anatomy. Volume V/5: the periodontium. Berlin:Springer-Verlag, 170-233.

Schwartz HS (1975). DNA breaks in P228 tumor cells in mice after treatment with daunorubicin and adriamycin. Res Commun Chem Pathol Pharmacol 10:51-54.

Scott JH, Symons NBB (1977). Introduction to dental anatomy. Edinburgh: Churchill Livingstone, 242-254.

Seidman AD, Scher HI (1991). The evolving role of chemotherapy for muscle infiltrating bladder cancer. Semin Oncol 18:585-595.

Seltzer S (1971). Endodontology. New York: McGraw-Hill, 1-32.

Serle J, Kerr JFR, Bishop CJ (1982). Necrosis and apoptosis: distinct modes of cell death with fundamentally different significance. Pathol Annu 17:229-259.

Sessle BJ (1966). Attrition and eruption rates of the rat lower incisor. J Dent Res 45:1571.

Shackleford JM (1971a). Scanning electron microscopy of the dog periodontium. J Periodont Res 6:45-54.

Shackleford JM (1971b). The indifferent fiber plexus and its relationship to principal fibers of the periodontium. Am J Anat 131:427-442.

Sharawy M, Bhussry BR (1986). Development and growth of teeth. In: Bhaskar SN, editor. Orban's oral histology and embryology. 10th edition. Toronto: CV Mosby, 24-44.

Shi Y, Glynn JM, Guilbert LJ, Cotter TG, Bissonnette RP, Green DR (1992). Role for c-myc in activation-induced apoptotic cell death in T-cell hybridomas. Science 257:212-214.

Shore RC, Berkovitz BKB (1979). An ultrastructural study of periodontal ligament fibroblasts in relation to their possible role in tooth eruption and intracellular collagen degradation in the rat. Arch Oral Biol 24:155-164.

Shore RC, Berkovitz BKB, Moxham BJ (1981). Intercellular contacts between fibroblasts in the periodontal connective tissues of the rat. J Anat 133:67-76.

Shore RC, Berkovitz BKB, Moxham BJ (1985). The effects of preventing movement of the rat incisor on the structure of its periodontal ligament. Arch Oral Biol 30:221-228.

Shore RC, Moxham BJ, Berkovitz BKB (1984). Oxytalan fibres in the periodontal ligament. In: Ruch JV, Belcourt AB, editors. Tooth morphogenesis and differentiation. Colloquiium of the Institut De La Santé Et De La Recherche Médicale 125:565-572.

Shuttleworth CA, Forrest L (1975) Changes in guinea-pig dermal collagen during development. Eur J Biochem 55:391-395.

Sicher H (1942). Tooth eruption: the axial movement of continuously growing teeth. J Dent Res 21:201-210.

Sims MR (1973). Oxytalan fibre system of molars in the mouse mandible. J Dent Res 52:797-802.

Sims MR (1975). Oxytalan-vascular relationships observed in histologic examination of the periodontal ligaments of man and mouse. Arch Oral Biol 20:713-716.

Sims MR (1976). Reconstruction of the human oxytalan system during orthodontic tooth movement. Am J Orthod 70:38-58.

Sims MR (1977). Oxytalan meshwork associations observed histologically in the periodontium of the mouse mandible. Arch Oral Biol 22:605-611.

Sims MR (1984). Ultrastructural analysis of the microfibrillar component of mouse and human periodontal oxytalan fibers. Connect Tuss Res 13:59-67.

Skladanowski A, Konopa J (1993). Adriamycin and daunomycin induce programmed cell death (apoptosis) in tumor cells. Biochem Pharmacol 46:375-382.

Slavkin HC (1989). Positional signalling and patterning for amelogenesis in mouse molar tooth development. Connect Tissue Res 20:91-100.

Slavkin HC (1990). Molecular determinants of tooth development: a review. Crit Rev Oral Biol Med 1:1-16.

Slavkin HC (1991). Molecular determinants during dental morphogenesis and cytodifferentiation: a review. J Craniofac Genet Dev Biol 11:338-349.

Slavkin HC, Bringas P Jr, Bessem C, Santos V, Nakamura M, Hsu MY, Snead ML, Zeichner-David M, Fincham AG (1989). Hertwig's epithelial root sheath differentiation and initial cementum and bone formation durin long term culture of mouse mandibular first molars using serumless, chemically-defined medium. J Periodont Res 24:28-40.

Slavkin HC, Hu CC, Sakakura Y, Diekwisch T, Chai Y, Mayo M, Bringas P Jr., Simmer H, Mak G, Sasano Y (1992). Gene expression, signal transduction and tissue-specific biomineralization during mammalian tooth development. Crit Rev Eukaryot Gene Expr 2:315-329.

Sloan P (1978). Scanning electron microscopy of the collagen fibre architecture of the rabbit incisor periodontium. Arch Oral Biol 23:567-572.

Sloan P (1979). Collagen fibre arcitecture in the periodontal ligament. J R Soc Med 72:188-191.

Sloan P (1982). Structural organisation of the fibres of the periodontal ligament. In: Berkovitz BKB, Moxham BJ, Newman HN, editors. The periodontal ligament in health and diease. Oxford:Pergamon Press, 51-72.

Sloan P, Shellis RP, Berkovitz BKB (1976). Effect of specimen preparation on the appearance of the rat periodontal ligament in the scanning electron microscope. Arch Oral Biol 21:633-635.

Smith CE, Warshawsky H (1975a). Histologic and three dimensional organization of the odontogenic organ in the lower incisor of 100 gram rats. Am J Anat 142:403-430.

Smith CE, Warshawsky H (1975b). Cellular renewal in the enamel organ and the odontoblast layer of the rat incisor as followed by radioautography using 3H-thymidine. Anat Rec 183:523-562.

Smith CE, Warshawsky H (1976). Movement of entire cell populations during renewal of the rat incisor as shown by radioautography after labeling with ^{3}H-thymidine. Am J Anat 145:225-260.

Sodek J, Ferrier JM (1988). Collagen remodelling in rat periodontal tissues: comparison for precursor reutilization confirms rapid turnover of collagen. Coll Relat Res 8:11-21.

Sodek J, Limeback HF (1979) Comparison of the rates of synthesis, conversion and maturation of type I and type III collagens in rat periodontal tissues. J Biol Chem 254:10496-10502.

Steenbergen C, Hill ML, Jennings RB (1987). Cytoskeletal damage during myocardial ischemia: changes in immunofluoresence staining during total in vitro ischemia in canine heart. Circ Res 60:478-486.

Stene T (1978). Effect of vincristine on odontoblasts in rat incisor. Scand J Dent Res 86:346-356.

Stene T (1979). Vincristine's effect on dentinogenesis in rat incisor. Scand J Dent Res 87:39-49.

Stene T, Koppang HS (1976). The effect of vincristine on dentinogenesis in the rat incisor. Scand J Dent Res 84:342-344.

Sturman GD (1957). A study of the eruption rate of the mandibular rat incisors. Yale J Biol Med 30:137-148.

Sugarbaker PH (1991). Early postoperative intraperitoneal adriamycin as an adjuvant treatment for advanced gastric cancer with lymph mode or serosal invasion. Cancer Treat Res 55:277-284.

Sugiyama M, Sakanashi T, Okamoto K, Chinami M, Hidaka T, Ogura R (1986). Membrane fluidity in Ehrlich ascites tumor cells treated with adriamycin. Biotechnol Appl Biochem 8:217-221.

Svejda J, Skach M (1973). The periodontium of the human tooth in the scanning electron microscope (Stereoscan). J Periodont 44:478-484.

Svoboda ELA, Brunette DM, Melcher AH (1979a). *In vitro* phagocytosis of exogenous collagen by fibroblasts from the periodontal ligament: An electron microscopic study. J Anat 128:301-314.

Svoboda ELA, Melcher AH, Brunette DM (1979b). Stereological study of collagen phagocytosis by cultured periodontal ligament fibroblasts: Time course and effect of deficient culture medium. J Ultrastruct Res 68:195-208.

Takita K, Ohshaki Y, Nakata M, Kurisu K (1987). Immunofluorescence localization of type I and type III collagen and fibronectin in mouse dental tissues in late development and during eruption. Arch Oral Biol 32:273-279.

Ten Cate AR (1969). The development of the periodontium. In: Melcher AH and Bowen WH, editors. Biology of the periodontium. London: Academic Press, 53-89.

Ten Cate AR (1972). Morphological studies of fibrocytes in connective tissue undergoing rapid remodelling. J Anat 112:401-414.

Ten Cate AR (1975). Development of the periodontal membrane and collagen turnover. In: Poole DFG, Stack MV, editors. Eruption and occlusion. London: Butterworth, 281-289.

Ten Cate AR, Mills C, Solomon G (1970). The development of the periodontium. A transplantation and autoradiographic study. Anat Rec 170:365-380.

Ten Cate AR, Syrbu S (1974). A relationship between alkaline phosphatase activity and the phagocytosis and degradation of collagen by the fibroblast. J Anat 117:351-359.

Tewey KM, Chen GI, Nelson EM, Liv LF (1984). Intercalative antitumor drugs interfere with the breakage-reunion reaction of mammalian DNA topoisomerase II. J Biol Chem 259:9182-9187.

Thayer WS (1977). Adriamycin-stimulated superoxide formation in submitochondrial particles. Chem Biol Interact 19:265-278.

Thesleff I, Jalkanen M, Vainio S, Bernfield, M (1988). Cell surface proteoglycan expression correlates with epithelial-mesenchymal interaction during tooth morphogenesis. Dev Biol 129:565-572.

Thesleff I, Partanen AM, Vainio S (1991). Epithelial-mesenchymal interactions in tooth morphogenesis: the roles of extracellular matrix, growth factors, and cell surface receptors. J Craniofac Genet Dev Biol 11:229-237.

Thesleff I, Vaahtokari SA, Vainio S (1990). Molecular changes during determination and differentiation of the dental mesenchymal cell lineage. J Biol Buccale 18:179-188.

Thomas HF, Kollar EJ (1989). Differentiation of odontoblasts in grafted recombinants of murine epithelial root sheath and dental mesenchyme. Arch Oral Biol 34:27-35.

Tonge CG (1963). The development and arrangement of the dental follicle. Trans Eur Orthod Soc 118-126.

Tonna EA, Weiss R, Stahl SS (1972). The cell proliferaive activity of paradontal tissue in aging mice. Arch Oral Biol 17:969-982.

Toto PD, Borg M (1968). Effect of age changes on the premitotic indes in the periodontium of mice. J Dent Res 47:70-73.

Toto PD, Kwan HW (1970). Coubling time of labelled periodontal cells of rats. J Dent Res 49:70-73.

Toto PD, Rubenstein AS, Gargiulo AW (1975). Labelling index and cell density of aging rats oral tissues. J Dent Res 54:553-556.

Trott JR (1962). The development of the periodontal attachment in the rat. Acta Anat 51:313-328.

Trump BF, Valigorsky JM, Dees JH, Mergner WJ, Kim KM, Jones RT, Pendergrass RE, Garbus J, Cowley RA (1973). Cellular change in human disease: a new method of pathological analysis. Hum Pathol 4:89-109.

Tsuruchi N, Kaku T, Kinoshita H, Amada S, Saito T, Kamura T, Tsukamoto N, Nakano H (1993). Ovarian mucinous cystadenocarcinoma with sarcoma-appearing mural nodule of anaplastic carcinoma. Gynecol Oncol 50:259-263.

Van den Bos T, Tonino GJM (1984). Composition and metabolism of the extracellular matrix in the periodontal ligament of impeded and unimpeded rat incisors. Arch Oral Biol 29:893-897.

Wang HW, Nanda V, Rao LG, Melcher AH, Heersche JNM, Sodek J (1980). Specific immunohistochemical localization of type III collagen in porcine periodontal tissues using the peroxidase-anti-peroxidase method. J Histochem Cytochem 28:1215-1223.

Weese JL, Nussbaum ML (1992). Gastric cancer-surgical approach. Hematol Oncol 10:31-35.

Weinreb MM, Assif D, Michaeli Y (1967). Role of attrition in the physiology of the rat incisor. I. The relative value of different components of attrition and their effect on eruption. J Dent Res 46:527-531.

Willingham MC, Yamada SS, Davies PJA, Ruterford AV, Gallo MG, Pastan I (1981). Intracellular localisation of actin in cultured fibroblasts by electron microscopic immunocytochemistry. J Histochem Cytochem 29:17-37.

Wils JA (1991). Perspectives in chemotherapy of advanced gastric cancer. Anticancer Drugs 2:133-137.

Wise GE, Fan W (1991). Immunolocalization of transforming growth factor beta in rat molars. J Oral Pathol Med 20:74-80.

Wise GE, Lin F, Fan W (1992). Effects of transforming growth factor-β_1 on cultured dental follicle cells from rat mandibular molars. Arch Oral Biol 37:471-478.

Yamada KM (1983). Cell surface interaction with extracellular materials. Annu Rev Biochem 52:761-799.

Yamasaki A, Rose GG, Pirero GJ, Mahan CJ (1987). Ultrastructural and morphometric analyses of human cementoblasts and periodontal fibroblasts. J Periodontol 58:192-201.

Yokose N, Ogata K, Ito T, Miyake K, An E, Inokuchi K, Yamada T, Gomi S, Tanabe Y, Ohki I (1993). Chemotherapy for minimally differentiated acute myeloid leukemia (AML-MO). A report on five cases and review of the literature. Ann Hematol 66:67-70.

Yoshikawa DK, Kollar EJ (1981). Recombination experiments on the odontogenic roles of mouse dental papilla and dental sac tissues in ocular grafts. Arch Oral Biol 26:303-307.

Zajicek G (1974). Fibroblast cell kinetics in the periodontal ligament of the mouse. Cell Tissue Kinet 7:479-492.

Zwarych PD, Quigley MB (1965). The intermediate plexus of the periodontal ligament: History and further observations. J Dent Res 44:383-391.

APPENDIX A

Solutions

Glutaraldehyde buffer mix (*p*H 7.1)

20.91 g of $Na_2HPO_4 \cdot 7H_2O$ (Dibasic sodium phosphate)
5.85 g of $NaH_2PO_4 \cdot H_2O$ (Monobasic sodium phosphate)

made to 1000 ml with distilled water.

Glutaraldehyde fixative (2.5%, *p*H corrected to 7)

10 ml of 25% Glutaraldehyde stock
37 ml of Glutaraldehyde buffer mix

made to 1000 ml with distilled water, and filtered prior to use.

Phosphate buffer wash (*p*H 7.2)

27.03 g of $Na_2HPO_4 \cdot 7H_2O$
7.56 g of $NaH_2PO_4 \cdot H_2O$

made to 1000 ml with distilled water.

Disodium Ethylenediaminetetraacetate (4.13% EDTA, *p*H 7.4)

41.3 g EDTA (disodium)
4.4 g NaOH pellets

The above chemicals were placed in a volumetric flask with 750 ml of distilled water, heated and stirred until dissolved. The solution was cooled to room temperature, the volume adjusted to 1000 ml with distilled water and the *p*H adjusted to 7.4.

Osmium Tetroxide (1% OsO_4, *p*H 7.3)

2.8 ml of stock salt solution

Stock salt solution :
40.0 g Sodium Chloride
2.0 g Potassium Chloride
1.0 g Calcium Chloride
made up to 500 ml with distilled H_2O

11.0 ml of 0.1 N HCl

10.0 ml of veronal acetate buffer

Stock veronal acetate buffer :
14.7 g Sodium veronal (barbital)
9.7 g Sodium acetate
made up to 500 ml with distilled H_2O

The above solutions were poured into a volumetric flask with 50 ml of distilled H_2O. 0.5 g of osmium tetroxide was added and allowed to dissolve at room temperature overnight. It was then stored in the refrigerator. Note that the veronal acetate was added last to avoid precipitation.

Epon Embedding Resin

Stock solution A

Epon resin 812	64 ml
DDSA (Dodecenyl succinic anhydride)	100 ml

Stock solution B

Epon resin 812	100 ml
NMA (Nadic methyl anhydride)	89 ml

The final solution was prepared in the following way:

Stock solution A	5 parts
Stock solution B	5 parts
DMP-30 (Dimethyl amino methyl phenol)	2%

Adriamycin (Doxorubicin Hydrochloride)

[Adria Laboratories of Canada, Ltd.]

10 mg in 5 ml of physiological saline (0.9%) resulting in a drug concentration of 2.0 mg/ml.

In a 100 g animal, a dose level of 5.0 mg/kg would be equivalent to 0.5 mg or 0.25 ml

3H-thymidine

[ICN Nuclear]

The specific activity was 50 Ci/mM and its concentration, 1.0 mCi/ml

In a 100 g animal, a dose level of 2.0 μCi/g would be equivalent to 200 μCi or 0.2 ml

Stains

Toluidine Blue

1 g of Borax (Sodium borate) was dissolved in 100 ml of distilled water and heated slowly. 1 g of toluidine blue was then added. The resulting solution was filtered and stored at 4.0 °C.

Uranyl Acetate

4.0 g of uranyl acetate was dissolved in 100 ml of 70% ethyl alcohol, and stored at 4.0 °C.

Lead Citrate

This solution was prepared according to the formulation of Reynolds (1963).

Iron hematoxylin

Solution A (Mordant)

5 g of Iron alum (Ferric ammonium sulfate) was dissolved in 100 ml of distilled water, taking care not to use yellow sulfate crystals. The solution was filtered before use.

Solution B (Regaud's Hematoxylin)

1 g of hematoxylin was dissolved in 10 ml of pure ethyl alcohol
10 ml of glycerine was added, and the solution was made to 100 ml with distilled water
The was left to ripen for at least 24 hours and filtered prior to use.

FIGURES

Abbreviations

The following abbreviations will be used to describe the figures in this Section:

A, Ameloblasts
Af, Apical foramen
c, collagen
Cc, Cellular condensation
Cl, Cervical loop
D, Dentin
Dis, Root sheath disruption
E, Enamel matrix
Es, Enamel space
Fb, Gingiva fibroblast
Ide, Inner dental epithelium
Lab, Labial
Lat, Lateral
L, Fibrous Lesion
Ling, Lingual
Med, Medial
m, mitocondria
n, nucleus
O, Odontoblast
Oo, Odontogenic organ
Ode, Outer dental epithelium
PDL, Periodontal ligament
P, Papilla/Pulp
Pf, Pulp fibroblast
rer, rough endoplasmic reticulum
Rs, Epithelial root sheath
Sr, Stellate reticulum

Length bars represent 100 μm on light micrographs and 5 μm on electron micrographs.

Sectioning artifacts associated with the alveolar bone are seen on the following Figures: 1.2.2.b-d, 1.2.3.a-f, 3.2.2

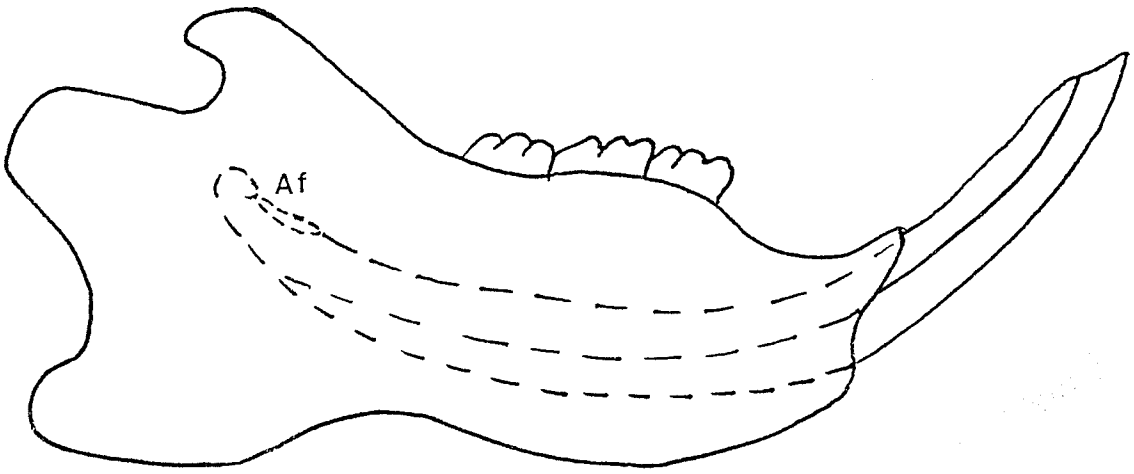
Af

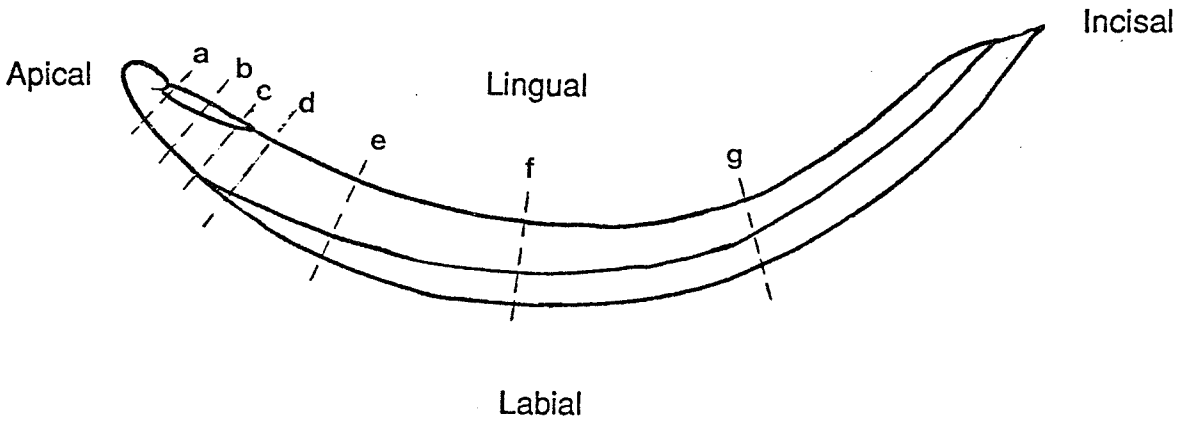
Incisal
Apical
a
b
c
d
e
f
g
Lingual
Labial

Figures 1.1.a to 1.1.g. Light microscopy cross sections of a control mandibular incisor, stained with toluidine blue.

Figure 1.1.a

Cross section through the "U"-shaped region of the odontogenic organ. The two lingual extensions have not approximated, resulting in a lingual apical foramen. (x 135)

Figure 1.1.b

Epithelial root sheath forming mesial and lateral limbs of the incisor. On the labial surface, tall columnar odontoblasts and ameloblasts; at the edge of the cervical loops, a condensation of spindle shaped cells, extends approximately 150 μm into the apical foramen. (x 70)

Figure 1.1.c

The medial and lateral arms of the root sheath nearly approximated. The cellular condensations of elongated, spindle-shaped cells adjacent to the cervical loops of the root sheaths appear as a scaffold, closing off the apical foramen. Dentin formation has progressed half way up the mesial surface of the incisor (x 70)

Figure 1.1.d

Root sheath approximation has resulted in closure of the apical foramen. Differentiation of odontoblasts, from ovoid to columnar cells, progresses lingually, parallel to dentin formation. The PDL comprises round to spindle-shaped cells. (x 70)

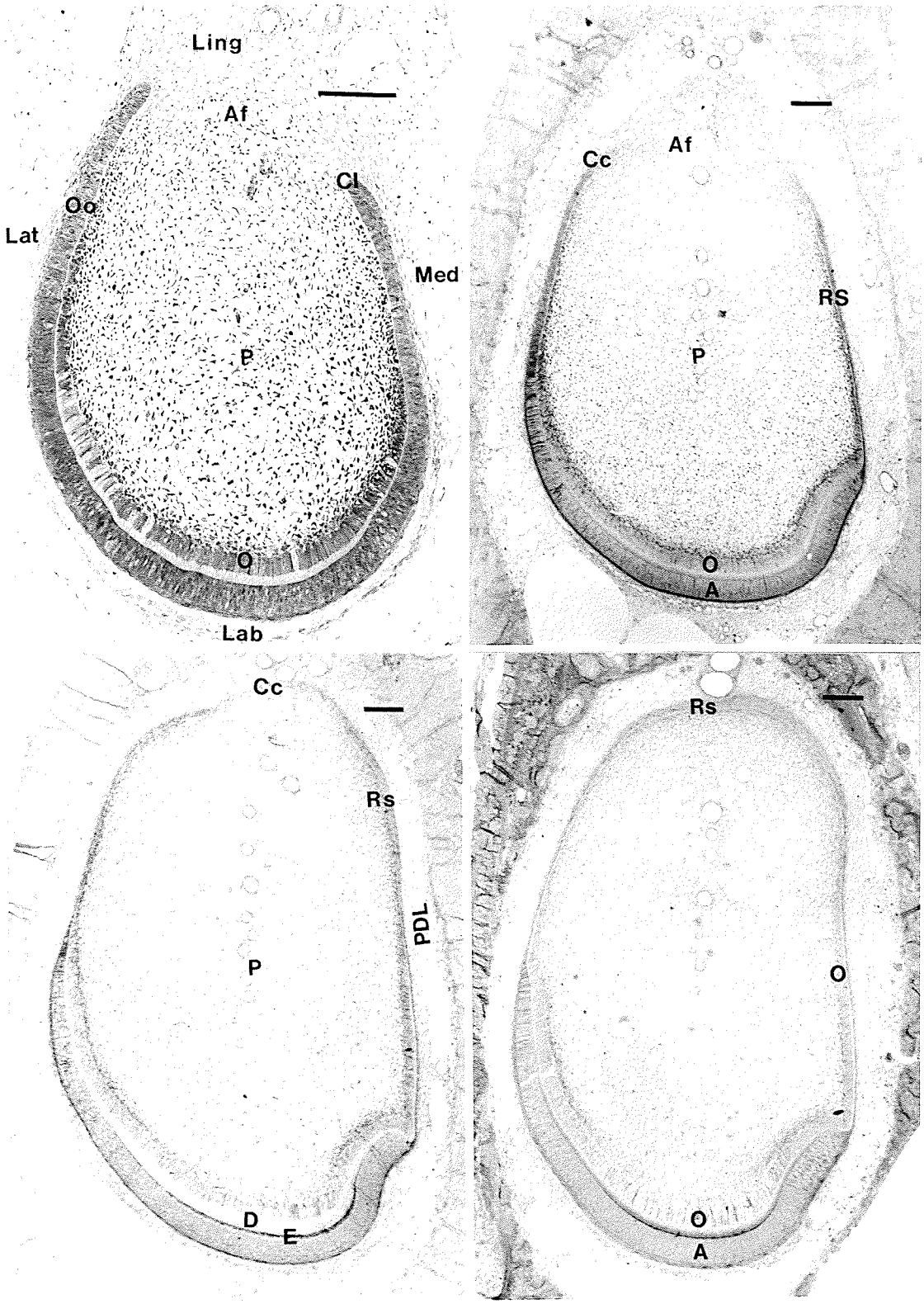
Ling
Af
Cl
Oc
Lat
Med
P
O
Lab
Cc
Af
RS
P
O
A
Cc
Rs
PDL
P
D
E
Rs
O
O
A

Figure 1.1.e

The lingual portion of the incisor is enclosed by a layer of dentin. The periodontal ligament has a definite fibrous organization. [Arrows [►] indicate the fibre orientation.] The component fibroblasts are oriented between the fibrous matrix. (x 70)

Figure 1.1.f

Dentin and enamel production is more advanced, resulting in a reduced pulp space. The PDL remains highly fibrous with an analogous orientation [arrows, ►] to that seen in Figure (1.1.e). (x 57)

Figure 1.1.g

Terminal end of the pulp chamber with PDL on the medial and lingual aspect. Orientation [►] of the fibres is perpendicular to the dentin surface. (x 57)


D
D
E
PDL
P
D
E
P
D
Es

Figure 1.2.1

Three dimensional reconstruction of incisor tooth, one week post-adriamycin administration. For diagrammatic simplicity, the reconstruction embraces an area from the apical end to where a complete dentin layer encircles the pulp. (x 100)

Letters denote light microscopy sections described in Figures 1.2.1.a - 1.2.1.e.

Cellular Disruption of Root Sheath
Dentin
Enamel
Odontogenic Organ
Root Sheath

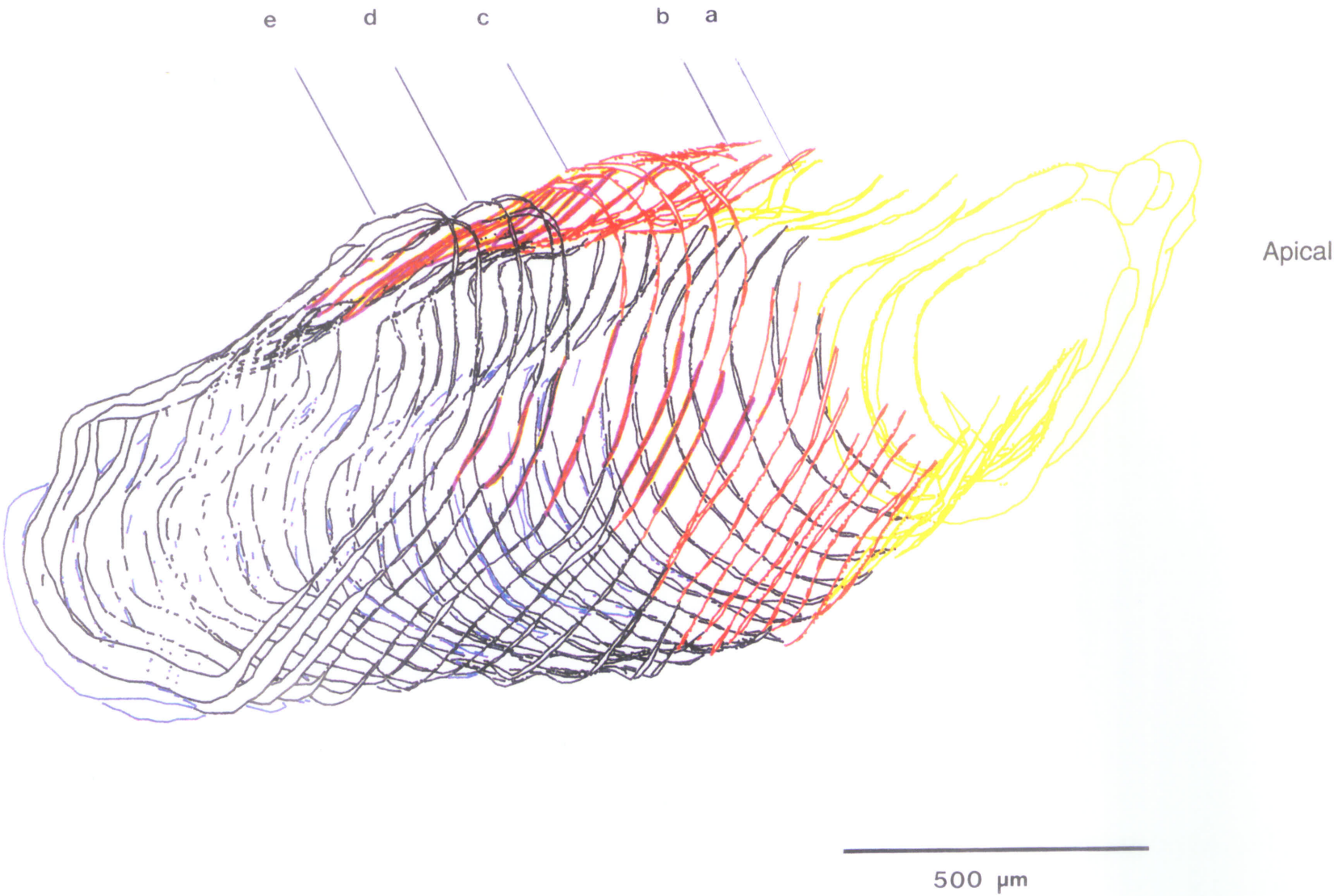
e
d
c
b
a
Apical
500 µm

Figure 1.2.1.a

Cross section through the "U" portion of the odontogenic organ, one week post-adriamycin administration. Adriamycin-induced pulpal cell death (apoptosis) is denoted by arrows [►]. (x 250)

Figure 1.2.1.b

Cross section through the epithelial root sheath with open apical foramen, one week post-adriamycin administration. Adriamycin-induced pulpal cell death (apoptosis) is denoted by arrows [►]. (x 250)

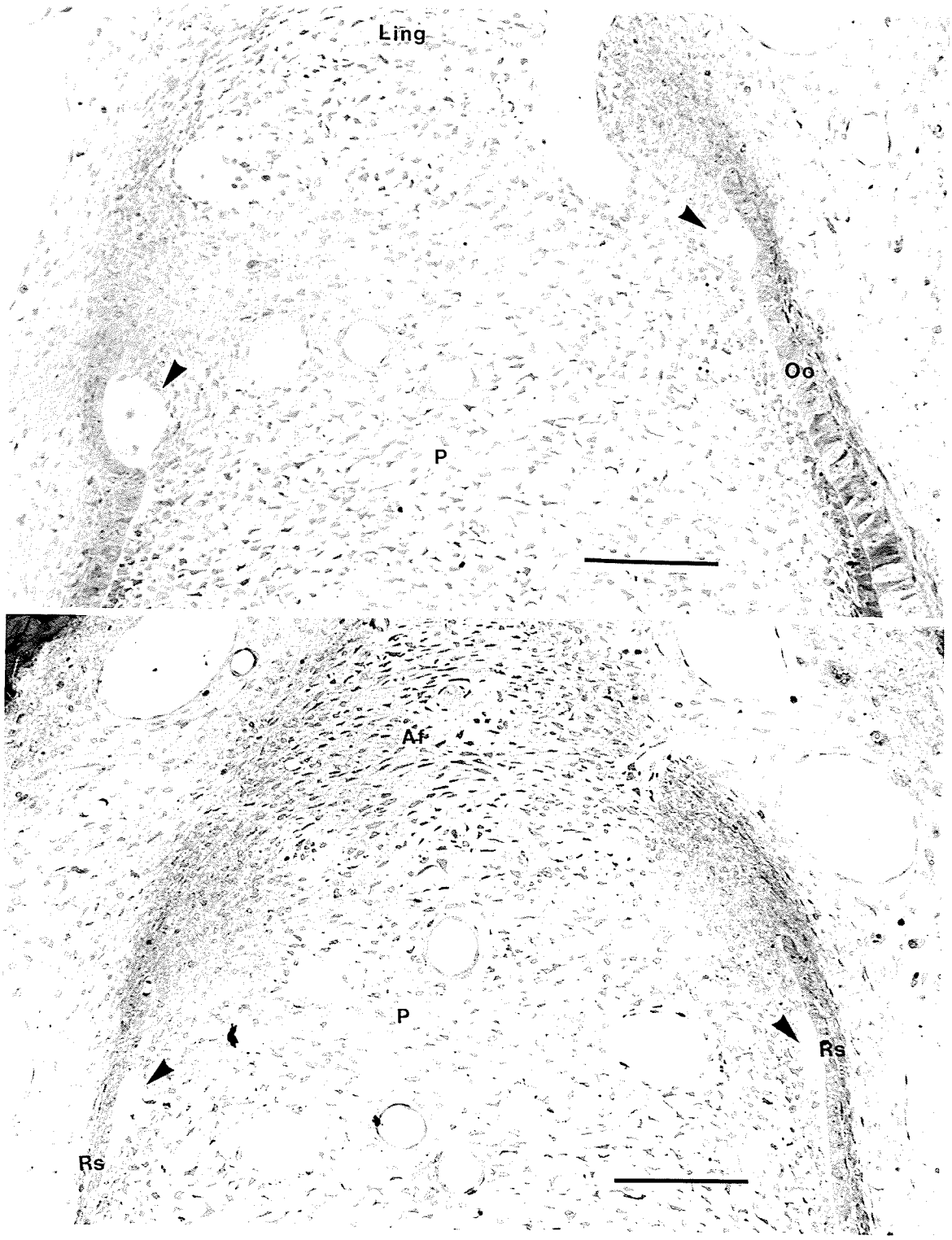
Ling
Oo
P
Af
P
Rs
Rs

Figure 1.2.1.c

Cross section through the epithelial root sheath with closed apical foramen, one week post-adriamycin administration. Adriamycin induced disruption of root sheath is delineated between arrows [►]. (x 250)

Figure 1.2.1.d

Cross section through incisor at region of early lingual dentinogenesis, one week post-adriamycin administration. Adriamycin induced disruption of root sheath is delineated between arrows [►]. (x 250)

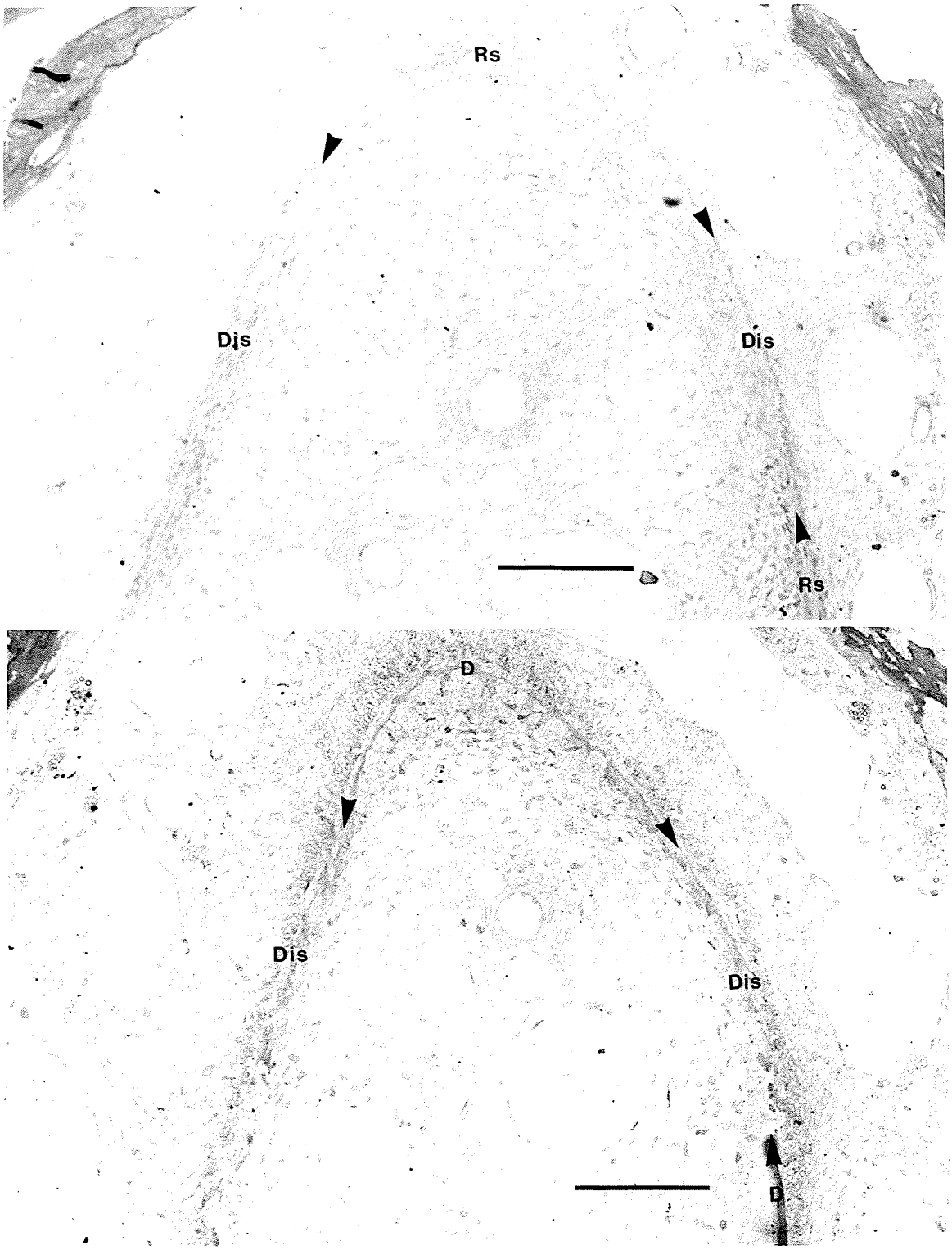
Rs
Dis
Dis
Rs
D
Dis
Dis
D

Figure 1.2.1.e

Cross section of incisor tooth, one week post-adriamycin administration. No cellular disruption noted. Dentin layer (D) has a convoluted, irregular pattern resembling osteodentin. (x 500)

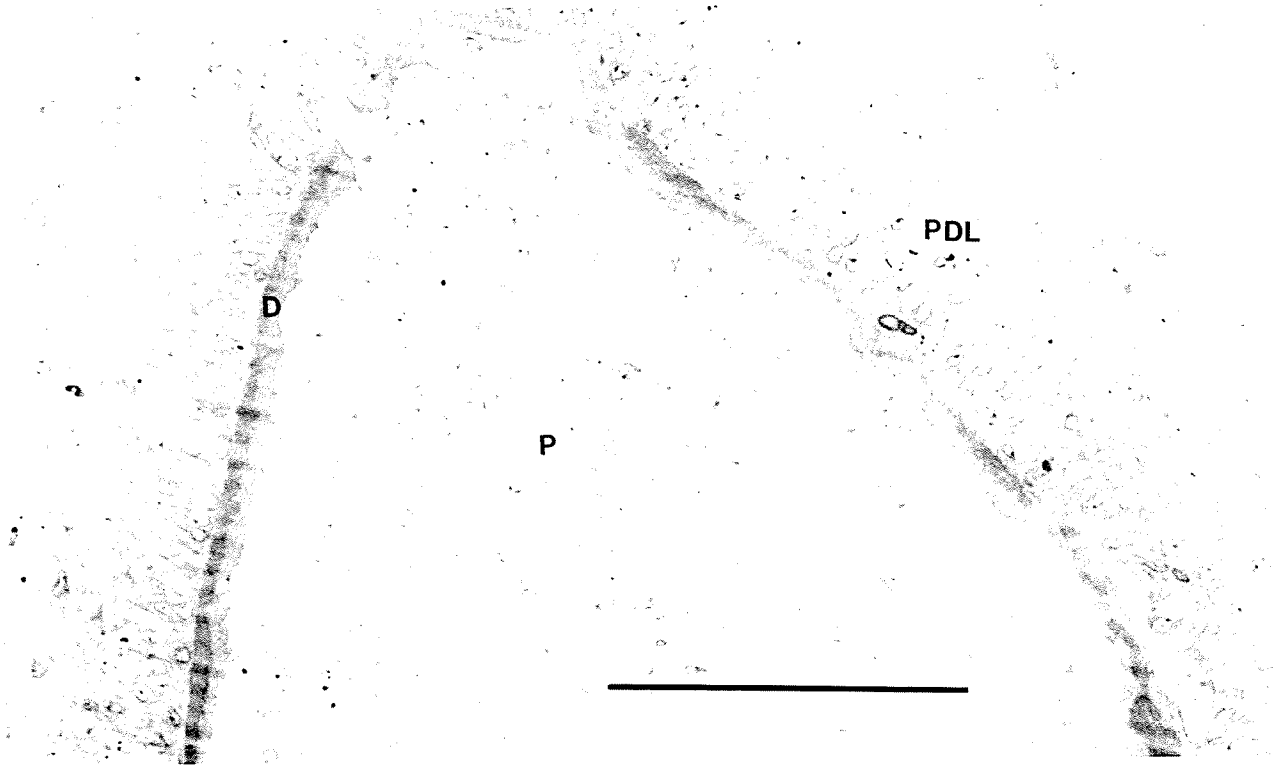
PDL
D
P

Figure 1.2.2

Three dimensional reconstruction of incisor tooth, two weeks post-adriamycin administration. For diagrammatic simplicity, the reconstruction embraces an area from the apical end to where a complete dentin layer encircles the pulp. (x 49)

Letters denote light microscopy sections described in Figures 1.2.2.a - 1.2.2.d.

Cellular Disruption of Root Sheath
Dentin
Enamel
Fibrous Lesion
Odontogenic Organ
Root Sheath

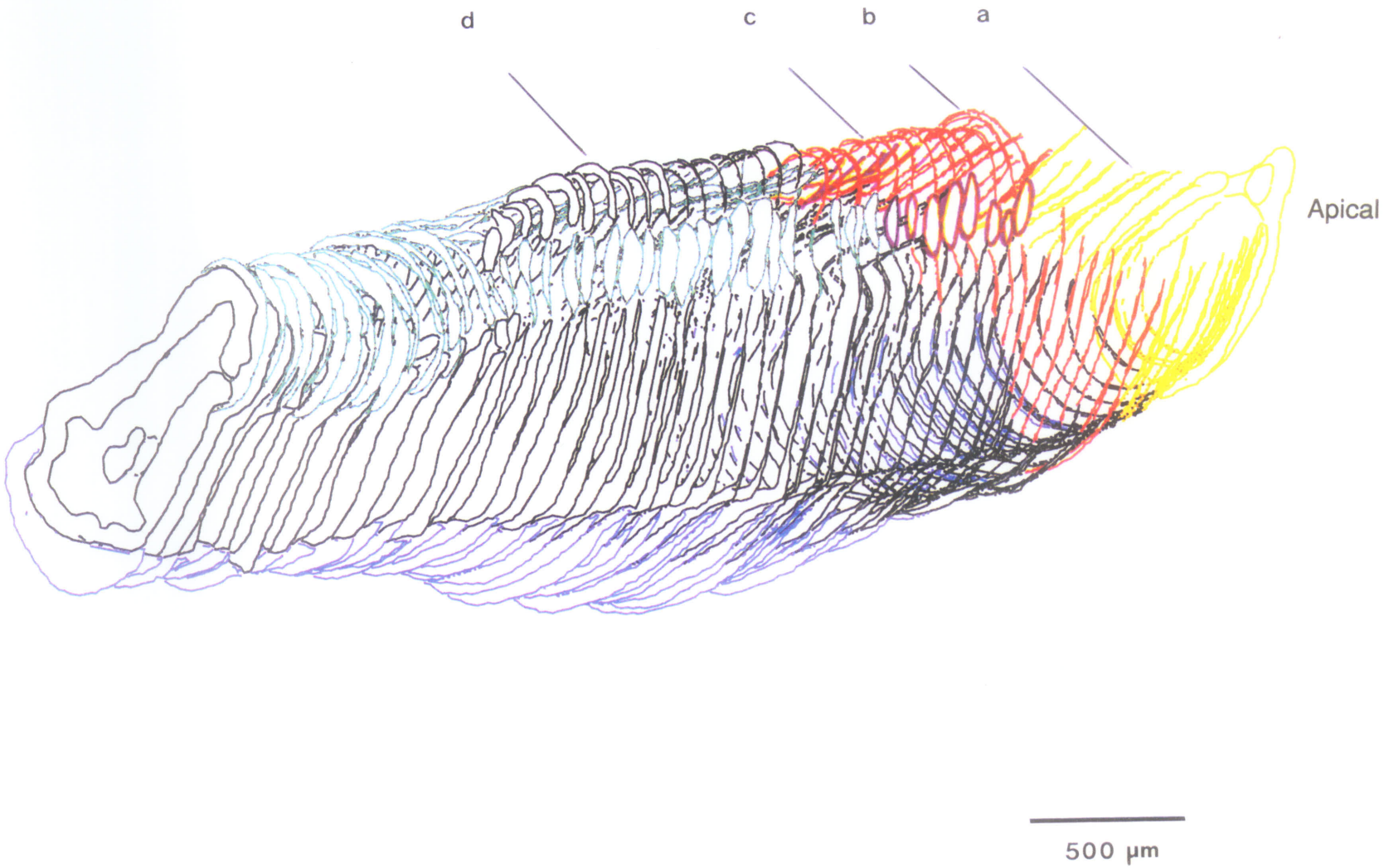
d
c
b
a
Apical
500 µm

Figure 1.2.2.a

Cross section through the "U" portion of the odontogenic organ, two weeks post-adriamycin administration. No areas of cellular apoptosis are noted. (x 250)

Figure 1.2.2.b

Cross section through the epithelial root sheath with closed apical foramen, two weeks post-adriamycin administration. Adriamycin induced disruption of root sheath is denoted between arrows [►]. (x 250)

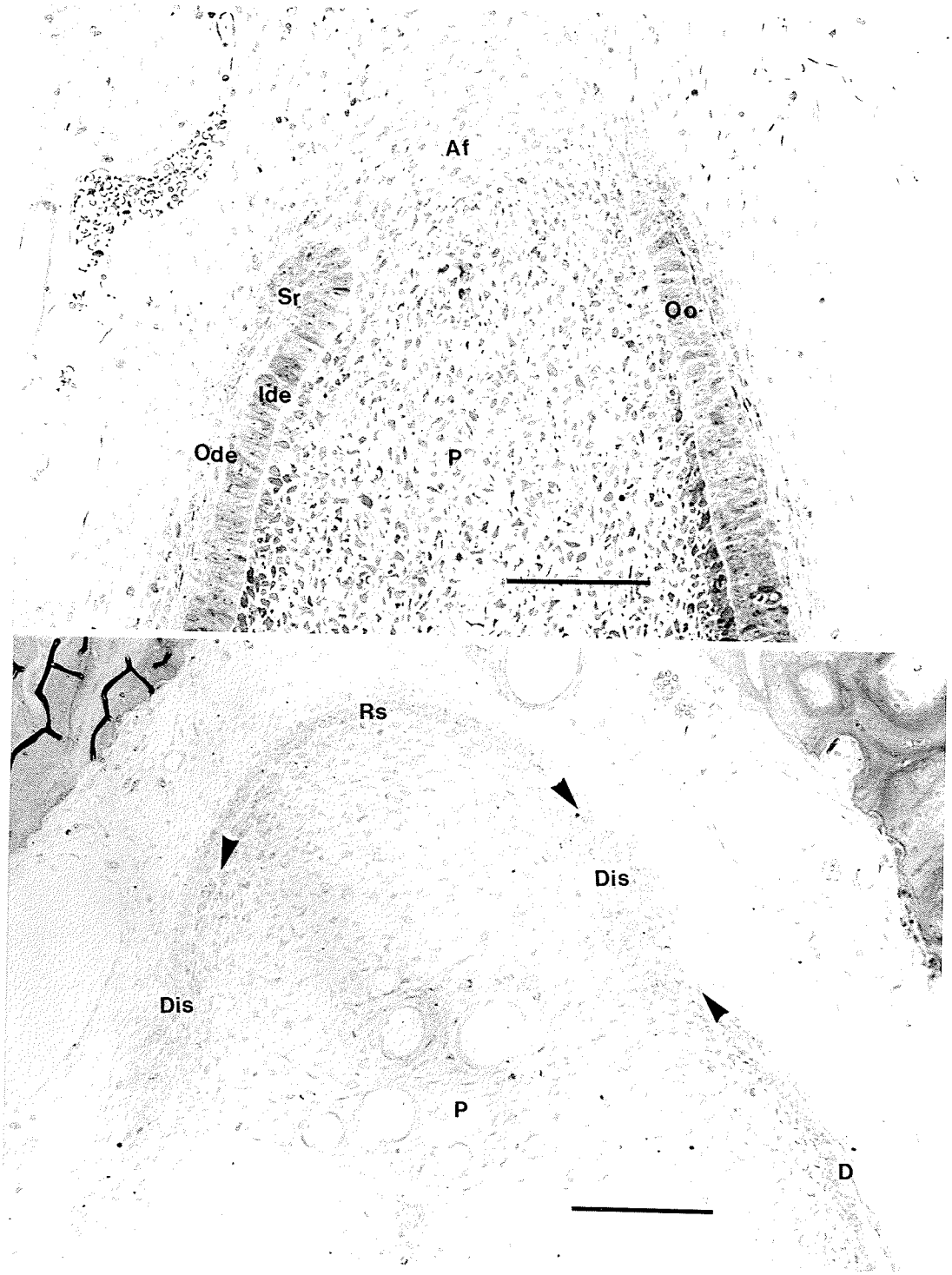
Af
Sr
Oo
Ide
Ode
P
Rs
Dis
Dis
P
D

Figure 1.2.2.c

Cross section through incisor at region of early lingual dentinogenesis, two weeks post-adriamycin administration. Adriamycin induced disruption of root sheath is delineated between arrows [►]. (x 200)

Figure 1.2.2.d

Cross section through incisor tooth with lingual dentin cap, two weeks post-adriamycin administration. Note that areas devoid of dentin are occupied by an adriamycin induced fibrous "lesion". (x 190)

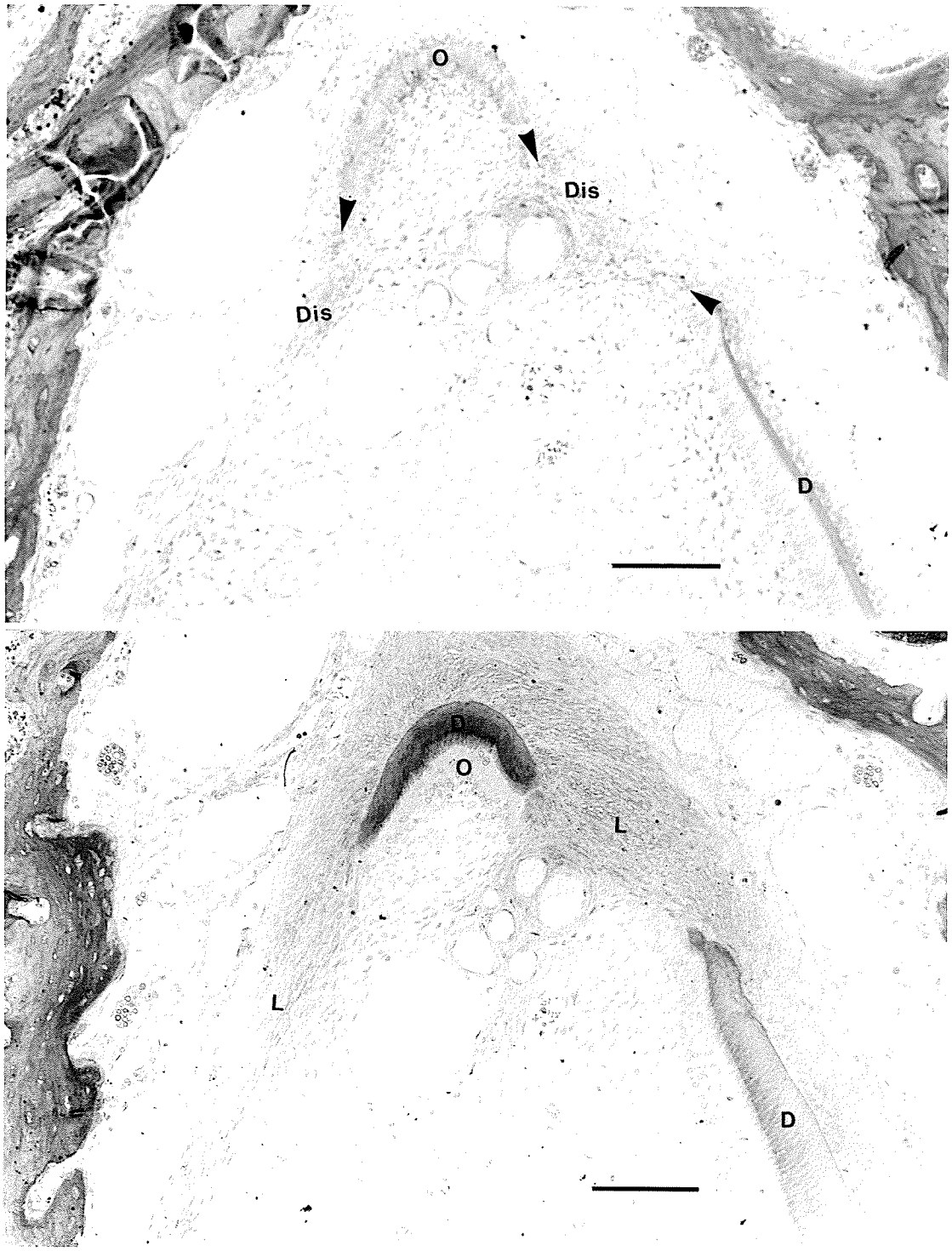
O
Dis
Dis
D
D
O
L
L
D

Figure 1.2.3

Three dimensional reconstruction of incisor tooth, three weeks post-adriamycin administration. For diagrammatic simplicity, the reconstruction embraces an area from the apical end to where only accessory canals are seen interrupting the dentin layer encircling the pulp. (x 30)

Letters denote light microscopy sections described in Figures 1.2.3.a - 1.2.3.f.

Cellular Disruption of Root Sheath
Dentin
Enamel
Fibrous Lesion
Odontogenic Organ
Root Sheath

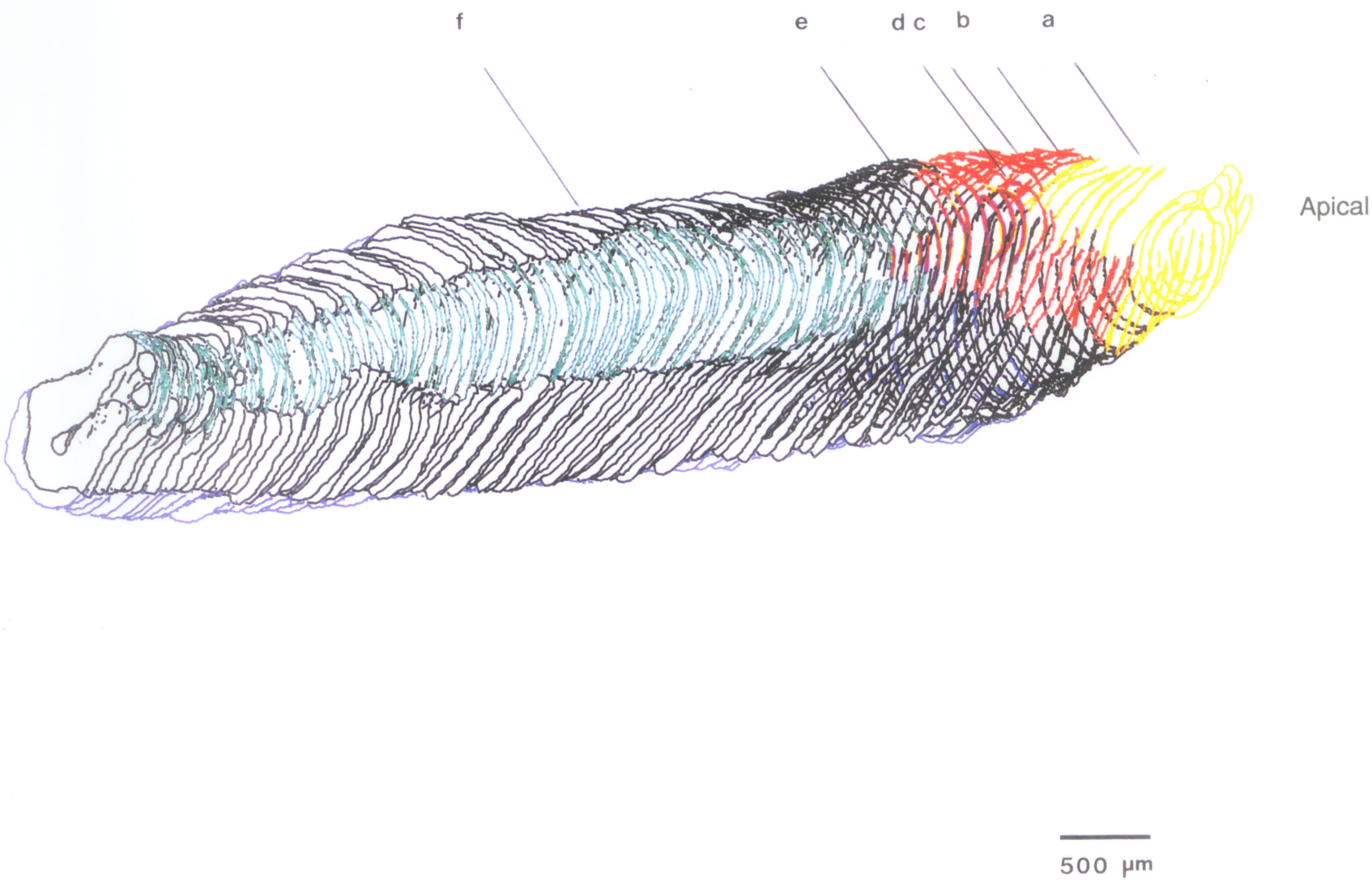
f
e
d c
b
a
Apical
500 µm

Figure 1.2.3.a

Cross section through the "U" portion of the odontogenic organ, three weeks post-adriamycin administration. No areas of cellular apoptosis are noted. (x 210)

Figure 1.2.3.b

Cross section through the epithelial root sheath with open apical foramen, three weeks post-adriamycin administration. No areas of cellular disruption are noted. (x 210)

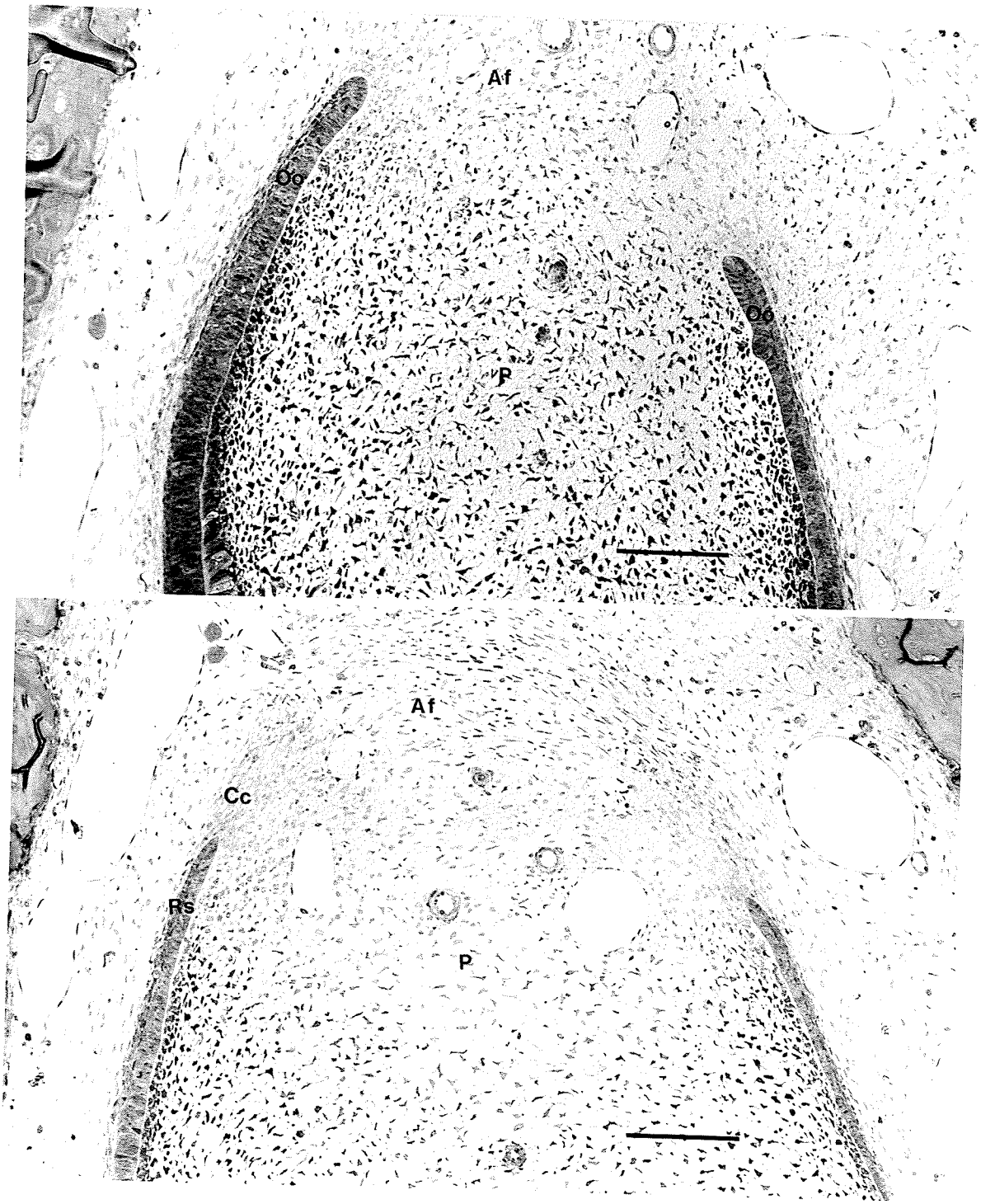
Af
Oo
Oo
P
Af
Cc
Rs
P

Figure 1.2.3.c

Cross section through the epithelial root sheath with open apical foramen, three weeks post-adriamycin administration. Cellular condensations present at the cervical loops of the root sheaths. No areas of cellular disruption are noted. (x 190)

Figure 1.2.3.d

Cross section through the epithelial root sheath with closed apical foramen, three weeks post-adriamycin administration. Adriamycin induced disruption of root sheath is denoted between arrows [►]. (x 190)

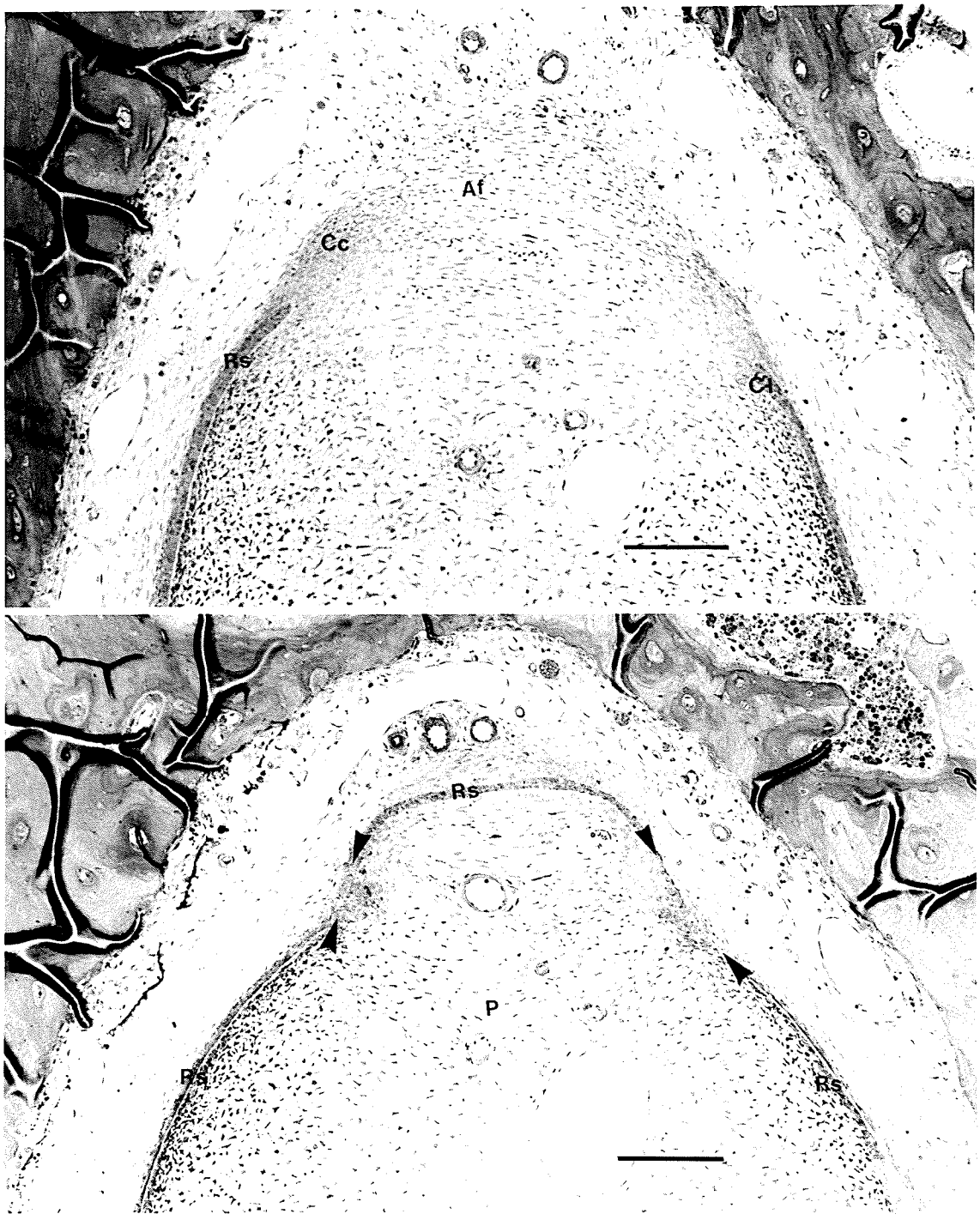
Af
Cc
Rs
Ch
Rs
P
Rs
Rs

Figure 1.2.3.e

Cross section through the incisor tooth, three weeks post-adriamycin administration. Adriamycin induced disruption of root sheath is denoted between arrows [►]. (x 190)

Figure 1.2.3.f

Cross section through the incisor tooth, three weeks post-adriamycin administration. Adriamycin induced fibrous "lesion" is seen coursing between the free edges of the medial and lateral dentin walls. Note artifact associated with dentin (D) (x 190)

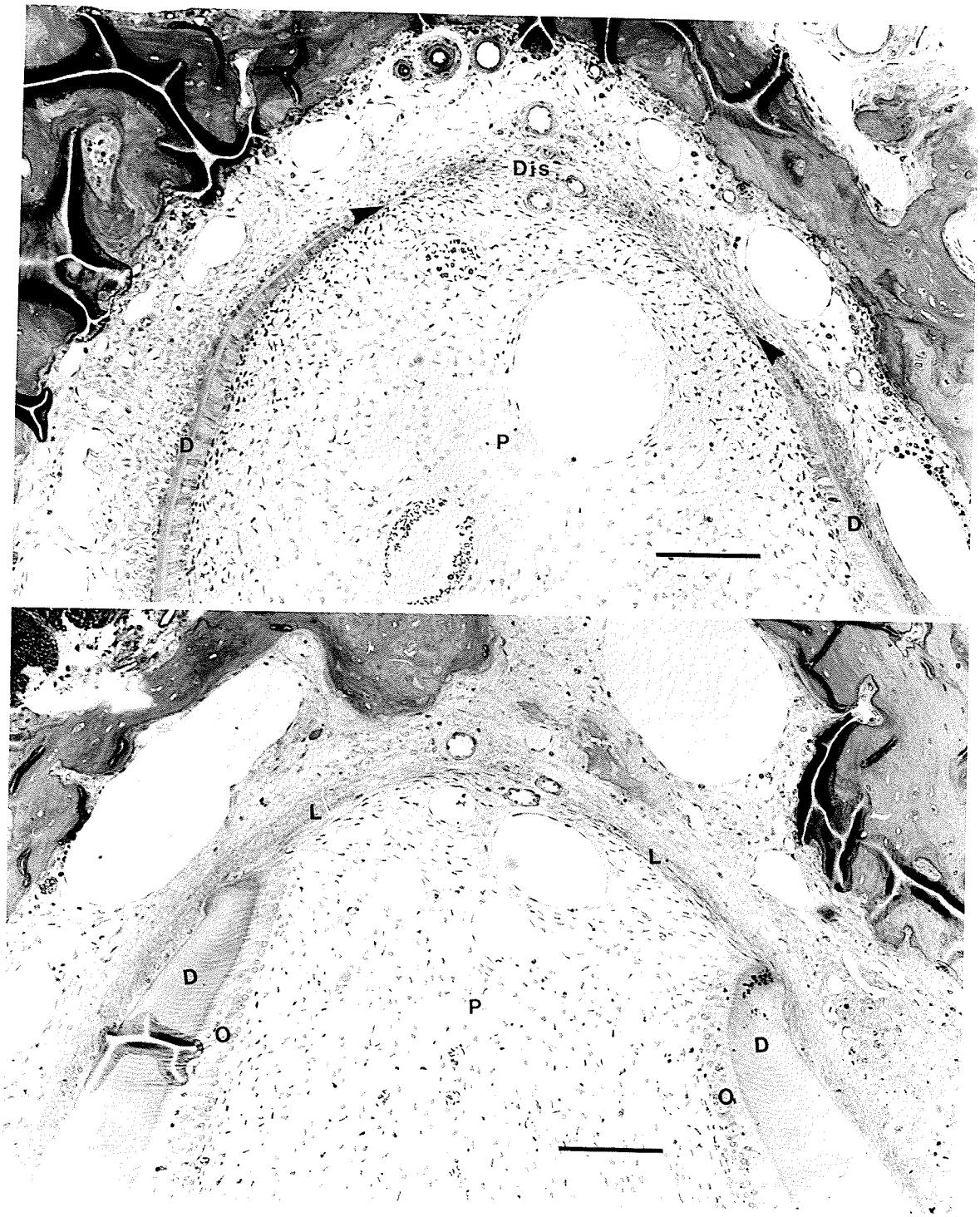
Dis
D
P
D
L
L
D
P
O
D
O

Figure 2

Three dimensional reconstruction of incisor tooth at:

i) Three Weeks post-adriamycin administration

ii) Two Weeks post-adriamycin administration

iii) One week post-adriamycin administration.

For diagrammatic simplicity, the reconstructions embrace an area from the apical end to where only accessory canals are seen interrupting the dentin layer encircling the pulp. (x 30)

Cellular Disruption of Root Sheath
Dentin
Enamel
Fibrous Lesion
Odontogenic Organ
Root Sheath

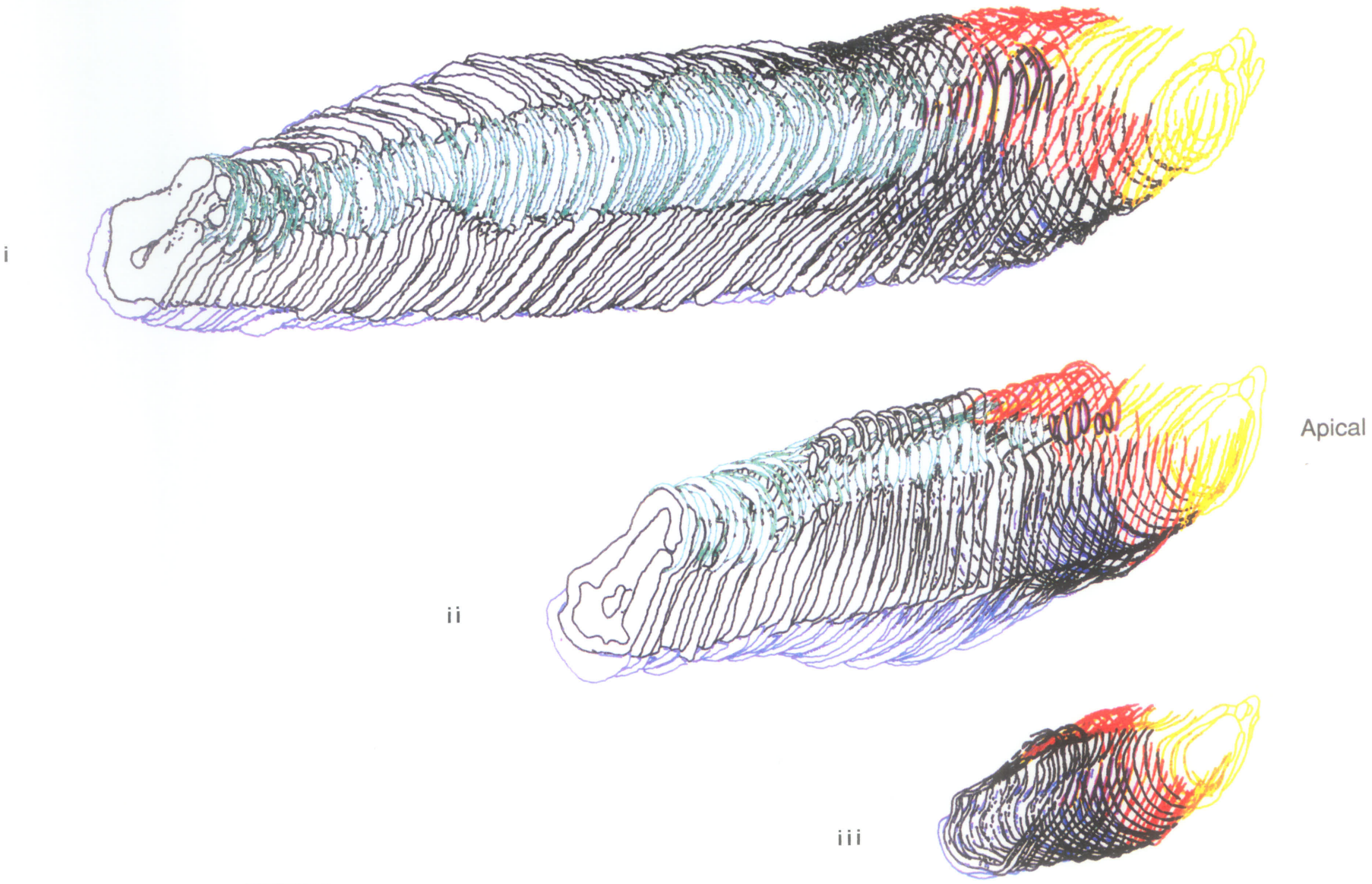
i
ii
iii
Apical
500 µm

Figure 3.1.1

Light microscopy section through the "U" portion of the odontogenic organ of a control. Representative regions of this Figure (3.1.1.a - 3.1.1.d) are subsequently shown as electron micrographs to illustrate the more detailed morphologic structure of the odontogenic organ and adjacent tissues. (x 200)

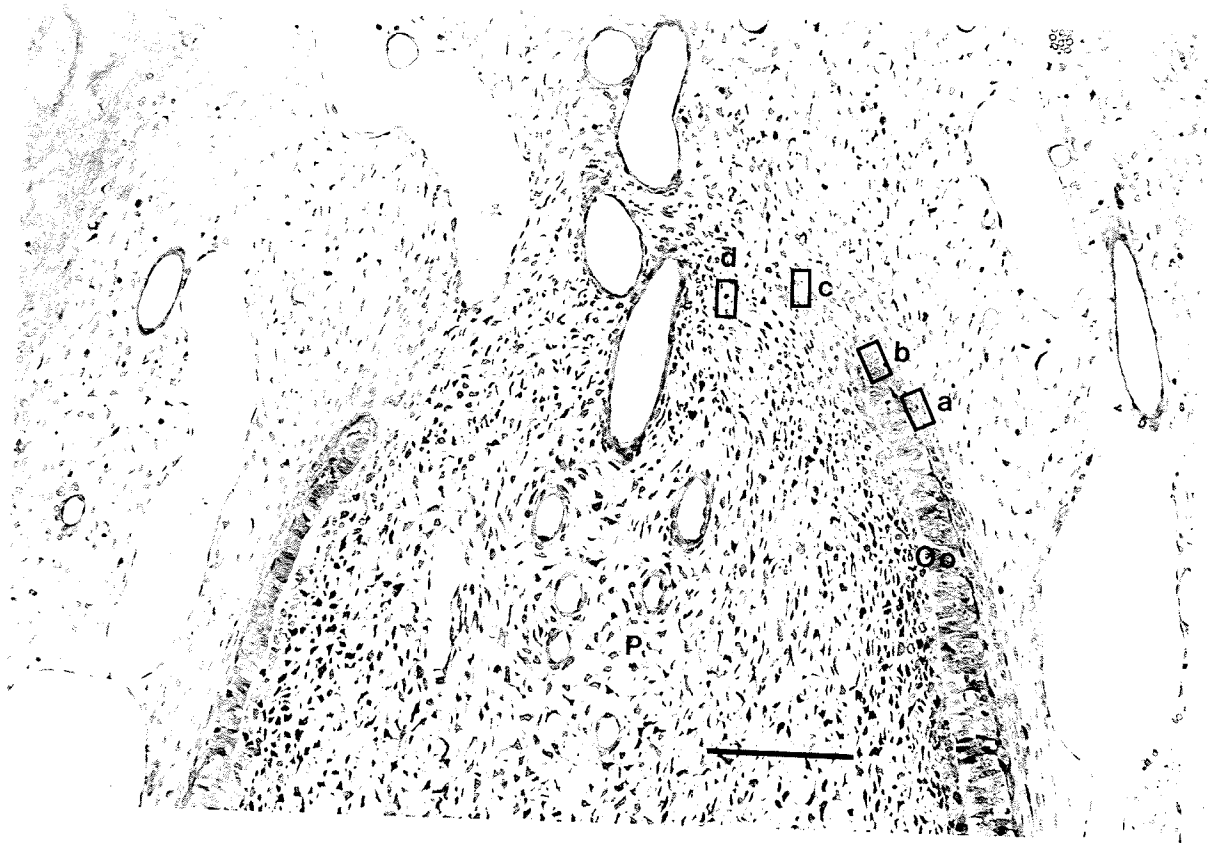
d
c
b
a
Co
P

Figure 3.1.1.a

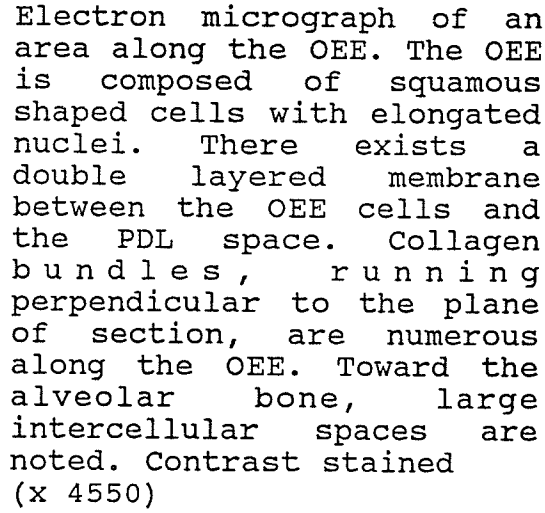

Electron micrograph of an area along the OEE. The OEE is composed of squamous shaped cells with elongated nuclei. There exists a double layered membrane between the OEE cells and the PDL space. Collagen bundles, running perpendicular to the plane of section, are numerous along the OEE. Toward the alveolar bone, large intercellular spaces are noted. Contrast stained (x 4550)

Figure 3.1.1.b

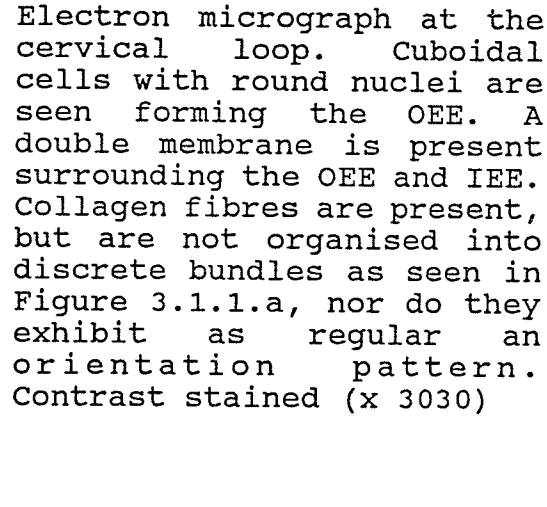

Electron micrograph at the cervical loop. Cuboidal cells with round nuclei are seen forming the OEE. A double membrane is present surrounding the OEE and IEE. Collagen fibres are present, but are not organised into discrete bundles as seen in Figure 3.1.1.a, nor do they exhibit as regular an orientation pattern. Contrast stained (x 3030)

Figure 3.1.1.c

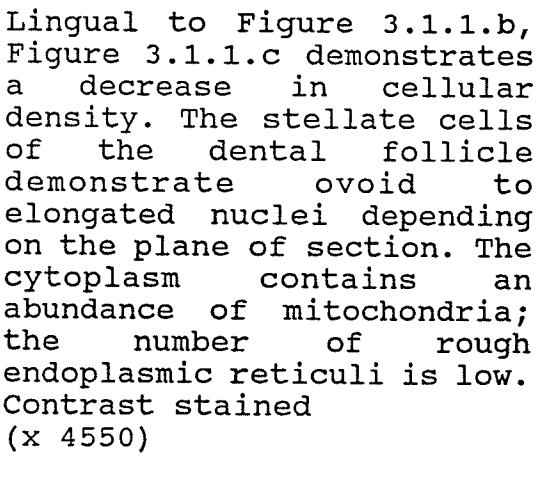

Lingual to Figure 3.1.1.b, Figure 3.1.1.c demonstrates a decrease in cellular density. The stellate cells of the dental follicle demonstrate ovoid to elongated nuclei depending on the plane of section. The cytoplasm contains an abundance of mitochondria; the number of rough endoplasmic reticuli is low. Contrast stained (x 4550)

Figure 3.1.1.d

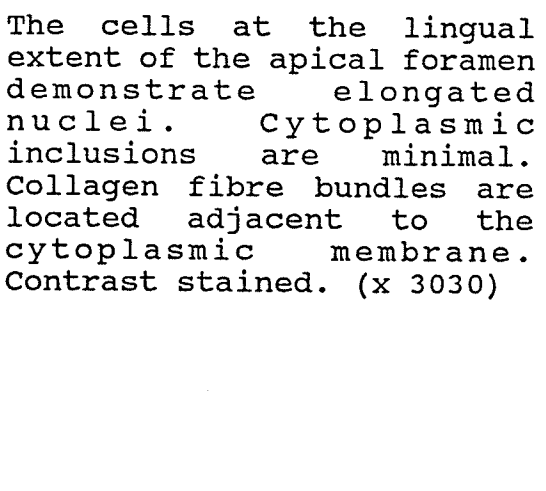

The cells at the lingual extent of the apical foramen demonstrate elongated nuclei. Cytoplasmic inclusions are minimal. Collagen fibre bundles are located adjacent to the cytoplasmic membrane. Contrast stained. (x 3030)

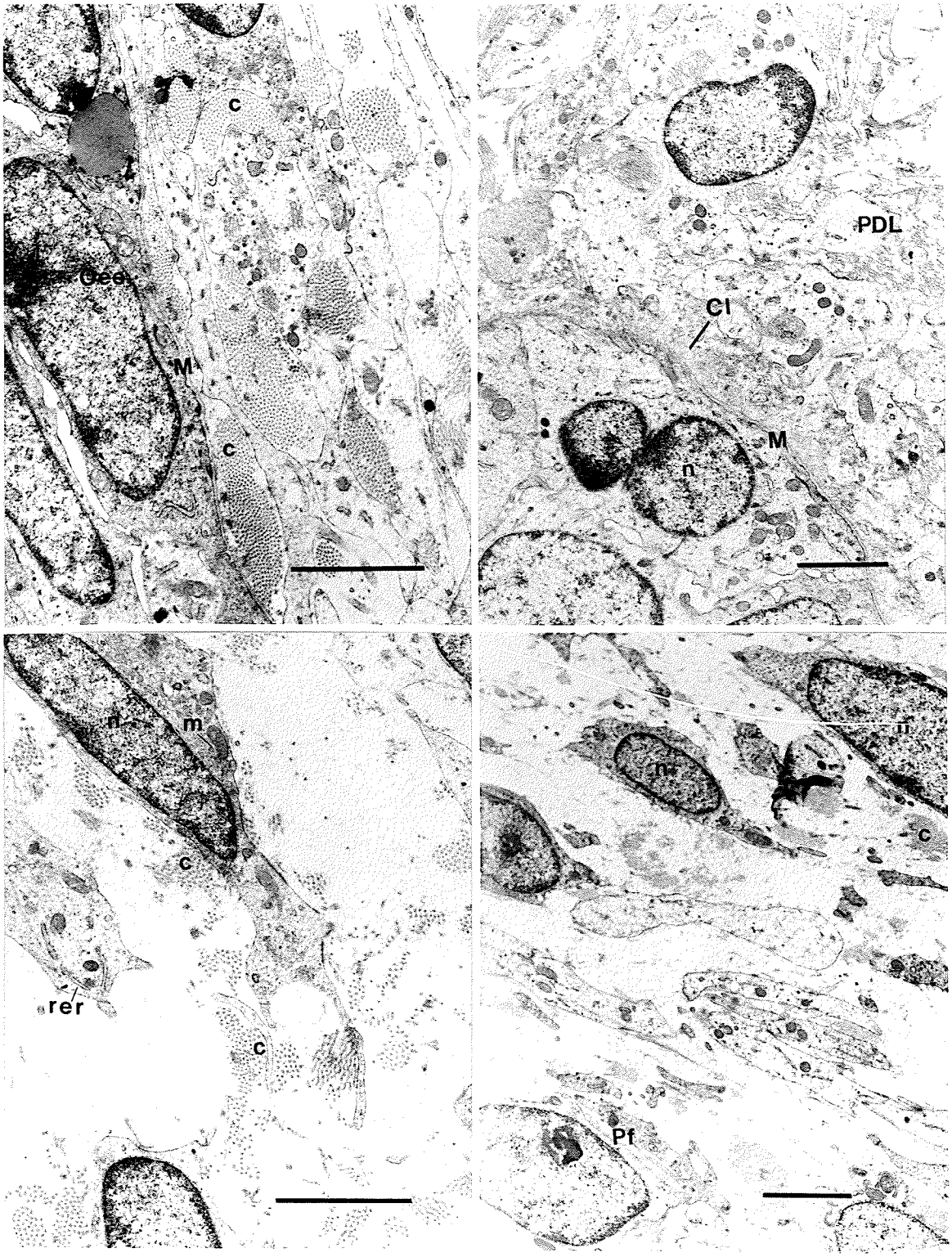
c
Oee
M
c
PDL
Cl
M
n
n
m
c
rer
c
n
c
Pf

Figure 3.1.2

Section through the "control" incisor at a point in development where the apical foramen is open, and the vertical limbs of the "U" are formed by epithelial root sheath. Representative regions of this Figure (3.1.2.a - 3.1.2.d) are subsequently shown as electron micrographs to illustrate the more detailed morphologic structure of the odontogenic organ and adjacent tissues. (x 200)

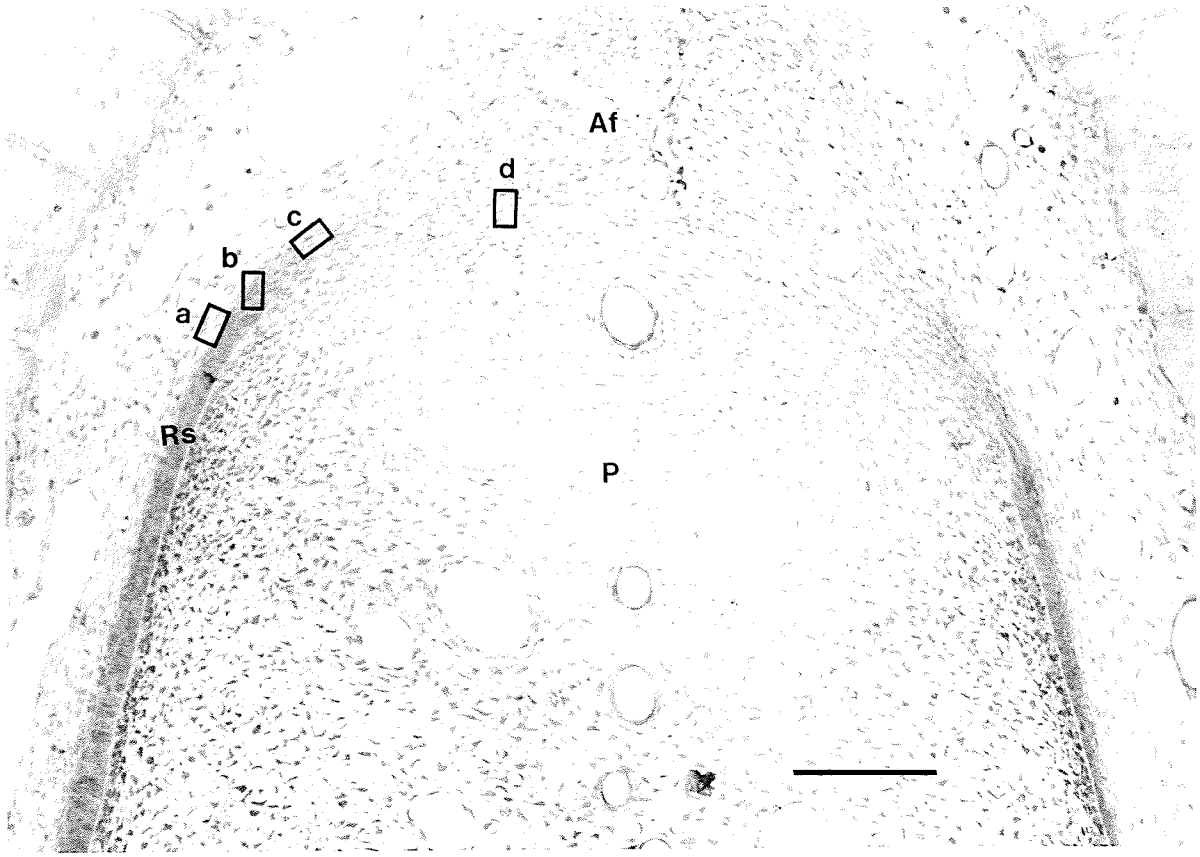
Af
d
c
b
a
Rs
P

Figure 3.1.2.a

Electron micrograph along the PDL side of the root sheath. The outer layer of the root sheath is enclosed by a double layer membrane. Collagen fibre bundles are near the root sheath, oriented perpendicular to the plane of section. Laterally, elongated follicular cells with ovoid nuclei are evident. The cytoplasm of these cells display polarity and contain lysosomes and RER. While the cells are tightly packed near the root sheath, greater intercellular spaces are noted laterally. Contrast stained (x 4550)

Figure 3.1.2.b

Electron micrograph illustrating the cellular organization at the cervical loop of the epithelial root sheath. At the cervical loop, the cells of the inner and outer layer are columnar with elongated nuclei. A double layered membrane surrounds the root sheath. Lateral to the cervical loop, the inner layer of follicular cells contain elongated nuclei and polarized organelles. There exists a zone which is low in cell density and appears to form a natural separation between the dental papilla and dental follicle. The dental papilla cells associated with the pulp exhibit a stellate appearance with associated collagen fibre bundles. These cells have not yet come into approximation with the inner layer of the root sheath. Contrast stained (x 1980)

Figure 3.1.2.c

Electron micrograph.
The follicle cells have attained a definite orientation, running from labial to lingual. The nuclei vary in shape from ovoid to squamous. While lysosomes are present, the number of cytoplasmic inclusions, ie. RER and mitochondria are low. Collagen fibre bundles are seen coursing between the cells, perpendicular to the plane of section. Contrast stained (x 3030)

Figure 3.1.2.d

The cells of the pulp demonstrate a stellate appearance with round to ovoid nuclei. The collagen fibre bundles associated with the pulp cells are coarse. Large intercellular spaces are present. Contrast stained (x 3030)

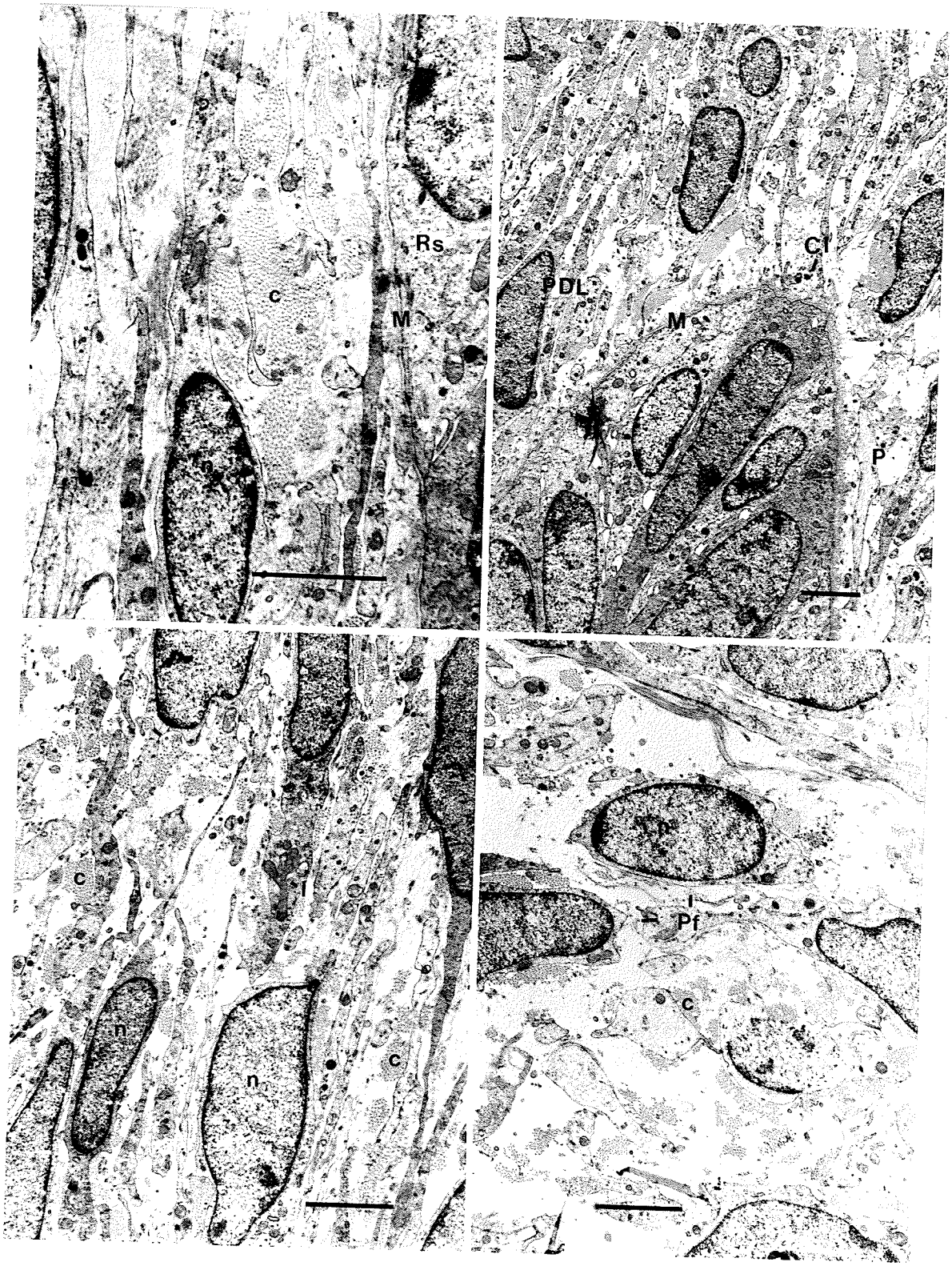
Rs
c
M
n
PDL
M
Cl
P
c
l
n
n
c
l
Pf
c

Figure 3.2.1

Light microscopy section through 3 week post-adriamycin induced "lesion", 2500 μm from the root apex. (Note: this immature "lesion" is not completely formed on the lingual surface of the incisor.) Representative regions of this Figure (3.2.1.a - 3.2.1.d) are subsequently shown as electron micrographs to illustrate the more detailed morphologic structure of the "lesion" and adjacent tissues. (x 190)

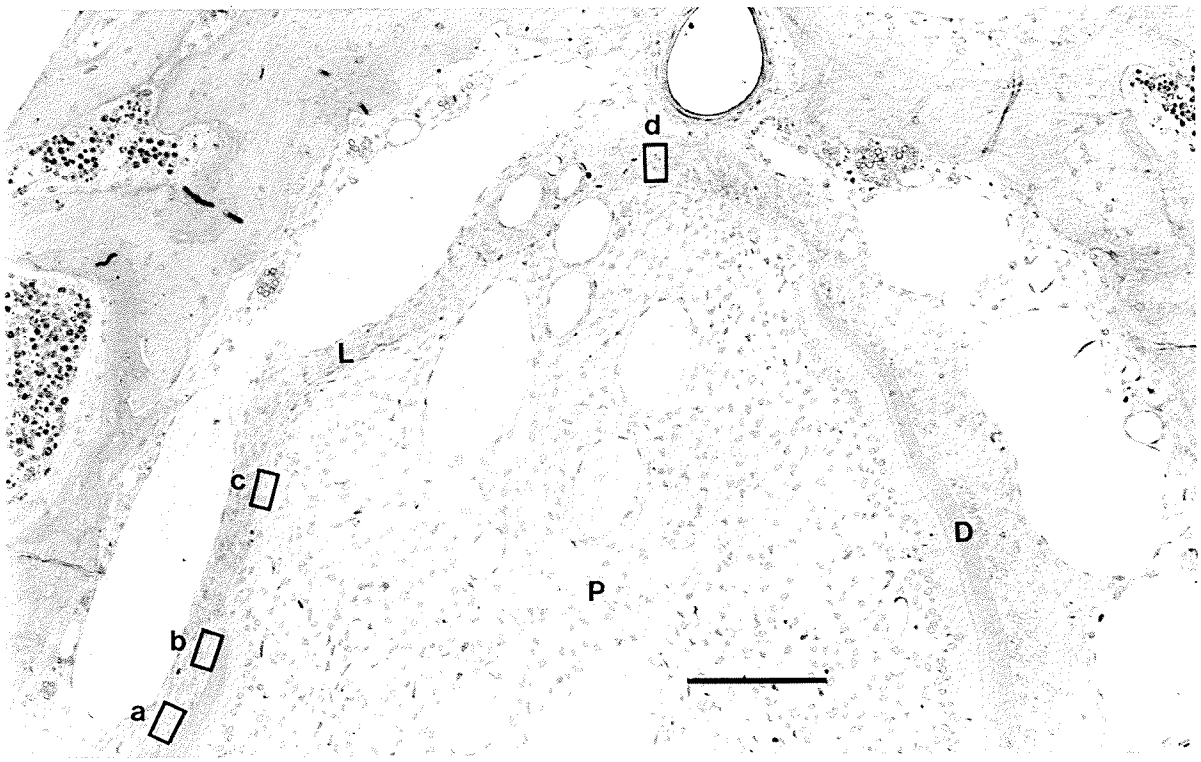
d
L
c
D
P
b
a

Figure 3.2.1.a

Electron micrograph representing an area of normal PDL labial to the "lesion" area. Near the dentin surface, flattened fibroblasts with elongated nuclei are noted. The cytoplasm, which is polarized, contains a large quantity of organelles, particularly RER and mitochondria. Collagen fibre bundles are seen running between the fibroblasts, perpendicular to the plane of section. The cells are tightly packed with little intercelluar space present. Contrast stained (x 3030)

Figure 3.2.1.b

Electron micrograph at the free edge of dentin. The odontoblast processes wrap around the dentin apex and come in contact with the lateral dentin surface. Collagen fibre bundles are present next to the odontoblasts and fibroblasts with elongated nuclei. Contrast stained (x 3030)

Figure 3.2.1.c

Stellate shaped pulp cells with round to ovoid nuclei. A low cell density is noted in the pulp with a fine, non-bundled collagenous matrix between the pulp cells. Lateral to the pulp, are intensely stained spindle shaped fibroblasts with elongated nuclei. The predominant cellular inclusions are RER and mitochondria. Contrast stained (x 3030)

Figure 3.2.1.d

Electron micrograph representing the region where the lateral and medial halves of the "lesion" have not yet approximated. The nuclei of the cells are ovoid and less intensely stained than the fibroblasts in the "lesion". The collagen fibre bundles demonstrate a delicate, fine appearance: RER and mitochondria still form the major of the cytoplasmic organelles. Contrast stained (x 3030)

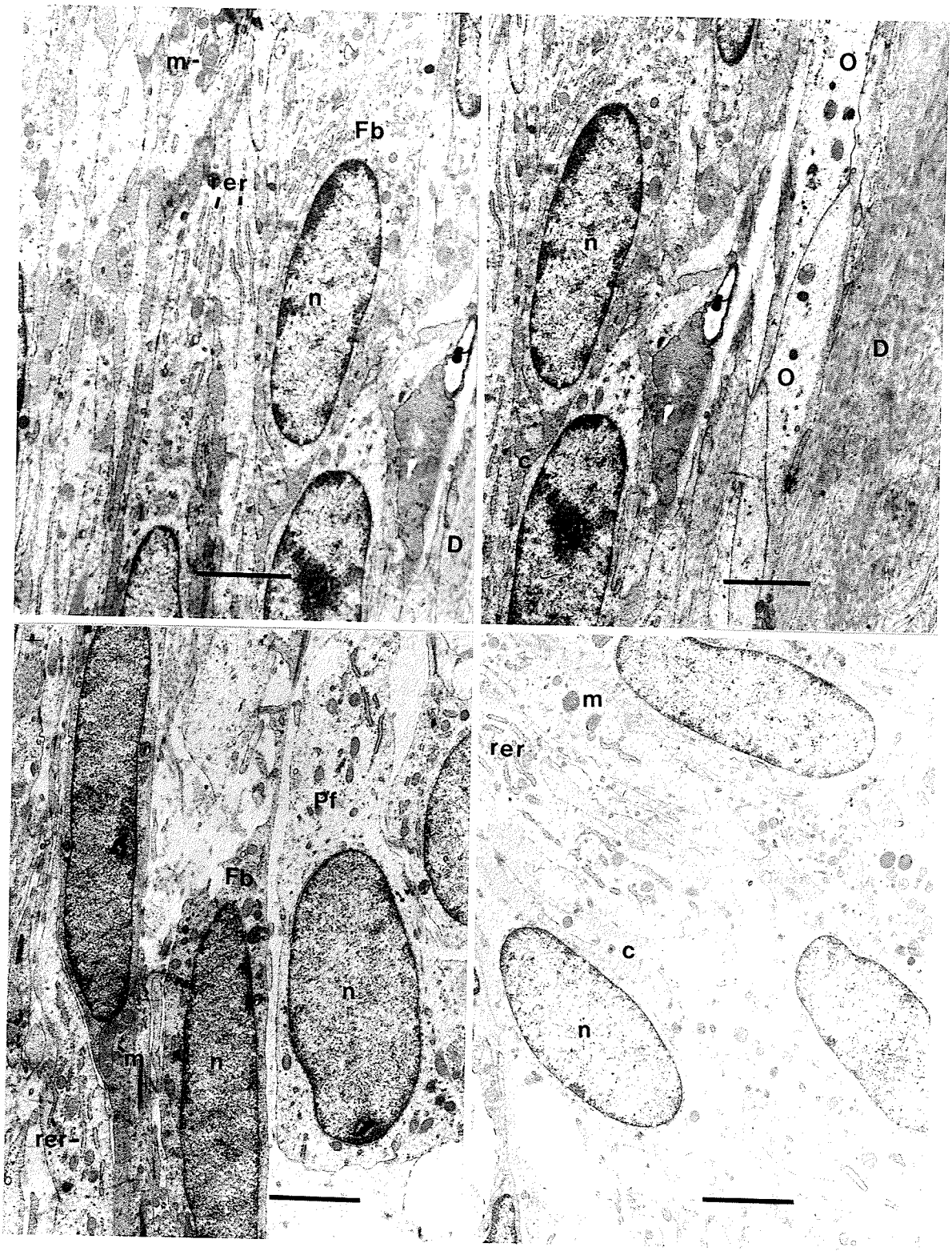
m
Fb
rer
n
D
O
n
O
D
c
Pf
Fb
n
m
n
rer
m
rer
c
n

Figure 3.2.2

Light microscopy section through 3 week post-adriamycin induced "lesion", 5100 μm from the root apex. (Note: this is a mature, fully formed fibrous "lesion".) Representative regions of this Figure (3.2.2.a - 3.2.2.d) are subsequently shown as electron micrographs to illustrate the more detailed morphologic structure of the "lesion" and adjacent tissues. (x 190)

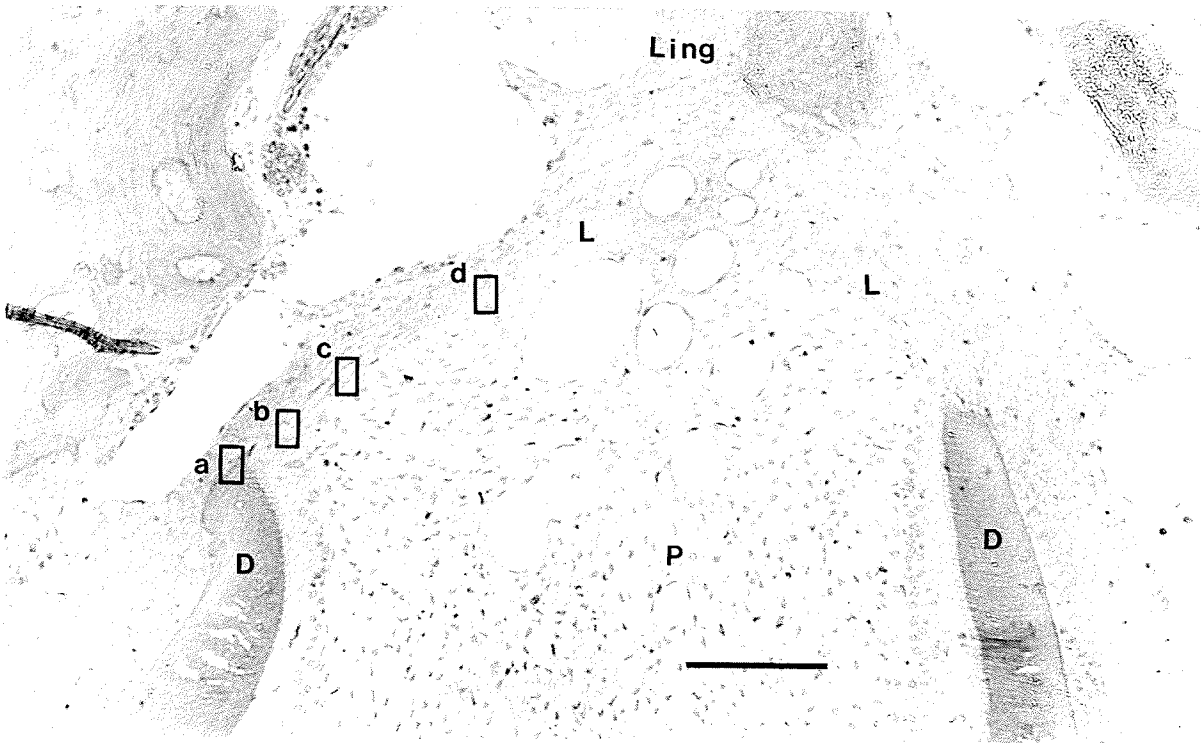
Ling
L
L
d
c
b
a
D
P
D

Figure 3.2.2.a

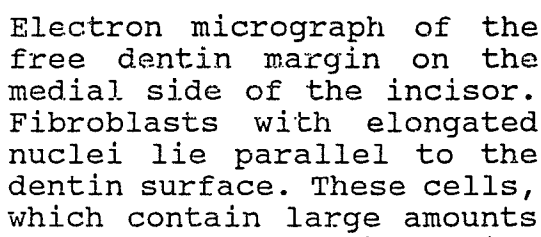

Electron micrograph of the free dentin margin on the medial side of the incisor. Fibroblasts with elongated nuclei lie parallel to the dentin surface. These cells, which contain large amounts of RER, are polarized with the organelles toward the lingual end of the incisor. Moving toward the alveolar bone, the cell density decreases, with more intercellular collagen bundles present. Contrast stained (x 1360)

Figure 3.2.2.b

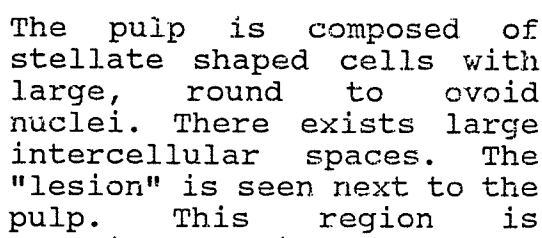

The pulp is composed of stellate shaped cells with large, round to ovoid nuclei. There exists large intercellular spaces. The "lesion" is seen next to the pulp. This region is comprised of tightly packed, intensely staining spindle shaped cells [as indicated by ←→], 6-8 cells in thickness. The cytoplasm of these cells contain relatively few organelles. Lingual to the intensely staining layer, fibroblasts with plump, ovoid nuclei are present. These cells contain a high quantity of organelles similar to the fibroblasts in Figure 3.2.2.a. (Note that the black wispy lines seen throughout are artifact) Contrast stained (x 1360)

Figure 3.2.2.c

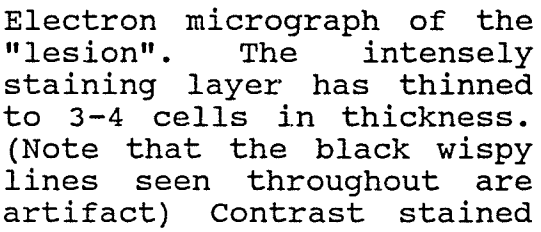

Electron micrograph of the "lesion". The intensely staining layer has thinned to 3-4 cells in thickness. (Note that the black wispy lines seen throughout are artifact) Contrast stained (x 1360)

Figure 3.2.2.d

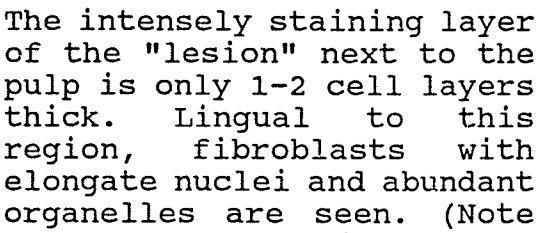

The intensely staining layer of the "lesion" next to the pulp is only 1-2 cell layers thick. Lingual to this region, fibroblasts with elongate nuclei and abundant organelles are seen. (Note that the black wispy lines seen throughout are artifact) Contrast stained (x 1360)

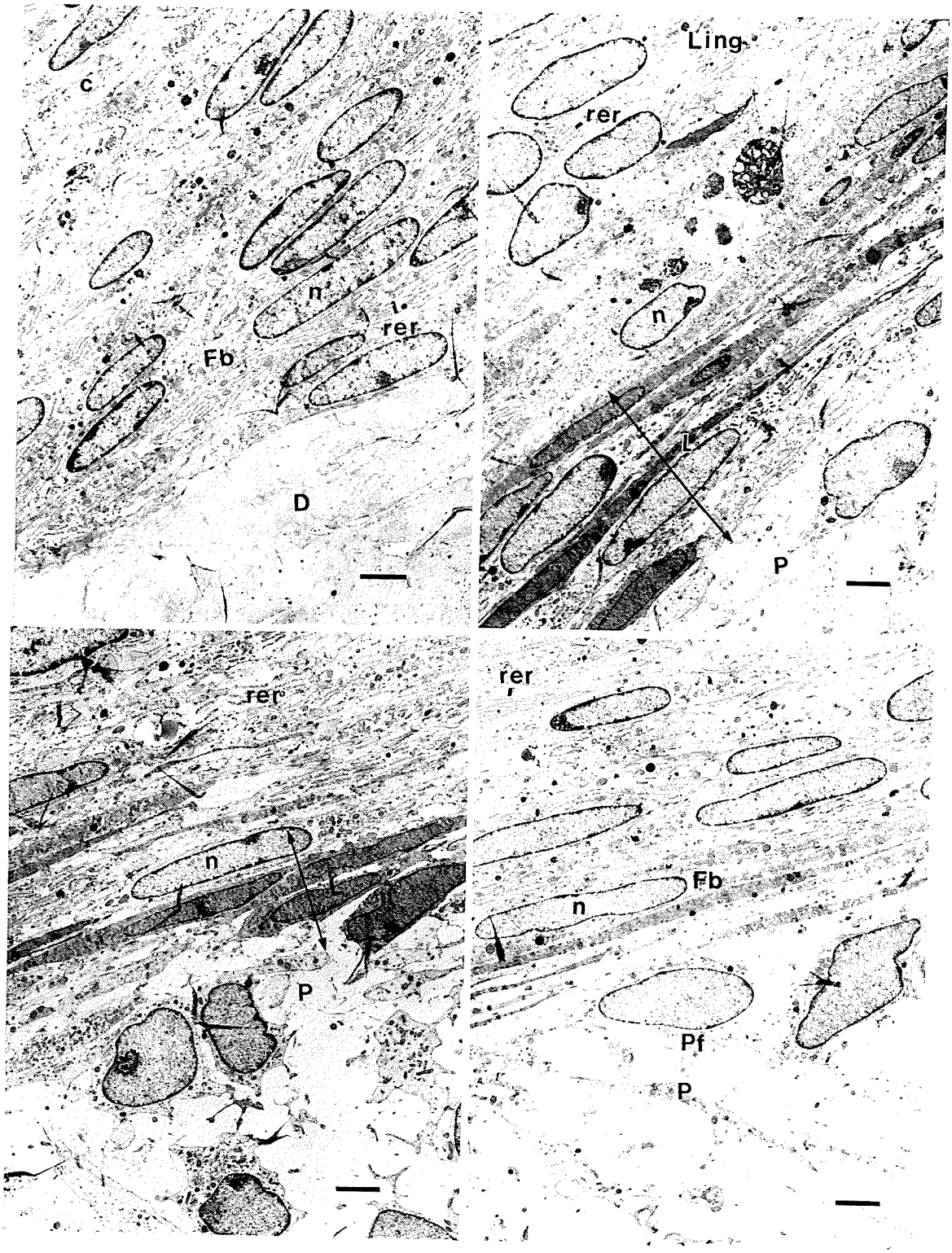
c
n
rer
Fb
D
Ling.
rer
n
L
P
rer
n
P
rer
Fb
n
Pf
P

Figure 4.1.a

Radioautograph illustrating ^{3}H-Tdr incorporation in the pulp and root sheath (1320 μm from the apex) in a control animal. Stained with iron hematoxylin (x 400)

Figure 4.1.b

Radioautograph illustrating ^{3}H-Tdr incorporation in the pulp and root sheath (1320 μm from the apex) in a 2 week post-adriamycin injected animal. Stained with iron hematoxylin (x 390)

Figure 4.1.c

Radioautograph illustrating ^{3}H-Tdr incorporation in the pulp and root sheath (1320 μm from the apex) in a 3 week post-adriamycin injected animal. Stained with iron hematoxylin (x 390)

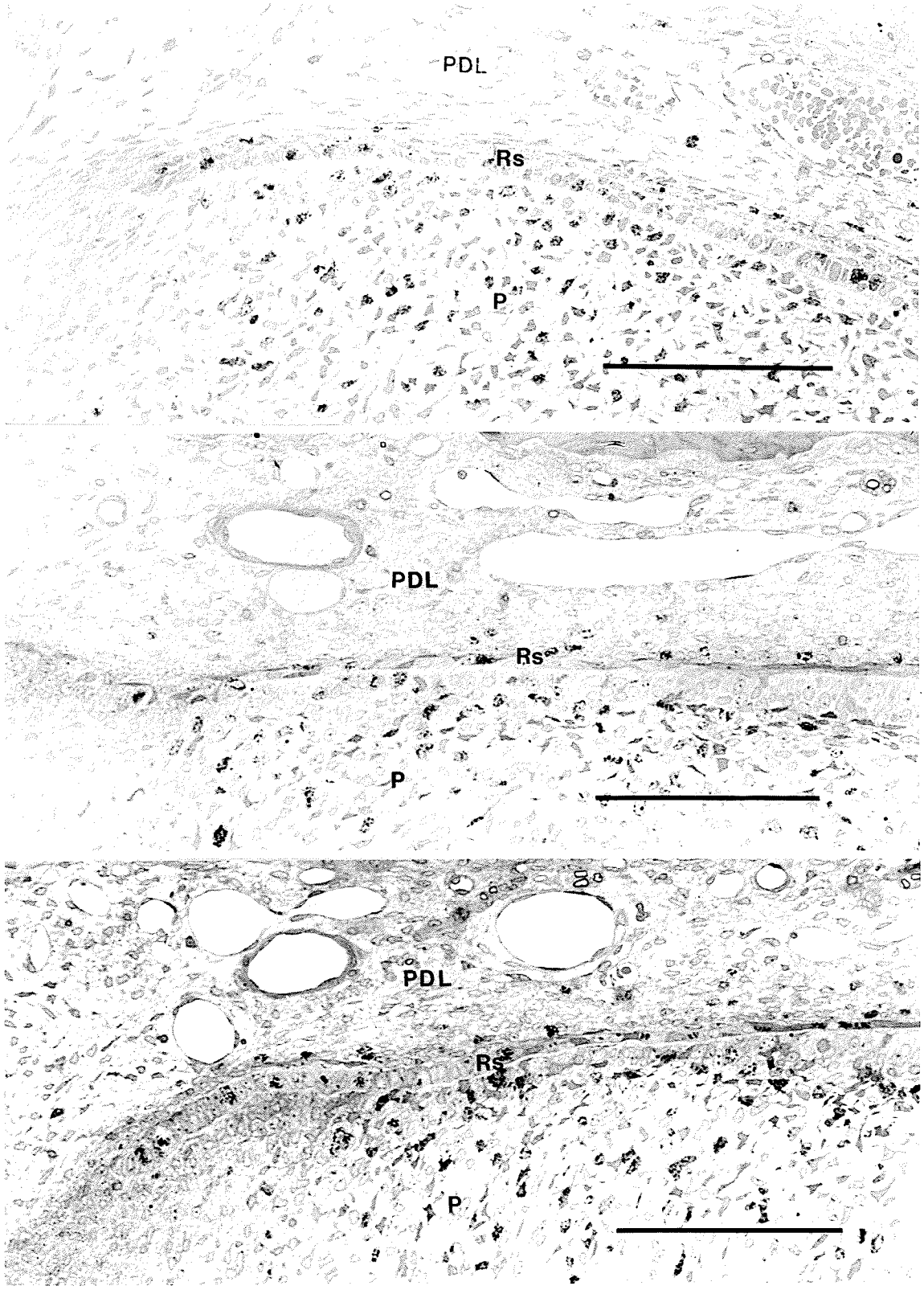
PDL
Rs
P
PDL
Rs
P
PDL
Rs
P

Figure 4.2.a

Radioautograph illustrating minimal ^{3}H-Tdr incorporation in the PDL (3300 μm from the apex) in a control animal. Stained with iron hematoxylin (x 780)

Figure 4.2.b

Radioautograph illustrating significant ^{3}H-Tdr incorporation in the adriamycin induced "lesion" (3300 μm from the apex) in a 2 week post-adriamycin injected animal. Stained with iron hematoxylin (x 780) [Note the artifact associated with dentin]

Figure 4.2.c

Radioautograph illustrating significant ^{3}H-Tdr incorporation in the adriamycin induced "lesion" (3850 μm from the apex) in a 3 week post-adriamycin injected animal. Stained with iron hematoxylin (x 390) [Note the artifact associated with dentin]

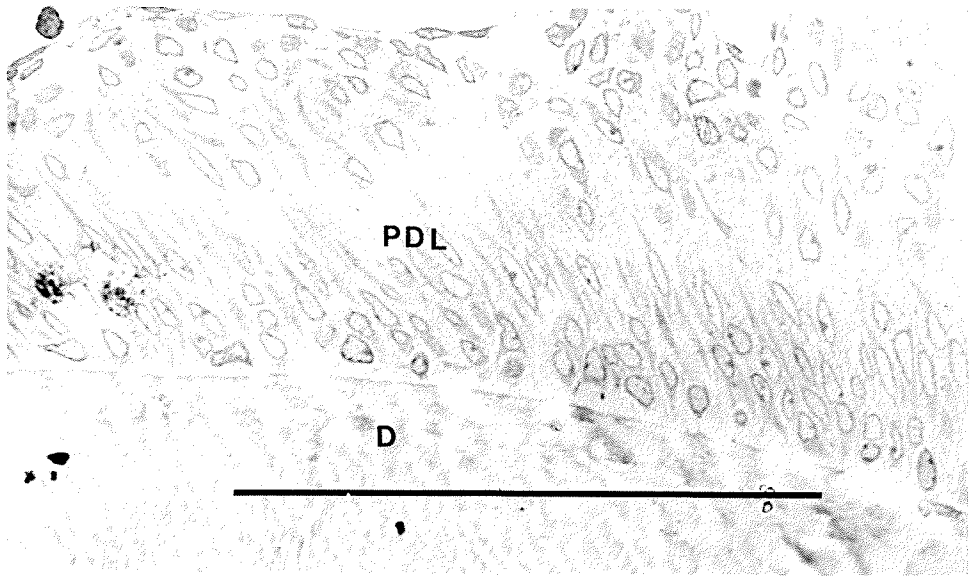
PDL
D

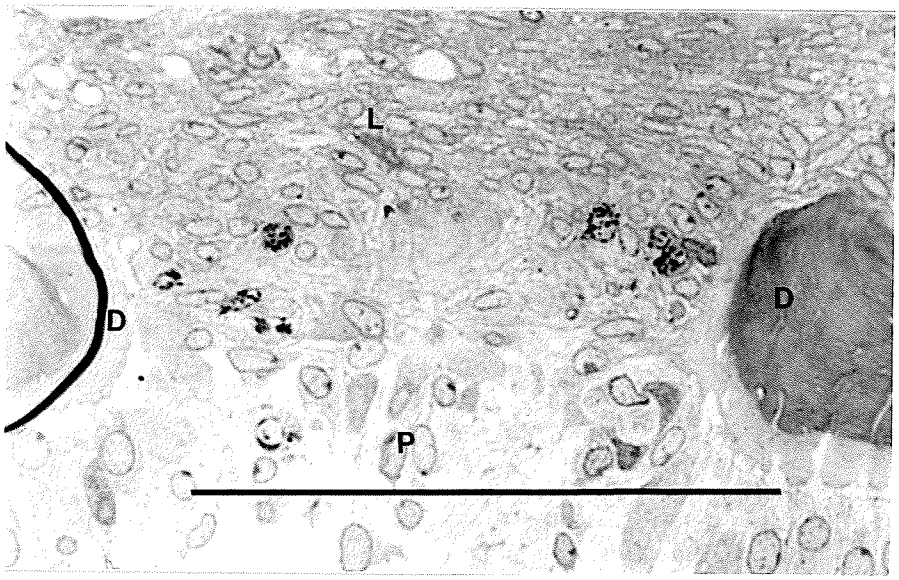
L
D
D
P

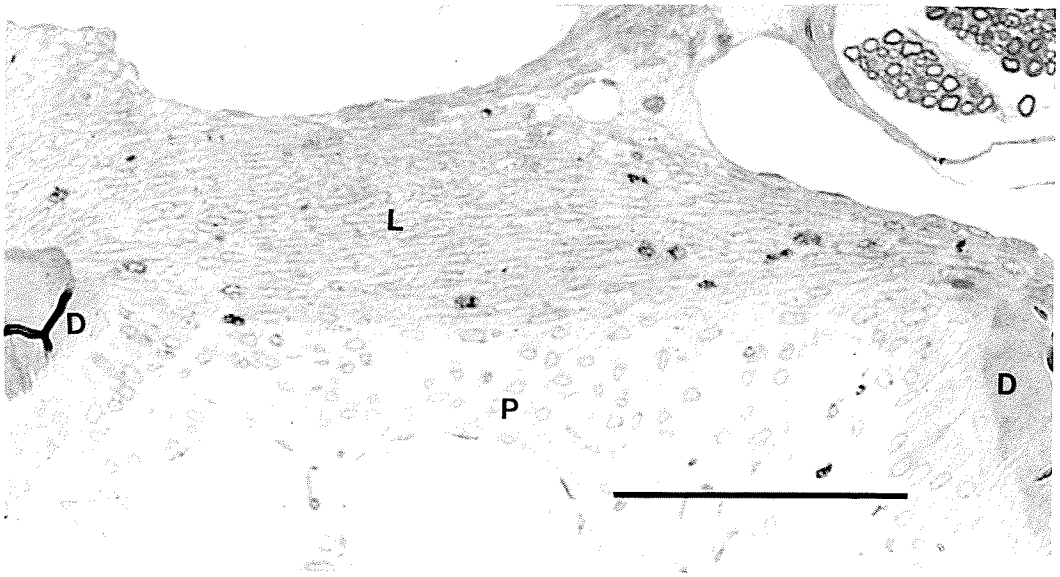
L
D
P
D

Figure 4.3.a

Radioautograph illustrating minimal ^{3}H-Tdr incorporation in the PDL of the lateral midroot area (3300 μm from the apex) in a 2 week post-adriamycin injected animal. Stained with iron hematoxylin (x 780)

Figure 4.3.b

Radioautograph illustrating ^{3}H-Tdr minimal incorporation in the lingual PDL (3300 μm from the apex) in a 2 week post-adriamycin injected animal. Stained with iron hematoxylin (x 780) [Note the artifact associated with dentin]

Figure 4.3.c

Radioautograph illustrating ^{3}H-Tdr incorporation in the adriamycin induced "lesion" (3300 μm from the apex) in a 2 week post-adriamycin injected animal. Stained with iron hematoxylin (x 780)

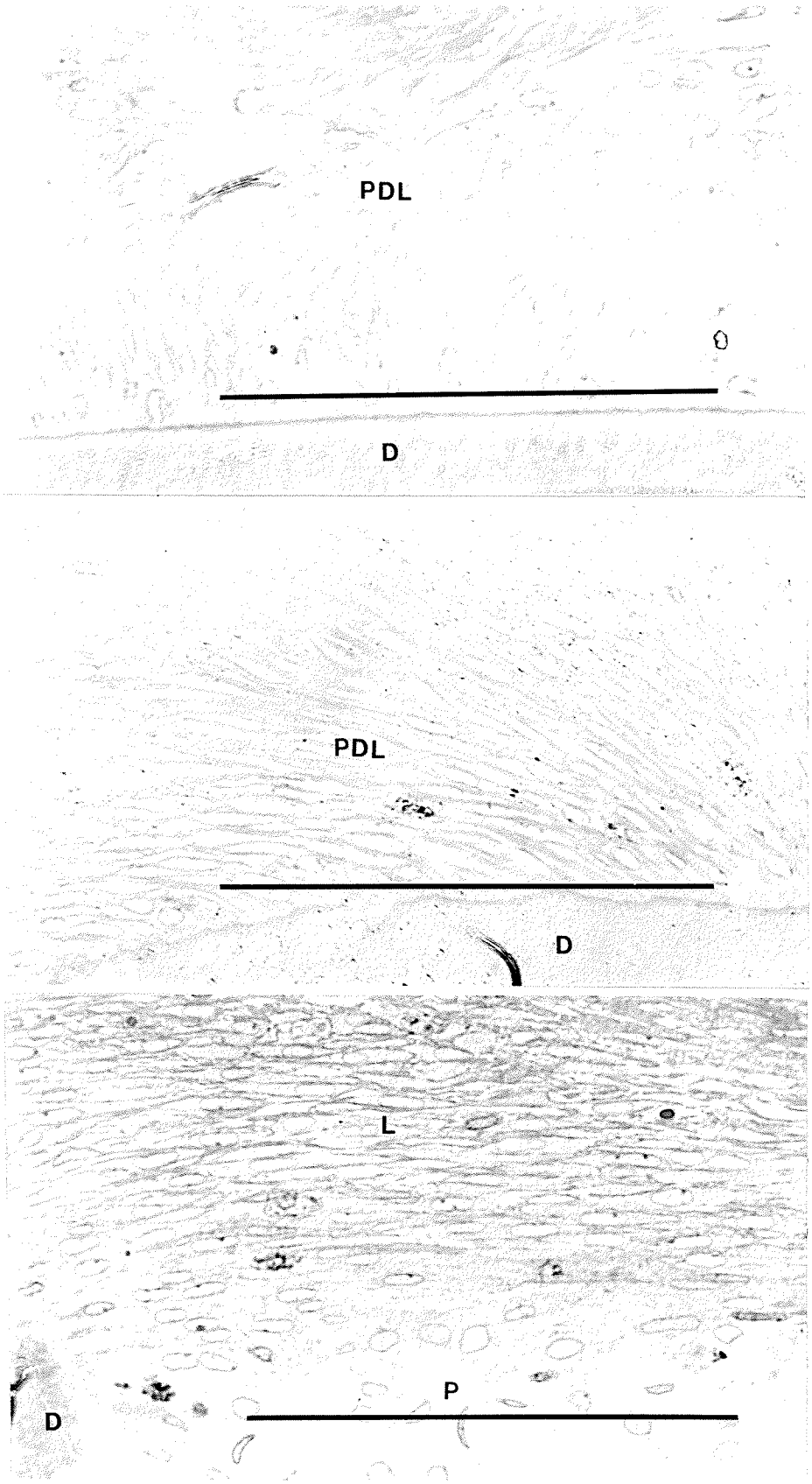
PDL
D
PDL
D
L
P
D